Spring August 2014

Engineering Probes to Detect Cholesterol Accessibility on Membranes Using Perfringolysin O

Benjamin B. Johnson
Umass Amherst

Engineering Probes to Detect Cholesterol Accessibility on Membranes Using Perfringolysin O

A Dissertation Presented

By

BENJAMIN B. JOHNSON

Submitted to the Graduate School of the

University of Massachusetts Amherst in partial fulfillment

of the requirements for the degree of

DOCTOR OF PHILOSOPHY

May 2014

Molecular and Cellular Biology

Engineering Probes to Detect Cholesterol Accessibility on Membranes Using Perfringolysin O

A Dissertation Presented

By

BENJAMIN B. JOHNSON

Approved as to style and content by:

_____

Alejandro P. Heuck, Chair

_____

Lynmarie K. Thompson, Member

_____

Daniel N. Hebert, Member

_____

Peter Chien, Member

_____

Barbara A. Osborne, Director

Molecular and Cellular Biology Program

ACKNOWLEDGMENTS

First I must thank Alejandro P. Heuck for his mentoring and support over the years that I have been a member of his lab. I have learned so much not only about my project but how to think about and approach science.

I would also like to thank my committee Lynmarie K. Thompson, Daniel N. Hebert and Peter Chien for their great support and their valuable input .

I will truly miss all of my co-works in the Heuck lab who worked with me in lab except Kyle. Having fun and interesting people around made even the bad day so much better: Fabulous, Lindsey Gouvin, Yuzhou Tang, Carolina Morell-Perez, Carlos M. Sanchez Correa , Dr. Devesh Kishore, Kathleen Burns, Francisca Sefakor Mote, William Boston-Howes, Sarah Kells, Dr. Paul C. Moe, , Kedar Mahagaokar, Kathryn Monopoli, Michael Buckner, Andrew Walsh, John Holt, and Nemat Sharaf

I would like to thank my girlfriend Amanda Hussey for all of her love and support as well as a considerable amount of proof reading.

Last but not least I would like to thank my family for without their support and guidance none of this would have been possible.

ABSTRACT

ENGINEERING PROBES TO DETECT CHOLESTEROL ACCESSIBILITY ON MEMBRANES USING PERFRINGOLYSIN O

MAY 2014

BENJAMIN B. JOHNSON

B.A., UNIVERSITY OF MASSACHUSETTS AMHERST

PH.D., UNIVERSITY OF MASSACHUSETTS AMHERST

Directed by: Professor Alejandro P. Heuck

Cholesterol is an essential component of mammalian cell membranes and it is important to regulate the structure and function of lipid bilayers. Changes in cholesterol levels are involved in many physiological and pathological events such as the formation of arterial plaques, viral entry into cells, sperm capacitation, and receptor organization. Determination of cholesterol trafficking and distribution is essential for understanding how cells regulate cholesterol.

A key factor in the regulation of cholesterol is cholesterol accessibility. Through it interactions in the membrane, cholesterol is sequestered below the surface of the membrane. Based on the composition of the membrane, a certain amount of cholesterol can be solubilized through interaction with the membrane. The remaining cholesterol is more solvent exposed and therefor accessible to interact with molecules outside of the membrane. This accessible cholesterol is

thought to regulate cholesterol homeostasis within the cell. A cholesterol probe capable of distinguishing changes in cholesterol accessibility within membranes would facilitate investigations in this area.

Perfringolysin O (PFO) is a cytolysin secreted by *Clostridium perfringens* that requires cholesterol in the target cell membrane for binding. The specificity of PFO for high levels of accessible cholesterol makes this toxin a potential tool for the detection of cholesterol distribution and trafficking. In an effort to adapt PFO into a molecular probe capable of sensing changes in membrane cholesterol accessibility, I have taken a non-lytic derivative of PFO and introduced several point mutations in the membrane-interacting domain 4 loops. These mutations altered the threshold of cholesterol concentration required in the membrane to trigger binding.

The cholesterol-dependent binding of each PFO derivative was tested on model membranes containing different percentages of cholesterol. Three PFO derivatives were selected to test their binding to macrophage plasma membranes. These three derivatives showed differential binding to cell membranes treated with β-methyl-cyclodextrin/cholesterol mixtures. These data showed that the produced PFO derivatives differentially bind to model and biological membranes containing different cholesterol accessibility.

TABLE OF CONTENTS

LIST OF FIGURES

CHAPTER 1

INTRODUCTION

1.1 Cholesterol

Cholesterol is a sterol that is essential for the viability of mammalian cells, as it is an important structural component of mammalian cell membranes. It helps to regulate membrane fluidity and stability, as well as reduce membrane permeability. Cholesterol is also the precursor to a number of steroid hormones, bile acids, and vitamin D.

Mammalian cells obtain cholesterol through two distinct pathways; one extracellular and one intracellular. The extracellular pathway involves the uptake of cholesterol from the blood stream via receptor-dependent binding of lipoproteins. The intracellular path involves cholesterol synthesis from within the cell in the endoplasmic reticulum (ER) from acetyl-CoA. Both of these pathways are tightly regulated respectively to each other and the needs of the cell. Cholesterol is unevenly distributed throughout cellular membranes, being largely localized on the plasma membrane and less so in the organelles. This distribution is important for many cellular functions and is maintained by a large number of tightly regulated processes within the cell

1.1.1 Cholesterol in health and diseases

Cholesterol, in addition to being an important structural component of cell membranes, has been shown to be involved in many physiological and pathological events such as the formation of arterial plaques, viral entry into cells, and receptor organization. Misregulation of cholesterol can lead to many disease

states, the most prominent of which is atherosclerosis. Atherosclerosis is associated with cholesterol metabolism that results in the formation of arterial plaques and, thus, the overall hardening of the arteries in humans. The primary cause of these plaques is the improper removal of cholesterol from the cells. Atherosclerosis is the number one cause of heart disease, the leading cause of deaths worldwide.

While not as prevalent as atherosclerosis, there are a large number of diseases caused by deficiency in cholesterol transport. Some examples of these are Niemann-Pick type C disease, familial hypercholesterolemias, Wolman disease, Tangier disease, Sitosterolemia, Smith-Lemli-Opitz syndrome, Cerebrotendinous xanthomatosis, congenital lipoid adrenal hyperplasia, and hypobetalipoproteinemias [1]. Niemann-Pick disease, for example, is a lysomal storage disease that is caused by the mutation of a cholesterol transport protein Niemann-Pick disease, type C (NPC1 or 2) that aids in the uptake of dietary cholesterol by moving it out of the late endosome for transport to the ER [2]. Niemann-Pick disease, while not very prevalent like all of the diseases listed above, is very serious and results in a progressive neurological decline followed by premature death.

Many other prominent diseases have been linked to cholesterol misregulation as these diseases result in abnormal cholesterol levels and distribution, but, at this time, it is still unclear whether misregulation of cholesterol causes or is merely just a result of the particular disease state. Alzheimer's Disease and some cancers are among those linked in this way [3].

While evidence of causality is still scarce, some have gone as far as to suggest cholesterol reducing drugs as a potential treatment for some cancers [2].

1.1.2 The role of cholesterol in mammalian cell membranes

Cholesterol consists of a hydroxyl group, four planar fused hydrocarbon rings, and a hydrocarbon tail (Fig. 1.1A). The hydroxyl group, in addition to mediating interaction with other membrane components, is important for orientation of the non-polar portions of the molecule [1]. In the membrane, cholesterol situates itself slightly below the surface of the membrane with the hydroxyl group interacting with the phospholipid head groups and the non-polar tail interacting with the tails of the other membrane components, mainly phospholipids and sphingolipids (Fig. 1.1B).

The interaction of cholesterol with membrane phospholipids and sphingolipids adjusts the melting temperature of the membrane to eliminate the liquid crystal phase transition in the host membrane. This creates an intermediate state in which the membrane has increased fluidity of the hydrocarbon chains below the transition temperature and decreases the fluidity above it [1]. At most biological temperatures, increases in cholesterol concentration will increase the order of the membrane and lower the motion of the hydrocarbon chains. This leads to an increase in packing and mechanical strength, as well as a resulting decrease in membrane permeability. These effects on the properties of membranes have been shown to alter the

A.

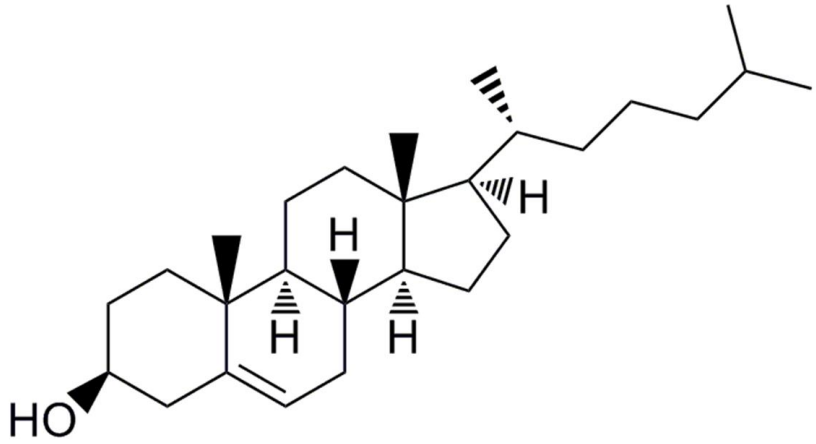

B.

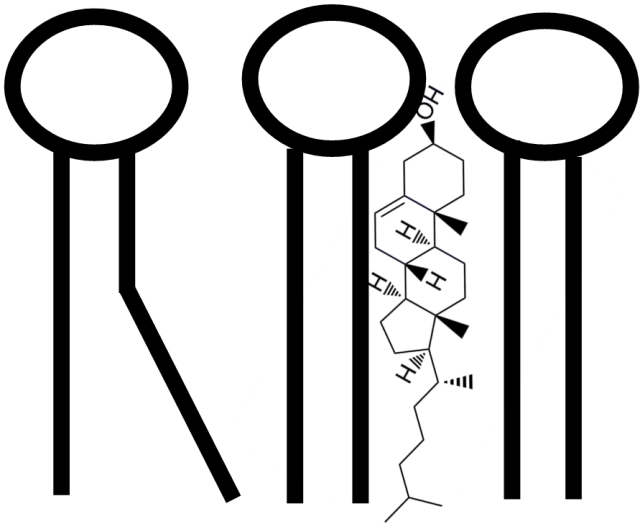

Figure 1.1 Cholesterol and the orientation of cholesterol in the membrane. A. The chemical structure of the cholesterol molecule. B. Depicts the energetically favorable placement of cholesterol in the membrane. Cholesterol is oriented below the membranes surface with the hydrophobic portion of the molecule interacting with the phospholipid tales and the hydrophilic hydroxyl group interacting with the phospholipid heads.

behavior of a number of integral membrane protein, including ion channels, membrane receptors, and enzymes [1]. The broad influence of cholesterol on such a large number of cellular processes is why cholesterol homeostasis is so important to the cell and so tightly regulated [1].

1.2 Cholesterol homeostasis

Due to cholesterol misregulation leading to such a large number of pathological states, cholesterol homeostasis is one of the most highly regulated biological processes[4]. Cholesterol can be acquired from food or produced within the cells; both acquisitions are tightly regulated in response to the other. In addition to this, cholesterol concentration in membranes is very unevenly distributed within the cell, leaving sharp gradient between the different membranes. While there are many proposed cholesterol transport mechanisms, it is still unclear how these gradients are maintained.

1.2.1 Extracellular cholesterol transport.

As a hydrophobic molecule, cholesterol must be transported in the blood stream by lipoproteins. There are five of these lipoproteins in the human blood stream: chylomicrons, very low density lipoproteins (VLDL), low density lipoproteins (LDL), intermediate density lipoproteins (IDL), and high density lipoproteins (HDL). Of these five proteins, HDL and LDL are predominantly responsible for the transport of cholesterol to and from cells in the blood stream. LDL is sometimes referred to as “bad” cholesterol as it takes cholesterol from the liver to various other tissues. HDL takes cholesterol collected from the bodies’ tissues and brings it to the liver. HDL is often referred to as “good” cholesterol

because it clears cholesterol from the blood stream as well as retrieving excess cholesterol from the cells.

Cholesterol levels in the blood stream are maintained by the liver and the intestines. The liver lowers serum cholesterol by removing VLDL and cholesterol containing chylomicron, which can then be excreted via bile to feces as well as releasing HDL. The liver can also raise serum cholesterol by synthesizing cholesterol and secreting it as LDL. By these processes, the liver can modulate the levels of cholesterol in the blood for cellular uptake [5]. In addition to the liver, the intestines can impact cholesterol homeostasis by modulating the levels of cholesterol absorption from food into the blood stream [6].

1.2.2 Regulation of Cholesterol Synthesis

In mammalian cells, cholesterol is produced in the ER, and is synthesized via a lengthy reaction sequence, requiring 30 enzymatic steps. The rate limiting step is the CoA reductase 3-hydroxy-3-methyl-glutaryl-CoA reductase (HMG-CoAR). This step has been the target of several cholesterol lowering drugs (statins),

Cholesterol synthesis is regulated by a family of sterol binding proteins, sterol regulatory element-binding protein (SREBP). The most prominent SREBP is SREBP2. When cholesterol levels are normal in the cell, SREBP2 is located in the ER in a complex with SREBP2 cleavage-activating protein (SCAP) and Insig-1. In this form, the complex is inactive. When cholesterol levels decrease, Insig-1 dissociates from the SREBP2/SCAP complex and is degraded [7] (Fig1.2) . The SREBP2/SCAP complex will then travel to the Golgi apparatus where SCAP will

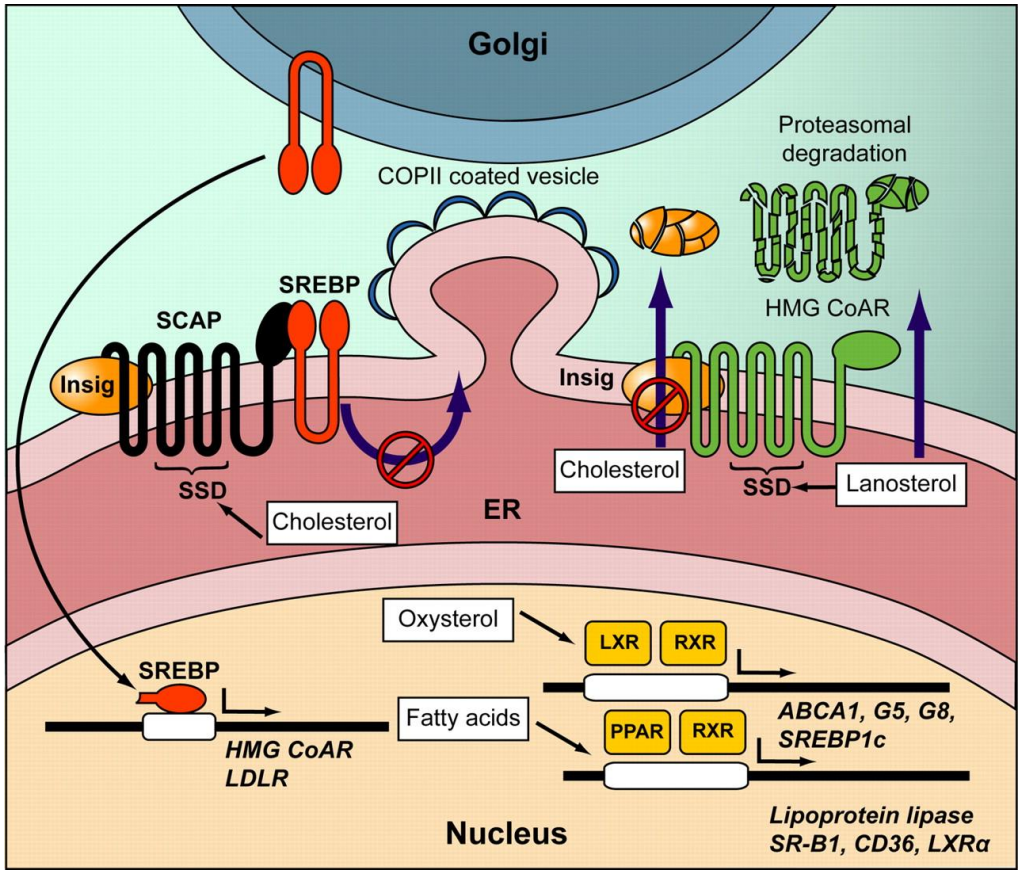

Figure 1.2 Schematic illustration of the transcriptional regulation of cholesterol homeostasis. In cases of high cholesterol, the inactive complex of SREBP2, SCAP, and Insig-1is located in the ER. When cholesterol levels decrease, Insig-1 dissociates from the SREBP2/SCAP complex and is degraded. The SREBP2/SCAP complex is transported to the Golgi where SCAP will cleave and release part of SREBP2 from the membrane. This fragment diffuses to the nucleus of the cell where it acts as a promoter by binding to sterol response element (SRE).

Figure taken with permission form Elina Ikonen (2006) Mechanisms for Cellular Cholesterol Transport: Defects and Human Disease, Physiological Reviews, Vol. 86 no. 1237-1261 October 1, 2006

cleave and release part of SREBP2 from the membrane. The water-soluble fragment will then enter the nucleus, of the cell where it acts as a promoter by binding to sterol response element (SRE). SRE is located in the promoter region of numerous genes involved in cholesterol synthesis. [8]. This results in a large increase in cholesterol production.

1.2.3 Cholesterol Uptake

Cholesterol, from nutrients, is taken up by the intestines and then packaged into lipoproteins for transport in the blood stream. Cholesterol then travels from the intestines to the liver by way of chylomicrons where it is repackaged into other lipoproteins for distribution to the cells. The lipoproteins packed in the liver, mainly LDL, can be easily taken up by cells. This process involves the LDL particle binding to the LDL receptor (LDLr) via a protein in its outer coat called ApoE/ApoB. The particle and the receptor are then both endocytosed through clathrin coated vesicles into acidic endocytic compartments [9]. In these vesicles, cholesterol esters are hydrolyzed by an acid lipase. The low pH in the early endosome causes the LDLr to dissociate for the LDL particle and the receptor is then recycled back to the cell surface [4]. (Fig 1.3) The remaining contents of the LDL particle, primarily cholesterol, moves on to the late endosomes where they are distributed to other cellular membranes by a yet unclear mechanism. This mechanism is, however, thought to involve two proteins NPC1 and NPC2. These proteins are suspected to be involved because inactivation of either protein results in Niemann-pick disease type C, the main symptom of which is an accumulation of cholesterol in the late endosome.

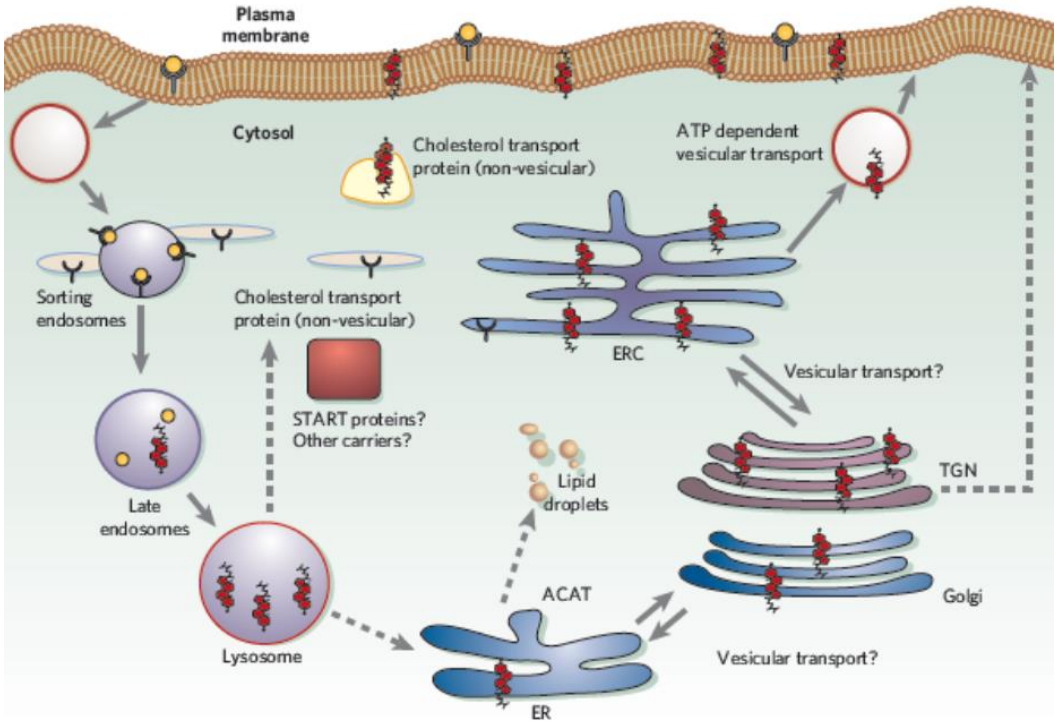

Figure 1.3 Intracellular cholesterol transport. LDL (yellow circles) carrying cholesterol and cholesterol esters bound to LDL receptors (light blue Y-shape). Cholesterol molecule are shown in red and the movement of cholesterol is depicted by the Gray arrows with the dashed arrows indicating that the mechanism by which this transport occurs is poor understood.

Figure taken with permission form Frederick R. Maxfield1 & Ira Tabas (2005) Role of cholesterol and lipid organization in disease, NATURE ,Vol 438 1 December 2005

1.2.4 Cholesterol Efflux

Most cells are incapable of degrading cholesterol. Therefore, cells need a mechanism by which cholesterol is transported outside of the cell and to the liver for reutilization or excretion. The main carrier of cholesterol back to the liver is HDL. HDL removes cholesterol from cells by passive diffusion of cholesterol into the HDL particle. The enzyme lecithin-cholesterol acyltransferase (LCAT) has been suggested to aid in this process. LCAT is located in the surface of lipo-protein particles mainly those containing HDL, and it has been shown to esterify cholesterol. The then esterified cholesterol will readily transfer to the HDL particle [10]. The HDL particle then circulates through the blood stream to the liver where it is absorbed. Cholesterol is removed by the scavenger receptor class B type1 (SRB1). While the LCAT pathway is the best defined mechanism of cholesterol removal, several other methods have been suggested, but poorly defined. It has also been shown that cholesterol can be removed in the absence of LCAT, so other methods are likely to emerge. [4].

1.2.5 Cholesterol Esterification and Storage

Cholesterol can be stored for extended periods of time in what are referred to as liquid droplets. They are large monolayer phospholipid vesicles with a neutral, lipid rich core consisting of steryl esters and triglycerides. These droplets are used for the storage of lipids, predominantly cholesterol and acylglycerols. The outer lipid monolayer has been shown to contain proteins that regulate lipid droplet dynamics and lipid metabolism. The net trafficking of cholesterol into or out of lipid droplets is linked to cellular cholesterol levels. Cholesterol is continually trafficked both in and out of lipid droplet, regardless of external cues,

although these cues do result in changes in the cholesterol balance. It is as of yet unclear by what mechanism cholesterol esters are trafficked into the lipid droplet. It has been shown that the transfer does not require energy input [11]. Some have suggested that the droplets may remain connected to the ER allowing for the simple diffusion of cholesterol esters. This is supported by the fact that the lipid droplets are likely derived from the ER. What, if anything, regulates this process remains very poorly understood.

The esterification of cholesterol for trafficking into lipid droplets involves the 3'-OH being fatty acylated to from a cholesterol ester. This process is accomplished via the enzyme acyl-CoA:cholesterol acyltransferase (ACAT). ACAT has two homologs expressed in most mammals (ACAT1 and ACAT2). They are both integral ER proteins, but are differentially expressed in various cell types. The degradation of cholesterol esters for trafficking out of lipid droplets involves the enzyme neutral cholesterol ester hydrololase (nCEH). This enzyme is located in the coat of the lipid droplets. As with ACAT, there are several homologous nCEHs in different cell types. The mechanism by which cholesterol esters move in, or cholesterol moves out, of the lipid droplets is very poorly understood.

1.2.6 Cellular Cholesterol Trafficking

Cholesterol is critical to many cellular functions, but it is far from evenly distributed throughout the organelles. Cholesterol is produced in the ER, but the majority of it resides in the plasma membrane. This requires cholesterol to be actively transported up a very steep gradient. In case of excess buildup of

cholesterol on the plasma membrane, cholesterol is returned to the ER of esterification and storage in lipid droplets. These two pathways appear to be independent due to the fact that they can be stimulated separately [12]. Maintaining this specific distribution of cholesterol is critical to cellular viability. As such, there are numerous mechanisms by which cholesterol can be distributed to different parts of the cell, through either vesicle or non-vesicle transport.

1.2.6.1 Non-Vesicle Transport of Cholesterol

Due to the hydrophobic nature of cholesterol, all non-vesicle transport requires a carrier protein with a hydrophobic pocket to solubilize the cholesterol molecule. While the exact identity of cholesterol carrier proteins remains elusive, several proteins have been implicated in cholesterol transport. These proteins include sterol carrier protein 2(SCP-2), caveolin, theoxysterol-binding protein-related protein (ORP) family, and steroidogenic acute regulatory (StAR) protein related lipid transport domain [4].

SCP-2 is a small soluble protein (13.3 Kd) formed by the cleavage of a larger protein SCP-X. SCP-2 has been shown to bind cholesterol, as well as other lipids. SCP-2 has also been shown to transport cholesterol between artificial membranes [13]. When SCP-2 is inhibited cellular distribution of cholesterol is disturbed [14]. In several tissue types, SCP-X remains almost completely involved with intake and is almost non-detectable in the cytosol [11]. While SCP-2 likely plays a role in cholesterol transport, the exact role is yet to be determined, and it is clearly not the sole mechanism of cholesterol transport.

StAR is responsible for shuttling cholesterol between the outer and inner membranes of mitochondria. StAR has been shown to bind cholesterol at a 1:1 ratio, and when knocked down, the transfer of cholesterol from the inner to the outer membrane is abolished [11]. Little else is known about the StAR proteins exact mechanism or what other proteins may be involved.

ORPs are a family of lipid binding proteins, many of which have been shown to bind cholesterol or cholesterol derivatives. Humans have at least 12 different ORPs, which are thought to play a role in regulation of lipid distribution and metabolism, cell signaling, and vesicular transport. It is not as of yet clear if ORPs directly play a role in cholesterol transfer, but when knocked down in yeast, they have been shown to greatly reduce the speed of cholesterol transfer from the ER to the plasma membrane.

Caveolin is a common membrane protein that oligomerizes on the surface of the membrane to create caveolae, cholesterol, and sphingolipid-rich invaginations. Whether or not caveolin is involved in cholesterol transport, though, is unclear. It has been shown to bind cholesterol, but this may just be for the purpose of organizing it on the membrane [15]. More study is needed to determine the mechanism by which it traffics cholesterol throughout the cell.

1.2.6.2 Vesicle Transport of Cholesterol

In addition to all of the methods listed above, cholesterol can also move as part of the membrane in a small vesicle. These vesicles are thought to travel between the ER and the plasma membrane in both directions. (Fig 1.3) When coming from the ER to the plasma membrane, cholesterol mostly goes through

the Golgi apparatus in a manner similar to protein secretion. This pathway is thought to be minor due to the fact that Golgi disassembly only reduces cholesterol transport to the plasma membrane by 20%, whereas protein secretion was reduced by 90% in the same cells. It has been suggested that vesicle transport could bypass the Golgi, but little evidence of this has been shown.

Cholesterol has been shown to return from the plasma membrane to the ER for esterification though the exact mechanism remains unclear. Loading cells with cholesterol causes vesicles to break off the plasma membrane in an ATP independent manner, though ATP is required for the delivery of these vesicles to the late endosome and lysosomes. This cholesterol is then trafficked to the ER in the same fashion as cholesterol taken from the media. This is supported by the fact that NCP-1 and NCP-2 deficient cells show significantly reduced transport of cholesterol for esterification. In addition to this path, retrograde transport of cholesterol through the Golgi has been implicated, but is at best a minor pathway.

1.3 Cholesterol Accessibility

Cholesterol modulates important membrane properties including permeability, fluidity, thickness, and domain formation. The cholesterol-dependent association of certain proteins and peptides with membranes has been often associated with the effect of cholesterol on one or more of these membrane physical properties. More recently, studies with molecules that directly interact with cholesterol, such as cyclic sugar polymers [e.g., cyclodextrins, 16], enzymes [e.g., cholesterol-oxidase, 17], and bacterial toxins [e.g., PFO, 18-21] have shown

that the accessibility of cholesterol at the surface of the membrane also plays a critical role in cell biology.

Cholesterol is insoluble in aqueous solutions, but it is readily soluble in phospholipid bilayers. The solubility limit of cholesterol in lipid bilayers is dictated by the nature of the phospholipids [acyl chain length and saturation, and head group size, 22]. If the concentration of cholesterol in a bilayer increases to levels above its solubility limit, cholesterol aggregates would form crystals and precipitate out into the aqueous solution [23-25]. Given its hydrophobic nature and how it situates itself in the membrane, at low concentrations, the interaction of cholesterol with other membrane components (lipids, proteins, etc.) reduces the ability of cholesterol to interact with water-soluble molecules at the membrane surface. In other words, when present in low amounts, cholesterol is not accessible to interact with water-soluble molecules such as PFO or cyclodextrins. As the concentration of cholesterol increases, the accessibility remains low until a saturation point is reached. The concentration of cholesterol at the saturation point will depend on the phospholipid or phospholipid mixture present in the membrane (Fig. 1.4A). At this point, a small increase in the sterol concentration causes a sharp increase in the ability of water-soluble molecules to interact with cholesterol [16, 17, 26]. Different models have been proposed to explain changes on cholesterol accessibility at the membrane surface: the cholesterol:phospholipid complex model and the umbrella model [27,28]. Despite their thermodynamic or steric basis, the models are not mutually exclusive [29, 30]. Recent molecular dynamics simulations of simple membrane models [31] suggested that cholesterol

accessibility is related to the overall cholesterol depth within the membrane bilayer and not to the appearance of a new pool of cholesterol molecules (sometimes referred as free cholesterol or active cholesterol). In favor of clarity in this chapter, I will refer to the effect that causes an increase in the interaction of cholesterol with water-soluble molecules, as an increase in cholesterol accessibility at the membrane surface (Fig. 1.4).

1.3.1 Role of Cholesterol Accessibility in Cholesterol Homeostasis.

As I have illustrated in the preceding section, cholesterol homeostasis is critical to cell viability, but the mechanisms by which it is controlled are not well understood. Recently, it has been proposed that cholesterol accessibility plays an important role in maintaining of the cholesterol gradients that exist between the organelles within the cell [21,32]. While it has been well documented that the plasma membrane (30-40 mol % cholesterol) has significantly more cholesterol than that of the ER (2-8 mol % cholesterol),it has been shown that the cholesterol accessibility of the two membranes is very similar[33,21]. This is possible because of the difference in the other membrane constituents that compose these membranes, and how strongly they interact with cholesterol. For example, sphingolipids interact strongly with cholesterol in the plasma membrane, and as a result, when this lipid is destroyed by sphingomyelinase, the cholesterol accessibility of the membrane increases greatly. This results in 15-30% of the plasma membrane cholesterol being transported back to the ER for esterification [34]. This action is believed to be the cell readjusting to the proper cholesterol accessibility. This indicates that imbalance of cholesterol accessibility

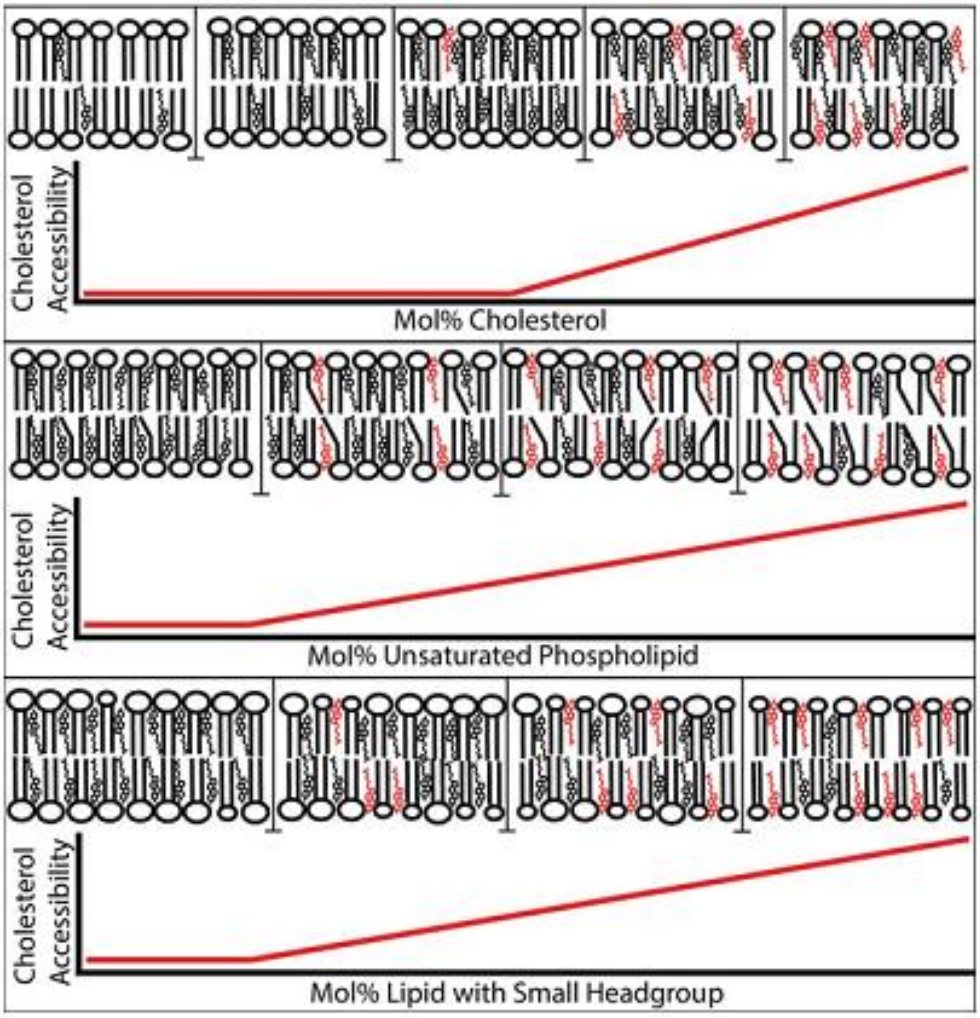

Figure 1.4 Cholesterol accessibility changes at the membrane surface as a function of the lipid composition. **A**. When interactions with other membranes components saturate the accessibility of cholesterol increases at the membrane surface. **B** At constant cholesterol concentration, an increase in the number of double bonds on the acyl chains of the phospholipids increases cholesterol accessibility. **C**. At constant cholesterol concentration, an increase in the concentration of phospholipids with smaller head groups increases cholesterol accessibility. The red lines depict a hypothetical increase on cholesterol accessibility. The actual change on cholesterol accessibility for each schematic graph may differ from a simple linear response. Some cholesterol molecules are colored red to visualize the increase on accessibility but they are indistinguishable from other cholesterol molecules in the membrane

triggers the trafficking of cholesterol from the plasma membrane to the ER. While the mechanism by which many of the sterol transport proteins work is still a mystery, they are mostly soluble proteins, and cholesterol accessibility seems very likely to play a factor in their binding to cholesterol. Cholesterol accessibility merely provides a simple means of maintaining the stark cholesterol gradient between the ER and the plasma membrane.

The activation of the SREBP2/SCAP complex has long been shown to be controled by the cholesterol levels in the ER (Fig. 1.2). The complex is retained in high cholesterol levels and released when cholesterol is low. Recent work has correlated this transition to the binding threshold of proteins known to have binding threshold linked to cholesterol accessibility (PFO, cyclodextrin) [21]. This would indicate that accessible cholesterol is what keeps INSIG-1 from being degraded in the SREBP2/SCAP complex in the ER. The result of this is a link between cholesterol accessibility and the regulation of cholesterol production.

1.3.2 Need for better cholesterol probes to study cholesterol in the cell

The complexity of the mechanism by which cholesterol homeostasis is regulated speaks to its supreme importance to the viability of all mammalian cells. The study of cholesterol homeostasis has been hindered by the redundancy of the mechanisms involved. Many different processes seem to act in unison to maintain proper cholesterol levels. We have reached the limit of what can be achieved through the knock down of single genes. In such a complicated system, better ways to track cholesterol and cholesterol accessibility are required to further define the system and all the players involved.

1.4 Current cholesterol probes

A diverse array of probes has been put forth as detection methods for cholesterol in the membrane. Among them, is everything from small molecules, like filipin, to whole proteins, like cholesterol dependent cytolysins (CDC) or cholesterol oxidases. In addition to standard probes, a large number of fluorescent cholesterol analogs have been created for the purpose of tracking cholesterol movement in the membrane.

Filipin is a polyene antibiotic that exhibits potent antifungal activity. Filipin is also highly fluorescent and binds specifically to cholesterol, presumably to the hydroxyl group of the cholesterol molecule [35]. While widely used, filipin staining tends to be somewhat ubiquitous at high concentration and uneven and prone to artifacts at lower concentration [36]. In addition, while filipin penetrates membranes, which can be useful, it also significantly disrupts them, which is very undesirable.

Cholesterol oxidase is an enzyme that converts cholesterol and oxygen into 4-cholesten-3-one and hydrogen peroxide. Hydrogen peroxide can then be detected by an oxidative coupling reaction in the presence of peroxidase that subsequently forms a chromogen or fluorophore, which can then be easily detected. Cholesterol oxidase activity has been shown to be dictated by cholesterol accessibility, because the cholesterol molecule has to at least partially leave the membrane to enter the active site of the enzyme. The main problem with cholesterol oxidase is that it oxidizes cholesterol by converting the sterol to a steroid and drastically changing its properties, thus causing it to no longer

condense or organize membranes in the same fashion. This can be very problematic, especially to longer term experiments.

Cholesterol analogs have proven very useful in tracking the movement of cholesterol. There are two kind of fluorescent cholesterol analogs; those that are intrinsically fluorescent and those that have a linked fluorophore. Intrinsically fluorescent cholesterol analogs, generally, more resemble cholesterol, but have low quantum yield and are prone to rapid photobleaching. As a result, larger amount of cholesterol analogs must be added to a cell that already contains cholesterol. This results in overloading of the cell. Cholesterol analogs with linked fluorophores are more photo-stable, allowing for lower density loading, but have issues with distribution and trafficking [37].

Cholesterol dependent cytolysins (CDC) are a family of pore forming toxins that bind to cholesterol containing membranes. They have primarily been used to detect high level of cholesterol, those over 30 mol%. This high cholesterol requirement led to CDCs being originally put forth as a method to detect lipid rafts. CDCs have also been used as an assay for the detection of high cholesterol disease states such as Niemann-Pick disease. More recently, the high binding threshold of CDCs was suggested to be the binding of accessible cholesterol by the protein. CDCs are somewhat limited by their high binding threshold, which makes them unsuitable for use on cholesterol poor membranes. [36]. While the previously discussed probes are capable of detecting cholesterol concentration, only CDC's are capable of detecting cholesterol accessibility

effectively. All currently available probes are imperfect and better probes are required to further the understanding of the role cholesterol plays in the cell.

1.5 Perfringolysin O

Perfringolysin O (PFO) is the prototypical example of a growing family of bacterial pore-forming toxins known as CDC [38, 39, 40]. CDCs are secreted by Gram-positive bacteria including *Bacillus, Listeria*, *Lysinibacillus*, *Paenibacillus*, *Brevibacillus, Streptococcus, Clostridium, Gardnerella*, *Arcanobacterium*, and *Lactobacillus* [see 39, 41, 42]. There are 30 members of the CDC family reported for Gram-positive bacteria and, surprisingly, two CDC-coding DNA sequences have been found in the Gram-negative *Desulfobulbus propionicus* and *Enterobacter lignolyticus*. However, in contrast with the Gram-positive bacteria that produce CDCs, the Gram-negative ones have not been shown to inhabit humans, or indeed animals, of any kind [43]. Despite their extremely diverse lineage, the majority of CDCs show an amino acid sequence identity greater than 39% when compared to PFO (figure1.5). The C-terminus (domain 4 or D4) of PFO is responsible for membrane binding and is the domain with the highest percentage of amino acid identity when sequences are compared with other CDC members.

Most CDCs possess a cleavable signal sequence, which targets the toxin for secretion to the extracellular medium. The secreted water-soluble toxins diffuse until encountering their target, a cholesterol-containing mammalian cell membrane (Fig. 1.6, step I). An exception to the cholesterol requirement, for targeting, was found for intermedilysin, which uses the human receptor CD59

		PFO	SPH	ALO	CLO	TLO	WLO	ALV	BVL	BRY	TLY	BLYb	BLYe	BLYc	NVL	SLO	SLOc	SLOe	LLY	PLY	MLY	PSY	SLY	ILY	ILO	LSO	LLO	VLY	PLO
Perfringolysin O	PFO		76	72	74	74	74	75	73	69	60	60	60	60	58	67	66	67	39	46	46	46	41	41	46	45	43	40	41
Sphaericolysin	SPH	90		80	82	82	82	77	80	69	58	57	57	56	54	66	65	65	37	42	42	42	41	37	45	45	43	37	38
Anthrolysin O	ALO	88	93		97	97	97	73	76	65	57	56	56	58	55	62	61	62	37	41	42	42	40	39	44	43	41	41	39
Cereolysin O	CLO	88	93	99		98	98	75	76	67	57	57	57	58	54	63	62	63	37	41	41	41	40	39	44	43	42	40	39
Thuringiensilysin O	TLO	88	93	99	99		98	75	77	66	57	57	57	57	54	63	62	63	37	41	41	42	40	39	44	43	42	40	39
Weihenstephanensilysin	WLO	87	93	99	99	99		75	77	66	56	57	57	57	54	63	62	63	37	41	41	42	40	39	43	43	42	40	39
Alveolysin	ALV	87	89	88	88	88	88		72	65	60	57	58	57	53	64	63	64	39	41	41	41	40	40	44	43	42	40	39
Brevilysin	BVL	88	93	91	91	92	92	87		68	58	57	57	58	57	64	63	64	39	42	42	42	40	39	46	44	42	39	40
Butyriculysin	BRY	85	86	84	84	84	84	81	84		58	55	55	57	56	64	63	63	37	43	43	43	40	39	45	44	42	40	39
Tetanolysin O	TLY	78	79	77	78	77	77	77	76	75		82	81	81	77	55	55	55	42	45	45	45	45	42	50	50	48	43	44
Botulinolysin B	BLYb	77	77	75	76	76	75	75	75	74	93		95	77	73	55	55	55	42	46	46	46	45	43	51	49	48	43	44
Botulinolysin E3	BLYe	77	77	75	75	75	75	75	74	75	93	98		74	72	54	54	54	42	44	45	44	45	42	51	49	49	43	43
Botulinolysin C	BLYc	79	79	78	79	78	78	77	77	77	93	90	90		83	54	54	54	42	46	46	47	46	46	49	49	48	45	43
Novyilysin	NVL	77	78	79	79	79	79	76	77	78	90	88	87	93		53	52	52	42	44	44	45	45	44	50	50	47	44	44
Streptolysin O	SLO	83	81	79	80	80	79	80	81	80	74	73	73	74	75		99	100	39	42	42	42	41	38	43	43	41	39	39
Streptolysin O c	SLOc	82	80	79	79	79	79	79	81	79	74	73	72	74	74	99		99	39	41	41	41	40	37	44	43	42	39	39
Streptolysin O e	SLOe	83	81	79	80	80	79	80	81	80	74	73	73	74	75	100	99		39	41	41	42	41	37	44	43	42	39	39
Lectinolysin	LLY	62	61	61	61	61	61	62	62	63	65	64	64	66	64	64	63	64		51	51	51	46	54	40	41	40	59	41
Pneumolysin	PLY	67	66	65	66	66	65	66	66	66	68	67	67	69	67	65	64	65	73		99	99	51	53	43	43	43	53	41
Mitilysin	MLY	67	66	65	66	66	65	66	66	66	67	67	67	69	67	65	64	65	73	100		100	50	53	44	43	43	53	41
Pseudopneumolysin	PSY	67	66	65	66	66	65	66	66	66	67	67	67	69	67	65	64	65	73	100	100		50	53	44	43	43	53	40
Suilysin	SLY	65	65	66	66	66	65	65	66	66	69	68	68	69	69	65	64	65	68	73	74	74		47	48	45	46	52	45
Intermedilysin	ILY	64	62	64	64	64	64	64	63	64	65	66	66	68	67	62	61	62	77	74	74	74	68		42	42	42	60	42
Ivanolysin	ILO	66	64	65	64	64	64	64	66	66	70	70	70	71	71	65	65	65	64	67	67	67	71	66		79	81	42	43
Seeligeriolysin O	LSO	67	66	65	65	66	65	67	67	65	71	70	71	71	70	66	66	66	64	66	66	66	69	64	91		85	41	43
Listeriolysin O	LLO	66	65	63	64	64	63	65	66	64	72	71	71	71	70	66	66	66	65	67	67	67	69	66	94	95		40	43
Vaginolysin	VLY	63	62	64	64	64	64	63	62	62	64	65	64	66	67	62	61	62	77	73	73	73	69	79	63	62	63		43
Pyolysin	PLO	60	58	58	59	59	59	60	61	61	61	60	60	63	63	60	60	60	62	61	61	61	64	63	63	62	62	60	

Figure 1.5. Analysis of the primary structure for the CDCs reveals a high degree of identity and similarity among them. Only the sequence for the conserved core of the CDCs was used for the analysis (corresponding to PFO amino acids 38–500). If more than one sequence was available for individual species, only one was used in the analysis. Sequence relationships were calculated using the MatGat 2.02 alignment program using the BLOSUM 62 matrix and open and extension gap penalties of 12 and 1, respectively (Campanella et al., 2003). The identity scores occupy the upper triangle (in bold) with scores higher than 70% shaded in dark gray, and those at 50–70% in light gray. Similarity scores in the lower triangle were shaded in dark gray if higher than 80% and in light gray if between 70 and 80%

for membrane targeting [44]. However, this toxin still requires cholesterol to insert into the membrane and form a transmembrane pore [45]. After binding, CDC monomers diffuse across the surface of the membrane and interact reversibly with other monomers until formation of a stable dimer [Fig. 1.6, step II, 46, 47]. These initial dimers grow by the incorporation of additional monomers into a large ring shaped complex (known as the pre-pore complex, [Fig. 1.6, step III, 48]. Each of these complexes contains 30-50 monomers, and upon insertion into the membrane, form large β-barrel pores [up to 250-300 Å in diameter, Fig. 1.6 step IV, 49, 50, 51].

PFO is secreted by *Clostridium perfringens* as a 52.6 kDa protein, and the crystal structure of the water-soluble monomer revealed four distinct domains [Fig. 1.7A, 52]. The overall three dimensional structure observed for PFO is conserved for all other CDCs whose high resolution structures have been solved [53-55]. Domain 1 (D1) consists of the top portion of the elongated molecule. D1 is the only domain that does not undergo large structural rearrangements during pore formation. Domain 2 (D2) adopts mostly a β-strand secondary structure that collapses vertically during pore-formation to allow the insertion of the β-hairpins that form the transmembrane β-barrel [49, 56-58]. Domain 3 (D3) contains both the β-sheet involved in the oligomerization of the toxin and the six short α-helixes that unfurl into two amphipathic β-hairpins to form the β-barrel [50, 51, 59]. D4 consists of a β-sandwich and contains a conserved Trp rich loop, as well as, three other conserved loops at the distal tip (Fig. 1.7B and C). D4 is responsible for

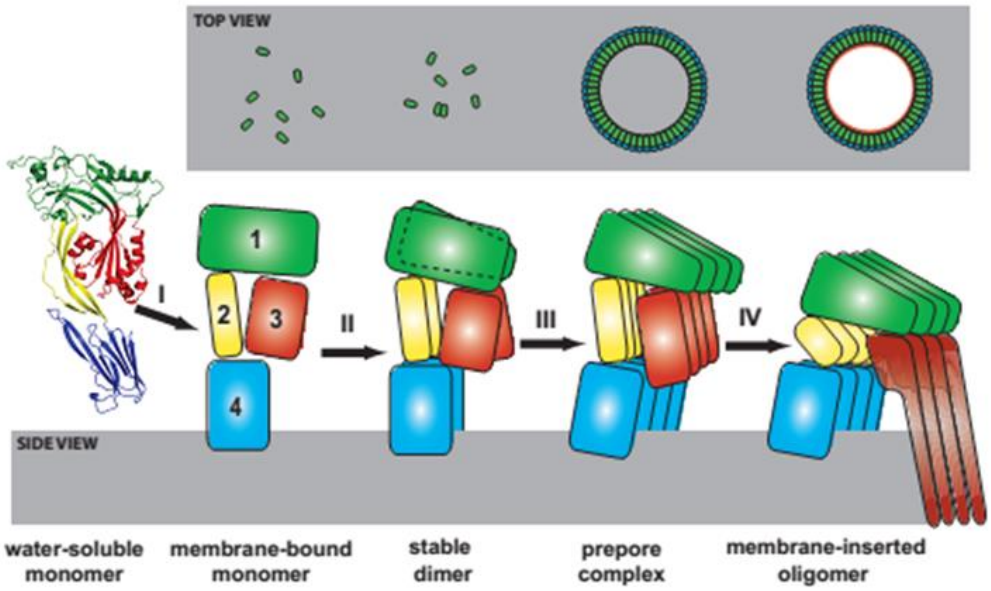

Figure. 1.6 Cartoon representation of the different steps/intermediates identified for the PFO mechanism of pore formation. A water-soluble monomer is secreted by the bacterium and binds to the target membrane via D4 (step I). Membrane-bound monomers diffuse across the membrane surface interacting transiently until they form a stable dimer (step II). The initial dimer starts growing with the addition of other monomers until completion of a circular ring or pre-pore complex (step III). In the last step, each monomer inserts two amphipathic transmembrane hairpins into the bilayer aided by the vertical collapse of D2 forming a large β barrel pore (step IV). Domains are numbered and color coded as follows: D1 (green), D2 (yellow), D3 (red), and D4 (blue). Only a few PFO monomers are shown in the side view at the bottom to simplify the figure. On the top is a schematic top view for each step of the pore formation mechanism shown below. The membrane bilayer is depicted by a gray rectangle.

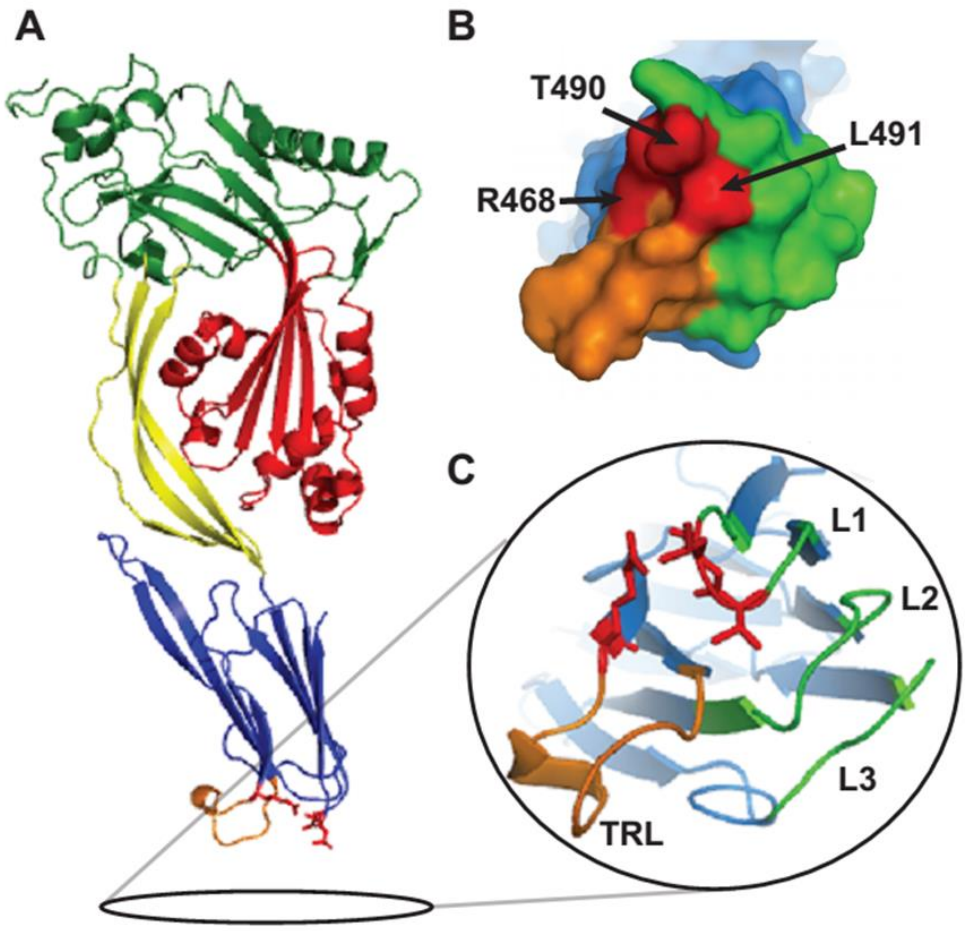

Figure 1.7 Three dimensional structure of PFO showing the location of important elements that modulate cholesterol interaction. A. Ribbon representation of the water-soluble PFO monomer with domains colored as indicated in Fig. 1.5. Also in color are three key residues that influence cholesterol interaction T490, L491, R468 (Red), and the Trp rich loop (TRL, orange). B. A view of the tip of D4 from the bottom showing the exposed surface of the Trp rich loop residues (orange), the three small loops (green), and the residues indicated in A (red). C. The ribbon rendering of the same bottom view of D4 shown in B. PFO (1PFO) structure representation was rendered using PyMol (DeLano Scientific LLC)

cholesterol recognition and the initial binding of the toxin to the membrane [26, 60].

1.5.1 Binding and pore formation mechanism

One of the unique features of the mammalian cell membrane is the presence of cholesterol. *C. perfringens* and other pathogens have exploited this property of mammalian membranes to target their CDCs without compromising the integrity of their own membranes. The cholesterol recognition of PFO is via D4. The full binding mechanism will be discussed in detail in section 1.5.3

1.5.2 Oligomerization on the Membranes Surface

Upon binding to a cholesterol containing membrane, PFO diffuses across the surface of the lipid bilayer and oligomerizes into a large ring shaped complex (Fig. 1.6). This complex contains 35-50 individual PFO monomers (~250-300 Å inner diameter) and it is referred to as the pre-pore complex [48, 49, 61]. Transition of the pre-pore complex to the final membrane-inserted complex occurs by the insertion of numerous β-hairpins (two per monomer) that perforate the membrane forming a large transmembrane β-barrel [50]. The conformation of the individual PFO monomers in the pre-pore complex is not vastly changed from that of their water-soluble form. There are subtle structural changes that are triggered by membrane binding and oligomerization of the protein that allow for proper alignment of the monomers and the overall geometry of the pore [59]. Formation of complete rings at the surface of the membrane seems to be regulated by the relatively slow formation of an initial CDC dimer [46, 47].

1.5.2.1 Nucleation of the Pre-pore Complex

Oligomerization of the CDCs is triggered by membrane binding and interaction with cholesterol (or exceptionally by interaction with a protein receptor for intermedilysin). Cholesterol binding is sufficient to trigger the conformational changes that unblock the hidden oligomerization interface in the water-soluble monomer [59, 62]. Blockage of the oligomerization interface in the monomer prevents premature oligomerization of the toxin in solution. This regulatory mechanism can be overridden if the monomers are present at high concentration in solution [e.g., for pneumolysin, 63, 64], but oligomerization is rare at physiological concentrations (i.e, nM range or lower).

The most significant of the conformational changes that follows membrane binding involves the exposure of the core β-sheet that comprises a larger part of D3. A short β-strand (β5) separates from the core β-sheet in D3 and exposes β4 for its interaction with the always-exposed β1 strand of another PFO molecule, promoting oligomerization [59, 65]. This conformational change is thought to be facilitated by a pair of Gly residues, G324 and G325, located in the loop between β4 and β5. These Gly residues are highly conserved, and act as a hinge between the two β-strands [66]. In addition to the separation of β5 from β4, it has been suggested that there is a disruption of the D2 and D3 interface. This disruption is thought to be caused by the rotation of D4, which breaks the weak interactions between D2 and D3. These conformational changes cause the rotation of D3 away from D1, and ultimately the unfurling of the transmembrane hairpins [47, 67].

Hotze et. al. have recently suggested that the initial interaction between two membrane-bound PFO monomers is weak and transient. This interaction is rarely of sufficient length to allow for the transition to a stable dimer with β1 and β4 strands properly aligned. However, if the transition occurs, addition of further PFO monomers to the complex becomes favorable and oligomerization ensues. Therefore, formation of a stable initial dimer constitutes the rate limiting step in oligomerization that diminishes the formation of uncompleted rings on the membrane surface [Fig. 1.6, step II, 47]. While it has been originally proposed that the separation of β5 from β4 happens upon membrane binding [66], it is still unclear whether these structural changes are caused by toxin binding or as a consequence of monomer-monomer oligomerization.

1.5.2.2 Alignment of Core β-sheets

Addition of monomers to the growing oligomer requires the proper alignment of the core β-strands of the newly added PFO monomer with a β strand at the edge of the oligomer. Formation of hydrogen bonds between adjacent β-strands is energetically favorable, but non-specific in nature. If the alignment is incorrect, proper growing of the oligomer would not be possible. It is critical to regulate the alignment of neighbor β-strands to prevent the formation of truncated pre-pore complexes. The correct alignment of adjacent β-strands among individual PFO monomers is dictated by π-stacking interactions between aromatic residues located in β1 (Y181) and β4 (F318) [66]. Modifications on either of these residues have proven to be extremely deleterious to the ability of PFO to form pores. Interestingly, despite being a critical interaction, it appears that only

Y181 is completely conserved among the CDCs. A few CDC family members do not contain an aromatic residue in the corresponding location of F318 in PFO, suggesting that proper alignment of adjacent β-strands may follow another regulatory mechanism for these members [i.e., lectinolysin, intermedilysin, vaginolysin, pneumolysin, mitilysin, pseudoneumolysin, and the two newly identified members, see 39, 41, 42].

1.5.3 Mechanism of Pore Formation

The last step in the cytolytic mechanism of PFO is the formation of the transmembrane pore. The pre-pore complex transitions into a membrane-inserted complex forming a large transmembrane β-barrel (Fig. 1.6, step IV). This transition involves the unfurling of six short α-helixes located in D3 down to two amphipathic β-hairpins, and the collapse of D2 to bring down the β-hairpins so they can span the hydrophobic core of the membrane. Large secondary and tertiary structural changes are required to coordinate the insertion of more than 140 individual β-strands and the removal of thousands of lipid molecules to form a β-barrel pore. The use of two β-hairpins per monomer to create a transmembrane β-barrel was first described for PFO [50, 68], and it is likely that this mechanism is also employed by other important pore-forming proteins like the membrane attack complex/perforin (MACPF) proteins [69-71].

A key step in the pore formation mechanism of the CDCs is the unfurling of six short α-helixes in D3 to form two extended amphipathic β-hairpins [50, 62, 72]. These conformational changes are necessary to minimize the exposure of hydrophobic residues in the water-soluble form of the PFO monomer [50, 73].

After insertion, the hydrophobic side of the amphipathic hairpin faces the non-polar lipid core, and the hydrophilic side faces the aqueous pore [Fig. 1.6, 50, 51]. The exact molecular mechanism for the pre-pore to pore conversion remains unknown, but thermal energy plays a key factor, since at low temperatures (e.g., 4 °C) the PFO oligomer remains locked at the pre-pore complex state [48, 74].

Sato et al have recently shown that in the pre-pore complex the β-strands that form the transmembrane pore are flexible and mobile [72]. These transmembrane β-hairpins are located high above the membrane in the pre-pore complex [56, 58] and are able to extend and test hydrogen bonding arrangements, but they do not fully form a β-barrel structure [72, 74]. This partially unfolded state of the β-hairpins is thought to represent an intermediate step in pre-pore to membrane-inserted complex transition for PFO [72]. The partial alignment of the β-hairpins in the pre-pore complex may constitute a kinetic barrier that deters the insertion of incomplete rings favoring the formation of complete pre-pore complexes.

The unfurling of the two α-helical bundles into two β-hairpins is favored by the formation of multiple hydrogen bonds, both between hairpins within a PFO monomer and between hairpins on adjacent monomers (Fig. 1.8). Crosslinking experiments revealed that the β-hairpins in the inserted β-barrel adopt a ~20 degree angle to the plane of the membrane, and the adjacent inter-monomer strands align themselves with a shift of two amino acids [Fig. 1.6, 72]. As mentioned above, PFO oligomerization is aided by the proper alignment of β-

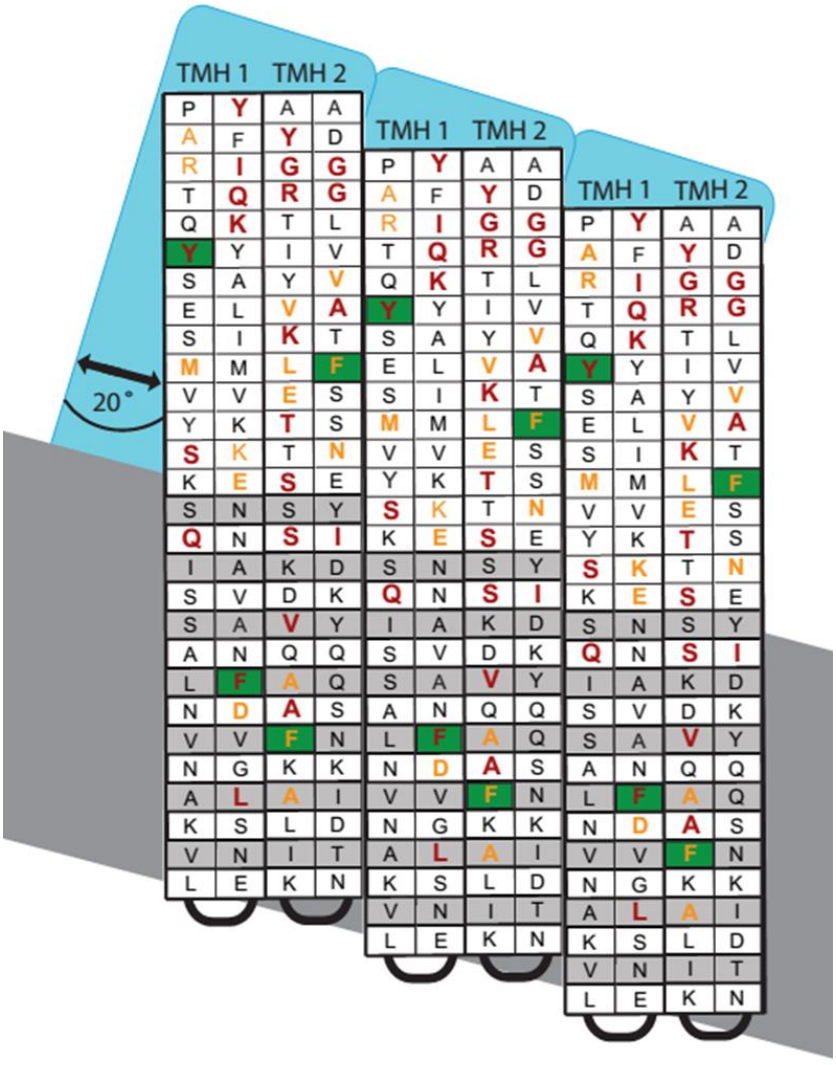

Figure 1.8 A schematic view that depicts the position and orientation of the transmembrane hairpins (TMH1 and TMH2) of PFO in the membrane-inserted complex as determined by Sato et al (2013). The tilted membrane and the rectangle representing the rest of the PFO molecule are depicted in gray and blue, respectively. The amino acids that compose the D3 β sheet and the transmembrane hairpins are depicted by their single letter code and color-coded according to conservation in the CDC family. Amino acids conserved in more than 90% of the 28 CDC members are shown in red, in orange if conservation was higher than 70% but lower than 90%, and in black if not highly conserved. Highlighted in green are the aromatic amino acids that are thought to be involved in π-stacking interaction that stabilize PFO pre-pore confirmation and help to align individual PFO monomers for pore formation (see text for details)

strands from adjacent monomers via π-stacking interaction between the completely conserved Y181 and the highly conserved F318. Inspection of the extended hairpins in the β-barrel conformation (Fig. 1.8) revealed another potential π-stacking interaction that may act to stabilize the hairpins in their extended conformation. These are the completely conserved F211 in the transmembrane hairpin 1 (TMH1) and highly conserved F294 (present in all but vaginolysin, lectinolysin, and intermedilysin of the 30 members) in the transmembrane hairpin 2 (TMH2). Interestingly, the F211C modification decreased the hemolytic activity of PFO [51] and the PFO derivative containing the F294C modification could not be stably produced [50].

The vertical collapse of D2 to bring D3 closer to the surface of the membrane is another important step in pore formation [56, 57]. In the pre-pore complex, PFO is positioned perpendicular to the membrane leaving D3 about 40 Å above the membrane surface [56, 58]. In this position, the β-strands that form the pore would barely reach the membrane surface and could not penetrate the membrane. The required vertical collapse of D2 would drop D3 to the membrane surface and allow the β-hairpins to punch through the membrane and form a β-barrel. Unfortunately, little is known about the mechanism of the transmembrane β-barrel insertion.

Formation of a pre-pore complex and formation of hydrogen-bonds between adjacent β-strands helps the toxin to overcome the energetic barrier of inserting non-hydrogen bonded β-hairpins [39]. The insertion of incomplete rings

may also occur, especially when free monomers are no longer available to complete the circular complex. Trapped metastable arc-like structures may form a pore by themselves, but the formation of a lipid edge at one side of the pore is not energetically favored, and the arcs would have a tendency to associate with other arcs or any proximal complete rings [75-77].

One of the most intriguing aspects of the CDCs cytolytic mechanism is what happens to the lipids that are displaced to form the pore. The insertion of the β-barrel requires the displacement of more than 1000 lipid molecules from the membrane [68]. It is not clear how such a large amount of molecules are removed from the center of the pre-pore complex, but the hydrophilic nature of the inner portion of PFO the β-barrel could aid in this process.

1.5.4 Domain 4 and cholesterol recognition and binding

Binding of PFO and other CDCs requires high levels of cholesterol in model membranes prepared with phosphatidylcholine [78-80]. Based on the requirement of high cholesterol levels, targeting of PFO to cholesterol rich domains or "lipid rafts" has been suggested. However, it has become clear that exposure of cholesterol at the membrane surface is a key factor to trigger PFO binding, and "lipid rafts" may not be necessary for toxin binding [18-21, 31, 62]. The localization of PFO oligomers on the surface of the membrane may change from the original binding site after insertion of the β-barrel [81, 82].

The binding of PFO to cholesterol containing membranes is modulated by amino acids located in the loops that connect the β-strands at the bottom of D4

[Fig. 1.7C, 20, 83, 84-87], however the precise molecular mechanism of CDC-cholesterol interaction remains poorly understood.

1.5.4.1 Cholesterol Recognition

The first step in the binding of a water-soluble CDC to the membrane involves the formation of a non-specific collisional complex between a monomer and the lipid bilayer. This step is diffusional and electrostatic interactions may play an important role [e.g., introduction or elimination of negative charges alters binding, 83, 86]. While on the membrane surface, insertion of non-polar and aromatic amino acids, and/or specific interactions with membrane lipids, may anchor the protein to the membrane [88]. However, non-polar amino acids are rarely exposed on the surface of water-soluble proteins, and therefore conformational changes are often required to expose these residues to the hydrophobic core of the membrane bilayer. As a result, multiple conformational changes are triggered during the transition of PFO from a water-soluble monomer to a membrane-inserted oligomer.

In model membranes prepared exclusively with phosphatidylcholine, > 30 mol% cholesterol is required to trigger binding of PFO [26, 80], streptolysin O [79], lysteriolysin O [89], or tetanolysin [78], but the amount of cholesterol needed does vary depending on membrane phospholipid composition. The "cholesterol threshold" can be reduced by the presence of double bonds in the acyl chains of the phospholipids or by the presence of phospholipids with smaller head groups [18, 19, 90]. Modifications to the phospholipids that form the membrane can alter the ability of PFO to detect cholesterol at the surface of the membrane [20]. Despite their influence on membrane binding, the presence of

phospholipids is not required, since cholesterol alone (in the absence of any other lipid) is sufficient to trigger PFO oligomerization and formation of ring-like complexes [62 and references therein]. Accessibility of cholesterol at the membrane surface seems to be the key to trigger the binding of PFO to membranes [19-21, 31].

1.5.4.2 Domain 4 and the Conserved Loops

PFO D4 consists of two four-stranded β-sheets located at the C-terminus of the protein (Fig. 1.9). There are four loops that interconnect the eight β-strands at the distal tip of the toxin, three short loops (L1, L2, and L3) and a longer Trp rich loop (also known as the conserved undecapeptide). These loops insert into the membrane upon binding and are presumably responsible for the interaction of the toxin with cholesterol [60, 83, 85]. Two of these loops (L2 and L3, Fig. 1.7C) connect β-strands from opposite β-sheets, while L1 and the Trp rich loop connect β-strands from the same β-sheet. L1 and the Trp rich loop are parallel to each other and abutted perpendicularly by L2 forming a pocket in the bottom of the protein. The loops that form the pocket are the most conserved segments in D4, and modifications to any of these loops affects the cholesterol binding properties of PFO [20, 85, 86, see below, 91]. The remaining L3 is far less conserved and distant from the pocket formed by the other three loops.

The Trp rich loop is the longest of the D4 loops, containing 11 residues (E C T G L A W E W W R). It is a signature feature of the CDCs and is highly conserved among species. The three-dimensional structure of this loop seems to be more variable [52-55], but this may simply reflect its flexibility [53]. Initially,

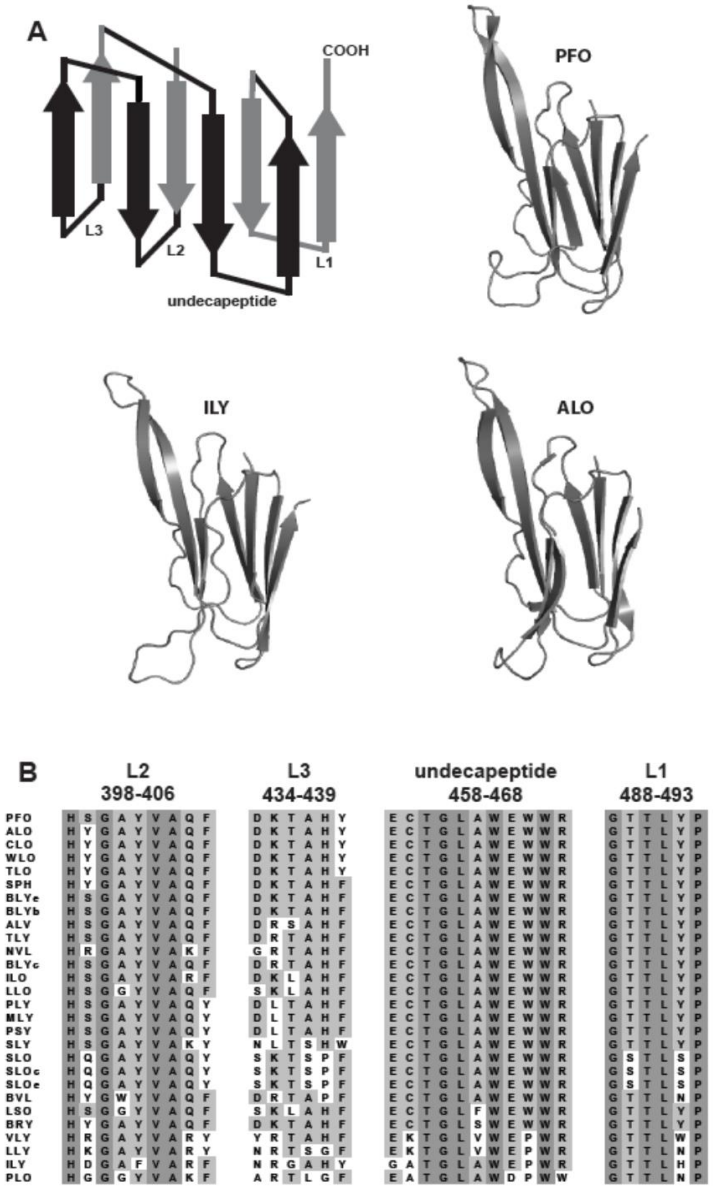

Figure 1.9 The three dimensional structure of D4 is highly conserved in the CDC family. (**A**) Comparison of D4 from three CDC homologs highlights the conserved architecture of this C-terminal domain. A cartoon, upper left, clarifies the threading of 2 β-sheets and loops in the β-sandwich and indicates the spatial organization of the undecapeptide, L1, and L2. The α-backbone for the D4 domains of PFO, ILY, and ALO were aligned using PyMol (DeLano Scientific LLC; available at www.pymol.org). (**B**) Alignment of the sequence for the 28 CDC family members reveals substantial conservation in loops L1, L2 and the undecapeptide. While integrity of the undecapeptide was long recognized for being critical to the cholesterol-dependent activity of these toxins, other loops are also important. Residues conserved in all sequences are shaded in black, and highly conserved residues are shaded in gray.

the Trp rich loop was thought to be responsible for cholesterol recognition and binding, and this idea was supported by several studies showing that modifications in it greatly decreased the pore-forming activity of the protein [91-97]. However, recent studies showed that the other loops in D4 are also responsible for cholesterol recognition [85]. The Trp rich loop has now been suggested to play a role in both the pre-pore to pore transition [83] and the coupling of monomer binding with initiation of the pre-pore assembly [87]. Dowd and colleagues recently showed that modification of a charged amino acid in the Trp rich loop (Arg 468, Fig. 1.7B) resulted in complete elimination of the pore-forming activity of PFO and had a significant effect on the membrane binding of the toxin [87, 91]. The R468A PFO derivative was not able to oligomerize after membrane binding, suggesting that this modification disrupts the previously reported allosteric coupling between D4 and D3 [26]. Despite the novel functions assigned to the Trp rich loop, its role in binding cannot be neglected since many modifications to this segment have been shown to have a significant effect in toxin-membrane interaction [91].

Unlike the flexible Trp rich loop, the three-dimensional structure of the other three short loops is more conserved. The L3 is located on the far edge of D4, away from a pocket formed by the Trp rich loop, L1, and L2 (Fig. 1.7C). Modifications introduced into L3 have been shown to have either a negligible effect on cholesterol interaction, or to decrease the amount of cholesterol required for binding [85, 86]. For example, the elimination of the charge of D434 in L3 increases the amount of protein able to bind to a given membrane. These results

suggest that L3 plays a limited role in cholesterol recognition, and its effect on binding may be related to nonspecific interactions with the membrane that stabilize the bound monomer at lower cholesterol levels.

1.5.4.3 Proposed Cholesterol Recognition Motif

PFO contains a proposed cholesterol recognition motif composed of only two adjacent amino acids in L1, T490 and L491 (Fig 1.9) [85]. These amino acids are completely conserved throughout all reported CDCs, and modifications to them greatly affect the binding of the protein to both cell and model membranes [85] . These data suggest a prominent role for these two amino acids in cholesterol recognition, however, other well conserved amino acids in that region have not been analyzed yet (e.g., H398, Y402 and A404). Moreover, no direct interaction between cholesterol and these two residues has been shown so far. The fact that both amino acids must be mutated to eliminate binding in a motif containing only two amino acids, coupled with the fact that there are many additional conserved amino acids in the vicinity, suggest that other amino acids may also play a role in cholesterol recognition and form part of the cholesterol binding site. Further studies are required in this area.

1.5.4.4 The Effect of Cholesterol Accessibility on PFO Binding

At this time, it is more or less accepted that cholesterol accessibility plays a pivotal role in the binding of PFO. The evidence for this is the high cholesterol bind threshold of PFO combined with that thresholds dependence on the interaction of the other membrane constituent with cholesterol [19]. While cholesterol accessibility is necessary for PFO binding, the analysis of PFO derivatives with modifications on D4 revealed that sterol accessibility is not

sufficient to trigger stable PFO-membrane association [86]. As mentioned above, native PFO readily binds to model membranes containing 40 mol% cholesterol [and an equimolar mixture of other phospholipids, see 86], revealing that cholesterol is accessible at the membrane surface. However, the PFO^{C459A} derivative was not able to bind to the same membranes, clearly indicating that the cholesterol molecules were not sufficiently accessible to trigger toxin binding. Binding of the PFO^{C459A} derivative was recovered when the cholesterol concentration was increased past 45 mol%, suggesting that the affinity of this derivative for cholesterol is lower than that of native PFO, and more cholesterol was required at the membrane surface to trigger stable binding. In addition to this, Tweten et. al. recently mutated most of the amino acids in the loops of D4 to alanine and tested the mutation effect on the binding of PFO [98]. These mutations greatly affected the amount of protein that could bind to a model membrane both positively and negatively; this shows that the protein was not simply binding to accessible cholesterol. It is not clear how cholesterol accessibility varies with increasing amount of cholesterol in the membranes. For simplicity, I have represented this variation as a linear function of cholesterol concentration, (Fig. 1.4) however, cholesterol accessibility may have a non-linear dependence in these systems. Further investigations are required in this area to establish the precise mechanism of PFO-cholesterol interaction as a function of cholesterol accessibility.

1.6 Mutations in Domain 4 Affect the Cholesterol Threshold Required to Trigger Binding

Our lab has recently shown that by modification of the C459 reside in the binding domain of PFO, we were able to decrease the "cholesterol threshold" of a PFO derivative [86]. While PFO has long been put forth as a probe for cholesterol-rich membranes, the advent of new PFO derivatives with varied "cholesterol thresholds" adds a layer of selectivity to the cholesterol sensing measurements. The development of PFO derivatives with varied binding thresholds would allow for the detection of various grades of cholesterol accessibility.

CHAPTER 2

MODIFICATIONS IN PERFRINGOLYSIN O DOMAIN 4 ALTER THE THRESHOLD OF CHOLESTEROL CONCENTRATION REQUIRED FOR BINDING

The majority of this chapter is the result of collaboration and is taken from:

Benjamin B. Johnson, Paul C. Moe, David Wang, Kathleen Rossi, Bernardo L. Trigatti, and Alejandro P. Heuck (2012)"Modifications in Perfringolysin O Domain 4 Alter the Cholesterol Concentration Threshold Required for Binding" Biochemistry 51.16 (2012): 3373-3382.

2.1 Introduction

Among the most powerful tools to determine the localization and fluctuations of molecules, in the physiological context of intact living cells, are fluorescence microscopy and related techniques. Visualization of cholesterol molecules in membranes is only limited by the molecular probes available to directly determine cholesterol levels [99, 100]. Cholesterol-binding reagents such as filipin have been widely used to stain cholesterol in cell membranes [101],[102]. However, given the ubiquitous distribution of cholesterol in mammalian cells, membrane permeable filipin, as well as other cholesterol fluorescent analogs commonly employed as imaging probes, [2],[100] stain all membranes (i.e., plasma and inner membranes) independently of their cholesterol levels [103]. Clearly, better molecular probes could facilitate the detection of cholesterol levels in cell membranes and their fluctuation in response to metabolic signals and drug therapies.

Non-lytic derivatives of the cholesterol-dependent cytolysin (CDC) Perfringolysin O (PFO) have been used to detect cholesterol rich microdomains in cell membranes [104]. The sharp transition observed for PFO binding to model membranes containing increasing amounts of cholesterol suggests that the toxin could be used as a molecular probe to detect cholesterol levels on cell membranes. Unfortunately, the promise of PFO as cholesterol imaging probe is limited by the narrow spectra of cholesterol concentrations that can be discriminated by the native toxin.

We have recently found that the C459A modification of the membrane interacting domain of PFO D4 alters the cholesterol concentration threshold required for binding [105]. I reasoned that additional modifications may yield PFO derivatives that bind to membranes containing more or less cholesterol than the native toxin. By combining the tunable properties of PFO D4 with the many fluorescent probes available [99], it would be possible to generate imaging reagents capable of detecting a broad range of distinct cholesterol levels in cell membranes.

I have modified residues located in the proximity of Cys459 and these modifications resulted in an increase, or decrease, in the amount of cholesterol required to trigger PFO binding. We then demonstrated these varied cholesterol requirements on both model and cell membranes.

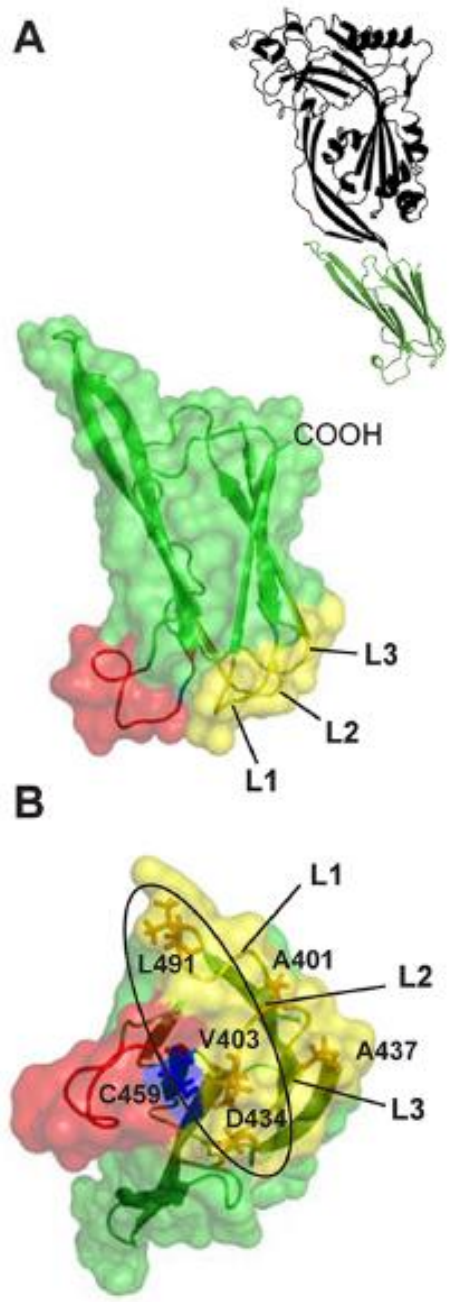

Figure 2.1 PFO D4 showing the location of residues modified in this study. A. Cartoon representation of the α-carbon backbone for PFO (upper right) with D4 showed in green, and for the α-carbon backbone and amino acids surface side-view of PFO D4. The conserved undecapeptide (red), the C459 (blue), the 3 loops (L1, L2, and L3) located at the tip of D4 (yellow) and the C-terminus are indicated. **B**. Bottom-view of the cartoon representation shown in A, with amino acids mentioned in the text shown as sticks and labeled. The central region containing mutations that affect the cholesterol threshold of the toxin is surrounded by an oval. The PFO D4 image was rendered in PyMol (DeLano Scientific).

Table 1: PFO Background Mutations Abbreviation

Table1: PFO Background Mutations Abbreviation	
	Mutations
nPFO	None, Wild Type
rPFO	C459A
FPFO	C459A-E167C-F318A
pPFO	C459A-E167C-F318A-Y181A

2.2 Results

2.2.1 The amount of cholesterol required to trigger PFO binding to a membrane is affected by amino acids located around the conserved Cys459.

The binding of PFO to model membranes is regulated by both the lipid composition of the membrane and the structure of the loops located at the distal tip of D4 (Fig. 2.1A). The presence of "free" cholesterol molecules at the membrane surface is required to trigger PFO-membrane association [19, 20, 39, 62]. However, how many of these "free" cholesterol molecules are required to trigger binding seems to be dictated by the structure of the D4 loops. Using POPC-cholesterol liposomes as model membranes, we have shown that the Cys459 to Ala substitution increased the threshold for cholesterol binding from 30 mol% to 35 mol% [20]. This was surprising because it has been shown that only the loop1 (L1), loop 2 (L2), and loop 3 (L3) in D4 mediate the specific interaction of PFO with cholesterol [83], with only two residues (Thr 490 and Leu491) being essential for cholesterol recognition [85]. It is clear from these data that the precise role of cholesterol in the cooperative cytolytic mechanism of PFO is far from being understood.

I first investigated if the phospholipid composition of the membrane affected the differential binding of native nPFO and the Cys-less rPFO, and second, if modifications to residues that are known to interact with the membrane upon PFO binding further affected the cholesterol binding threshold of the toxin [60]. The cholesterol content of the liposomes was varied from 25 mol% to 50 mol% and the phospholipid composition was fixed at a 1:1:1 molar ratio of POPC, POPE, and SM (the most abundant human plasma membrane phospholipids). In membranes containing just POPC:cholesterol, the cholesterol threshold for nPFO and rPFO binding are 40 mol% and 44 mol% cholesterol [20]. In membranes containing POPC, POPE, and SM, the cholesterol thresholds for nPFO and rPFO binding was 36.5 mol% and 41.5 mol% cholesterol, respectively. Interestingly, despite this both PFO derivatives showed a lower cholesterol threshold when using a more complex phospholipid mixture, the cholesterol mol% difference between the PFO derivatives remained constant (Fig. 2.2A).

Four mutants in the Cys-less rPFO derivative, L491C (in L1), A401C and V403C (in L2), and A437C (in L3) [Fig. 1, 60] were initially tested to evaluate the effect of D4 mutations on the cholesterol dependent binding of PFO. The pore forming activity of these derivatives is similar to that of nPFO when measured using liposomes containing high cholesterol [60]. Two of the analyzed mutants, $rPFO^{L491C}$ and $rPFO^{V403C}$ showed a 4-5 mol% increase in the cholesterol concentration required to trigger binding (Fig. 2.2A). No major change was observed for the A437C mutant and a minimal change for the A401C substitution. A close inspection of the structure of the D4 distal tip shows that the Leu491 and

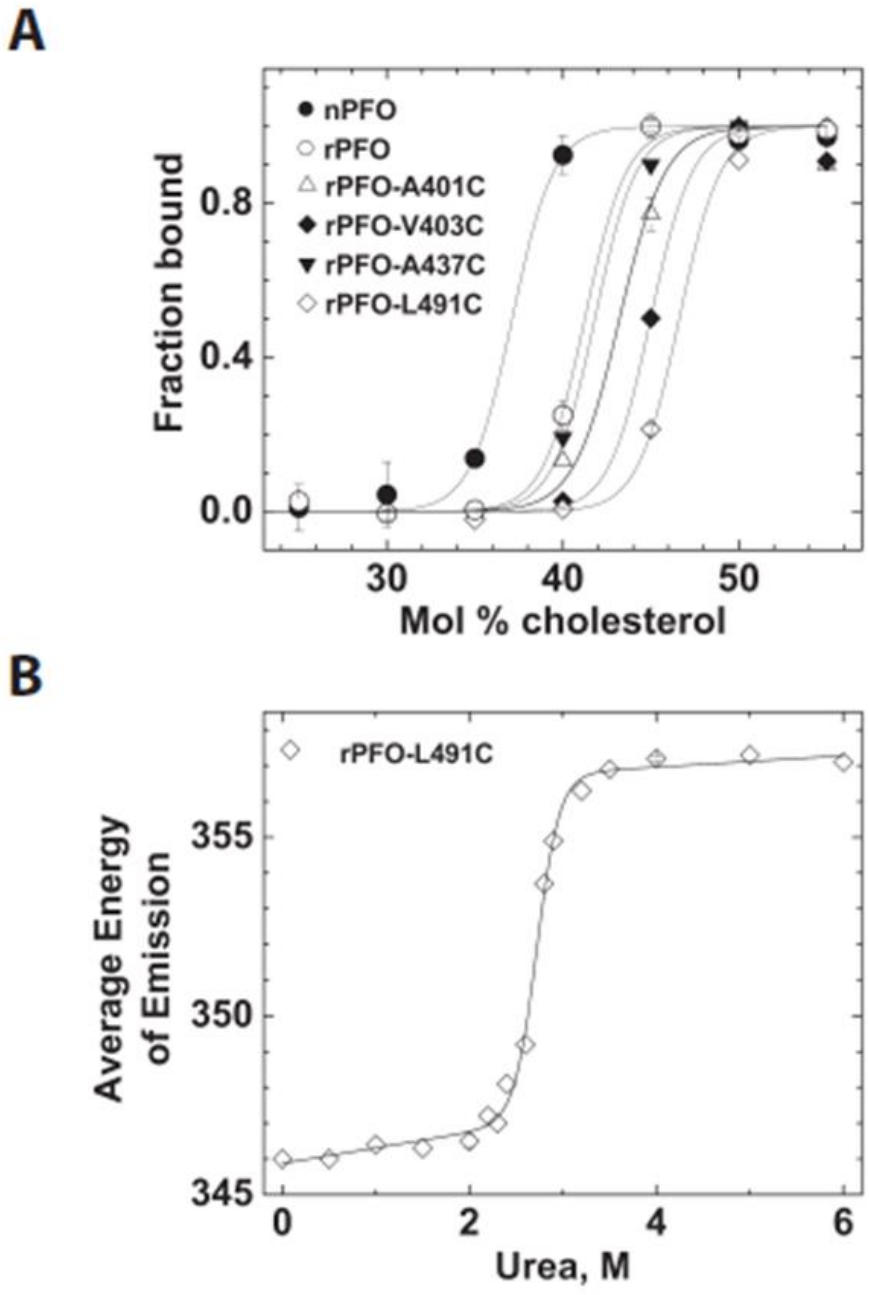
A
nPFO
rPFO
rPFO-A401C
rPFO-V403C
rPFO-A437C
rPFO-L491C
Fraction bound
0.0
0.4
0.8
30
40
50
Mol % cholesterol
B
rPFO-L491C
Average Energy of Emission
345
350
355
0
2
4
6
Urea, M

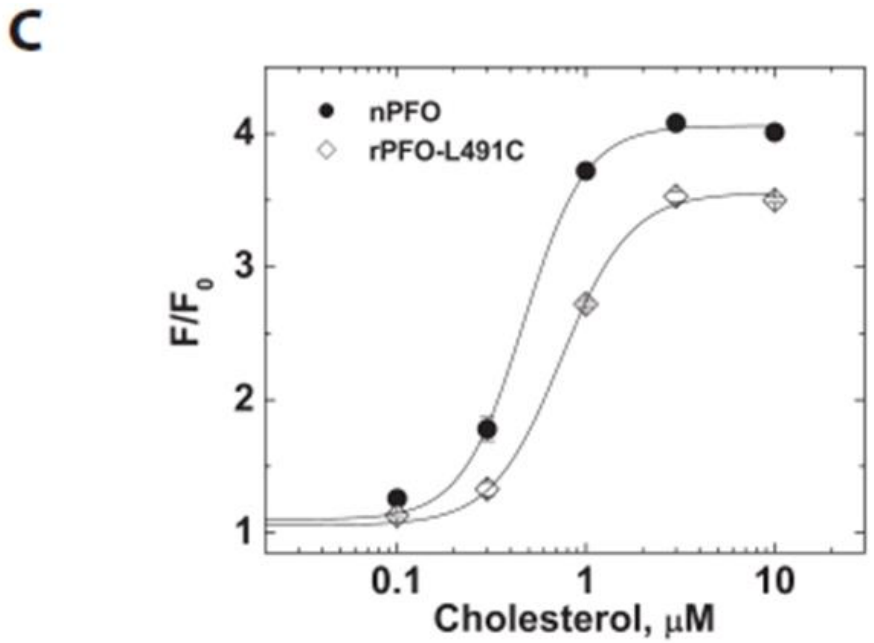

Figure 2.2 Mutations on D4 alter the cholesterol threshold of PFO. **A**. The fraction of bound PFO derivatives (0.1 μM final concentration) to liposomes of varying cholesterol content and POPC, POPE and SM in a constant 1:1:1 ratio (0.1 mM total lipid final concentration) was determined using intrinsic Trp fluorescence as described in experimental procedures. The cholesterol threshold for both nPFO and rPFO were lower than the ones observed with POPC:cholesterol (28), but the difference in the cholesterol threshold (~5 mol% cholesterol) was not significantly affected by the change on the phospholipid composition of the membrane. More than 4 mol% increase in the cholesterol threshold was observed for the $rPFO^{V403C}$ and $rPFO^{L491C}$ mutants. **B**. Urea denaturation for $rPFO^{L491C}$, the derivative with the highest cholesterol threshold. The average energy of emission for each fluorescence emission spectrum was obtained at given urea concentrations. The data were fitted assuming that the average energy of emission of the folded and unfolded states varies linearly with urea concentration. **C**. Binding of nPFO (filled circles) and $rPFO^{L491C}$ (open diamonds) to cholesterol dispersed in aqueous buffer solution. Trp emission intensity for 0.1 μM protein was measured as described in experimental procedures before (F0) or after (F) addition of the indicated amount of cholesterol. Most data points show the average of at least two independent measurements and their range.

Val403 residues are proximal to Cys459 (Fig. 2.1B), while the A401 and A437 are more distant from the undecapeptide. To evaluate the potential effect of D4 mutations on the conformational stability of the protein we determined the free energy for the unfolding of $rPFO^{L491C}$, the protein with the highest cholesterol threshold, using equilibrium urea denaturation [Fig. 2B, 20]. No significant difference on the $\Delta G_{U\text{-}F}{}^{water}$ was observed between the rPFO and $rPFO^{L491C}$ mutant [13.6 ± 1.5 kcal mol^{-1} [20] and 13.2 ± 1.6 kcal mol^{-1}, respectively]. These results suggest that mutations that altered the cholesterol threshold of rPFO did not affect the stability of the toxin. Moreover, nPFO, and $rPFO^{L491C}$ bound similarly to cholesterol dispersed in aqueous buffer (Fig. 2C) [62], suggesting that the change in the cholesterol threshold is not related to the ability of the proteins to bind cholesterol. The lower maximum F/F_0 observed for $rPFO^{L491C}$ is typical for PFO derivatives containing the Cys459 to Ala mutation, which have higher F_0 [20].

2.2.2 A standard scale to evaluate binding properties of PFO mutants.

The changes in the intrinsic Trp fluorescence that follows membrane binding of PFO derivative have been effectively used to determine the fraction of protein bound as a function of cholesterol concentration [19-21, 26, 62]. The step-like increase on Trp emission intensity for PFO derivatives occurred at a precise cholesterol concentration (Fig. 2.2A). Each PFO derivative is therefore characterized by a cholesterol threshold defined as the cholesterol concentration at which the increase in Trp emission is half of the emission when binding is complete. Since the absolute cholesterol threshold (mol%) depends on the lipid

composition of the membranes (see above) and there are small variations in the cholesterol concentration among identically prepared liposome batches (~5 mol% in our hands), it is convenient to define a relative value for the cholesterol threshold rather than an "absolute" value. The difference in the cholesterol threshold (Δmol% cholesterol obtained with the same membranes) between nPFO and the PFO mutant under study is a more robust parameter to characterize the cholesterol binding properties of PFO derivatives. A negative value of Δmol% cholesterol indicates a derivative that binds at lower cholesterol concentrations than nPFO, and a positive value indicates that higher cholesterol concentrations are required for binding. For example, we previously found that rPFO required more cholesterol than nPFO for membrane binding [20]. Using the above defined relative scale the corresponding Δmol% cholesterol for rPFO is +3.6. The absolute cholesterol threshold value for any PFO derivative can be calculated using the Δmol% cholesterol data if the value for nPFO is known for a particular membrane system. Therefore, I determined the cholesterol threshold for nPFO by quantification of the lipid composition of liposomes containing 1:1:1 POPC:POPE:SM and various amounts of cholesterol (Fig. 2.3A). The cholesterol threshold of nPFO was 36.5 ± 1 mol% cholesterol for this membrane system.

2.2.3 Mutations on D4 can increase or decrease the Δmol% cholesterol of PFO derivatives.

Our ultimate goal is to obtain probes that differentially bind to cellular membranes containing different cholesterol levels. We therefore introduced single amino acid mutations into PFO D4 using the parental rPFO$^{E167C\text{-}F318A}$ derivative

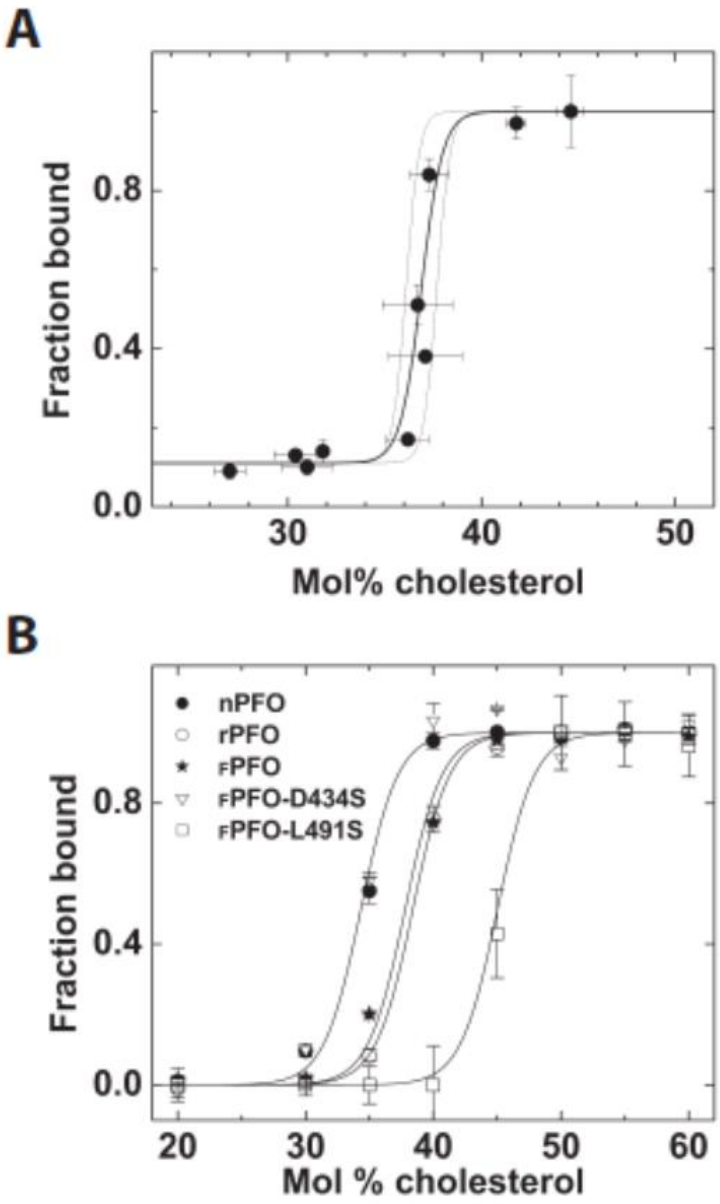

Figure 2.3 Cholesterol thresholds in PFO derivatives can differ up to 10 mol% cholesterol. A. Determination of the cholesterol threshold for nPFO (200 nM final concentration) on POPC:POPE:SM membranes containing the indicated mol % of cholesterol (100 µM total lipids final concentration). The mol % of cholesterol was determined by individual quantification of cholesterol and total phospholipids. Cholesterol was quantified using Amplex® Red and total phospholipids by phosphate determination after acid hydrolysis as described in section 2.4.7. Thin lines are a guide for the eye to indicate average range for data in the transition. **B.** Cholesterol dependent binding of $_{F}PFO^{D434S}$ (open triangles) and $_{F}PFO^{L491S}$ (open squares) derivatives selected for cellular studies compared to nPFO (filled circles), rPFO (open circles), and FPFO (filled star). Binding measurements were done as indicated in Fig. 2.2 Data points are the average of at least two measurements and their standard deviation.

(hereafter named FPFO). The F318A mutation renders a protein that oligomerize on liposomal membranes but is not lytic at 1/1000 protein/total-lipid ratio concentrations [59], and increases by more than 20-fold the magnitude of toxin required to cause 50% hemolysis in sheep red blood cells (Fig. 2.4). The E167C mutation introduces a unique site for labeling with a fluorescent or other probe of choice, and this modification does not affect the properties of the toxin[56, 62]. We first evaluated the cholesterol threshold for the parental $_{F}$PFO derivative, which contains the same D4 as rPFO. The Δmol% cholesterol for $_{F}$PFO was +3.2 ± 0.5, very similar to that observed for rPFO (Fig. 2.3B). This result clearly indicated that neither the F318A mutation in D3, nor the E167C mutation in D1, affected the cholesterol binding properties of the toxin. Our next goal was to scan the D4 loops for mutations that reduced or increased the cholesterol threshold of $_{F}$PFO.

The first candidate to decrease the cholesterol threshold was the charged D434 residue located in L3 of PFO D4. The negatively charged Asp was modified to Ser, a non-charged amino acid that can form hydrogen bonds with the polar groups of the lipids at the membrane surface. The Δmol% cholesterol for the $_{F}$PFO^{D434S} decreased ~3 units, rendering a derivative with a lower cholesterol threshold than the parental $_{F}$PFO derivative and very similar to the one for nPFO (Fig. 2.3B).

With the goal of increasing the cholesterol threshold of $_{F}$PFO derivative to higher cholesterol concentrations we targeted the L491 residue because it has been shown that the L491A mutation decreased PFO binding as determined using

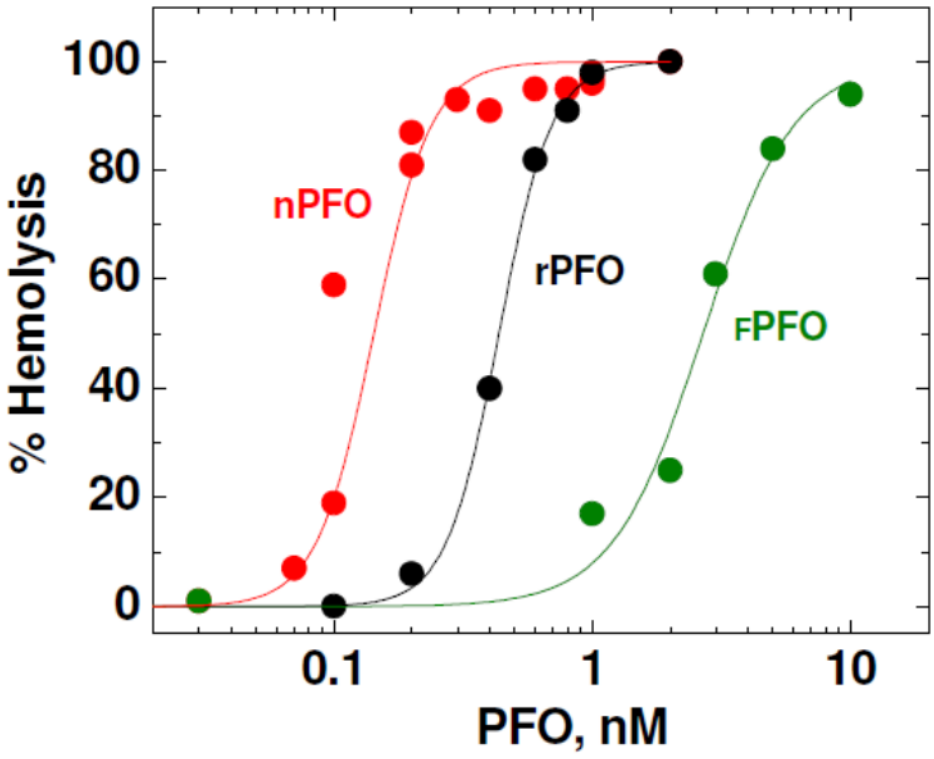

Figure 2.4 Percentage of hemolysis of sheep red blood cells for PFO derivatives as a function of protein concentration. Washed sheep red blood cells (RBC) were exposed to the indicated concentration of FPFO(●), rPFO(●), and nPFO(●), with addition of BSA to maintain overall protein levels. This mixture was then incubated for 30 minutes at 37°C. Unlysed RBC were removed by centrifugation. The extent of hemoglobin release was quantified by measuring the absorbance of the supernatants.

surface plasmon resonance [85]. We replaced the hydrophobic Leu for the more polar residue Ser generating the FPFOL491S derivative. As expected, FPFOL491S showed a cholesterol threshold seven units higher than the parental FPFO (Fig.2.3B). Both $_{F}PFO^{D434S}$ and $_{F}PFO^{L491S}$ were selected for cellular studies because the cholesterol threshold between them differ more than 10 mol % cholesterol.

2.2.4 Cholesterol was essential for PFO binding to murine macrophages-like cells.

We tested if the binding of the parental $_{F}PFO^{Alexa488}$ derivative was dependent on cholesterol at the surface of the plasma membrane of murine macrophage-like cells (RAW 264.7) using two independent assays. First, we incubated RAW 264.7 cells with filipin to block cholesterol at the membrane surface [36, 106, 107]. While filipin fluorescence was seen both at the cell surface, as well as intracellularly, (Fig. 2.5A), $_{F}PFO^{Alexa488}$ was found only at the surface of untreated murine macrophage-like cells. In contrast, when cells were first treated with filipin no significant binding of $_{F}PFO^{Alexa488}$ was detected on the cell surface (Fig. 2.5A). Cholera toxin subunit B associates with lipid rafts in plasma membranes by binding to the ganglioside, GM1 in a cholesterol independent manner [108]. Labeling of cells with $CTxB^{Alexa594}$ was not affected by filipin treatment, demonstrating that filipin treatment did not disrupt the plasma membrane but specifically blocked $_{F}PFO^{Alexa488}$ binding. Second, we tested the cholesterol dependence of $_{F}PFO^{Alexa488}$ binding to RAW 264.7 cells by removing cholesterol from the membrane surface using incubation with mβCD [109]. Cells were incubated with 0.05 mM, 0.5 mM, or 5 mM mβCD for 3 h at 37 ^{o}C. Treatment of

cells with 0.5 mM or higher mβCD concentrations prevented labeling with $_{F}PFO^{Alexa488}$, whereas treatment with 0.05 mM (Fig 2.5B) or lower concentrations had no apparent effect (data not shown). In contrast, mβCD treatment of cells did not affect the extent of $CTxB^{Alexa594}$ binding. It is clear from these data that binding of $_{F}PFO^{Alexa488}$ to RAW 264.7 cells membranes was dependent on the presence of cholesterol and regulated by the cholesterol levels at the membrane surface.

2.2.5 The sensitivity of PFO mutants for cholesterol concentration was conserved on RAW 264.7 cells membranes.

The cholesterol content of the cell membranes can be altered by incubations with mβCD or mixtures of mβCD:cholesterol [109]. Incubations with mβCD alone or with high mβCD:cholesterol ratios reduce the cholesterol concentration on the plasma membrane. In contrast, incubation with low mβCD:cholesterol ratios increase the cholesterol content of the cells [106, 110]. We therefore incubated RAW 264.7 cells with 2.5 mM mβCD alone or with mixtures of 2.5 mM mβCD:cholesterol at ratios ranging from 20:1 to 3:1 in order to decrease and increase the normal levels of cholesterol in the plasma membrane (Fig. 2.6). Binding of $_{F}PFO^{Alexa488}$ was not observed in cells treated with mβCD alone (as in Fig 2.5B), or with a mβCD:cholesterol ratio of 20:1 (Fig. 2.6). Cells treated with a mβCD:cholesterol ratio of 15:1 were labeled faintly (slightly less than untreated cells) by $_{F}PFO^{Alexa488}$. In contrast, treatment of cells with mβCD:cholesterol ratios of 8:1 or lower resulted in substantially more labeling with $_{F}PFO^{Alexa488}$.

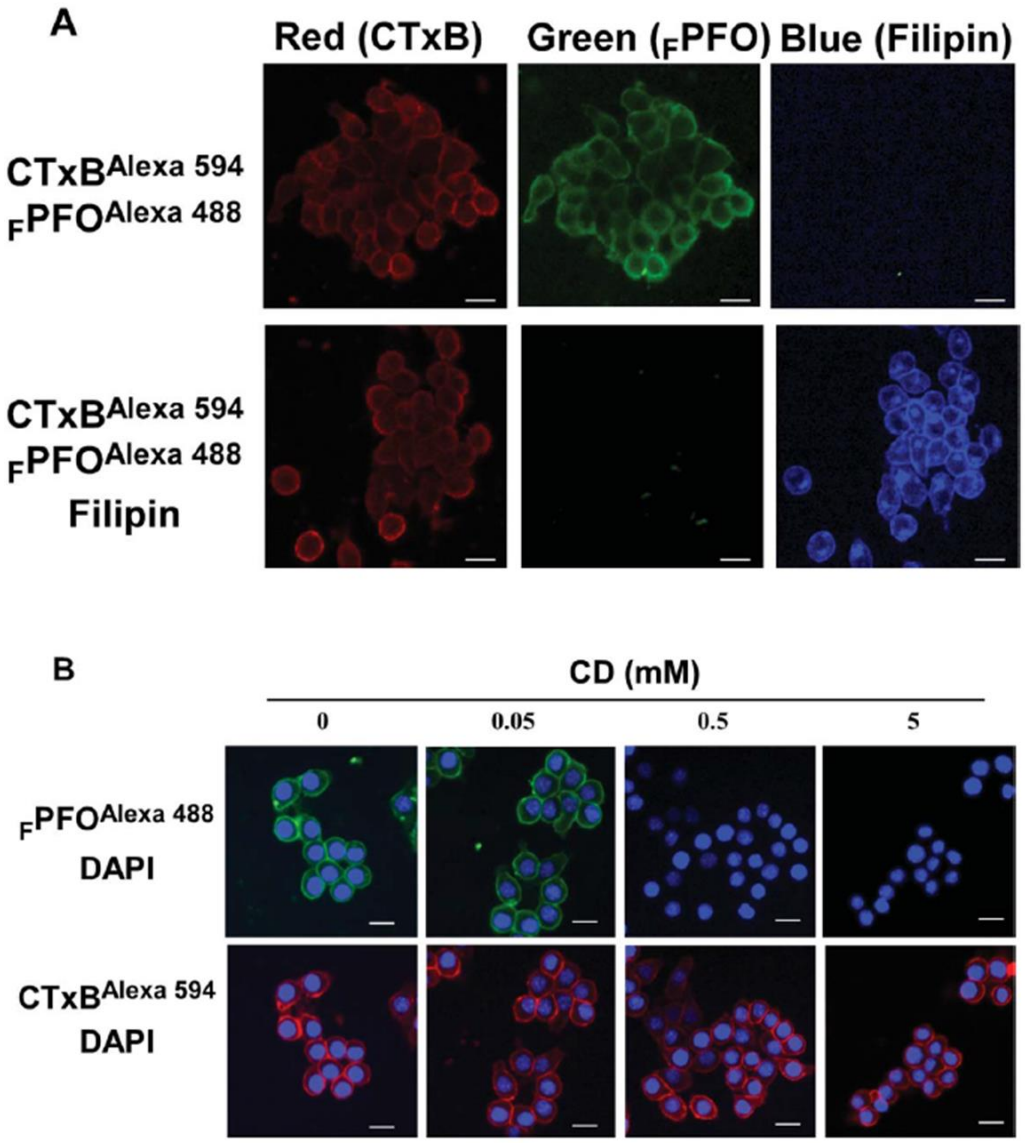

Figure 2.5 Cholesterol modulates $_{F}$PFO binding to RAW 264.7. **A**. Filipin blocks $_{F}$PFO^{Alexa488} binding to the cell surface. Fixed RAW 264.7 murine macrophage-like cells were incubated without (top row) or with 7.6 µM filipin (bottom row) for 60 min at 20-23 ^{o}C. Cells were washed and incubated with $_{F}$PFO^{Alexa488} (40 nM) and CTxB^{Alexa594} (5 µg/mL) (the latter as a marker for the cell surface). **B.** Depletion of cholesterol using mβCD inhibits $_{F}$PFO^{Alexa488} binding. Cells were treated for 2 h without (panels marked "0") or with the indicated amount of mβCD. Cells were then fixed and incubated with $_{F}$PFO^{Alexa488} and CTxB^{Alexa594} for 90 min, and then stained with DAPI for nuclear DNA as described in experimental procedures. Labeled cells were imaged by wide field fluorescence microscopy using standard filter sets for TRITC ("Red" CTxB labeling), FITC ("Green", $_{F}$PFO^{488Alexa}), or DAPI ("Blue", filipin labeling in A, DAPI labeling in B). Scale bars represent 10 µm.

The FPFOD434S-Alexa633 derivative was bound to the plasma membrane even when cells were treated with m□CD alone, suggesting that the cholesterol dependent properties of PFO derivatives observed with model membranes are conserved on natural membranes (i.e., RAW 264.7 cells). A slight increase in ratio of 20:1, and more than two fold increase when cells were treated with ratios of 15:1 or lower. Interestingly, untreated cells did not significantly bind the $_{F}PFO^{L491S\text{-}Alexa488}$ derivative, suggesting that the cholesterol availability in these cells is lower than the one obtained in model membranes with 50 mol% cholesterol. Binding of this derivative was observed only on cells overloaded with cholesterol using the lowest mβCD:cholesterol ratios (Fig. 2.6). Taken together, our data clearly indicate that engineered PFO derivatives (e.g., $_{F}$PFO) could be tuned to associate with cellular membranes containing different cholesterol levels.

2.3 Discussion

My studies on the role of the membrane interacting domain of PFO showed that mutations in amino acids located in the proximity of the conserved Cys459 modulated the threshold of cholesterol required to trigger toxin-membrane association. Cholesterol was required at the plasma membrane for PFO binding to RAW 264.7 cells as determined by both filipin inhibition, and cholesterol depletion using mβCD. The cholesterol-dependent properties of PFO derivatives were consistent on model as well as natural membranes, and not significantly affected by the lipid composition. Mutations of conserved residues increased or decreased the cholesterol threshold for PFO binding, suggesting that

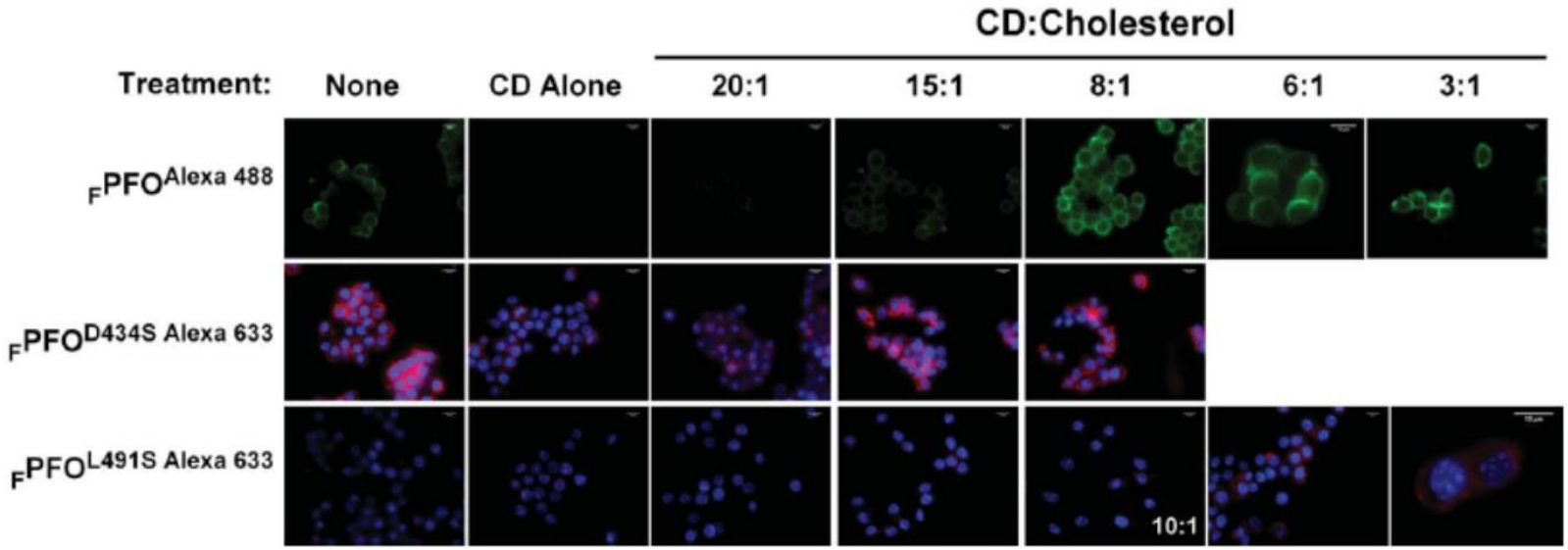

Figure 2.6 Different cholesterol levels are distinguished by PFO derivatives on murine macrophage-like cells membranes. RAW 264.7 cells were incubated for 3 h at 37 ºC either with no additions (panels marked "None"), 2.5 mM mβCD alone, or with 2.5 mM mβCD complexed with cholesterol at the indicated mβCD:cholesterol ratios. After 3 h, cells were washed, fixed, and incubated with 38 nM of either $_{F}PFO^{Alexa\ 488}$ (top row), $_{F}PFO^{D434S\ Alexa\ 633}$ (middle row) or $_{F}PFO^{L491S\ Alexa\ 633}$ (bottom row). Cells labeled with $_{F}PFO^{D434S\ Alexa\ 633}$ or $_{F}PFO^{L491S\ Alexa\ 633}$ were also incubated with DAPI (middle and bottom rows). Cells treated with mβCD:cholesterol ratios of 6:1 and 3:1 were not incubated with $_{F}PFO^{D434S\ Alexa\ 633}$ (middle row). Scale bars represent 10 μm.

PFO has evolved to recognize optimal cholesterol accessibility on cell membranes. High levels of cholesterol are required in model membranes to trigger binding of PFO and other related CDCs [26, 78-80]. Similar high-cholesterol dependent effects have been observed for the enzymatic activity of cholesterol modifying enzymes [e.g., cholesterol oxidase, 111, 112] and for the rate of removal of sterols from the membrane surface by cyclodextrins [16, 113]. The high cholesterol levels needed for these membrane processes has been related to the tight interaction of cholesterol molecules with surrounded phospholipids [114, 115]. Cholesterol becomes accessible at the membrane surface only after the sterol-phospholipid interaction is saturated [116, 117]. The interactions of cholesterol with phospholipids make the phospholipid-sterol mixtures in membranes non-ideal, and therefore the thermodynamic parameter that more precisely relates to the cholesterol concentration with the accessibility of sterol molecules at the membrane surface is the chemical activity. Cholesterol accessibility is influenced by changes in the length and saturation of the acyl chains of the phospholipids present in the membrane, as well as by the size of the phospholipid head groups [22]. Given that the levels of cholesterol on the plasma membrane seem to be tightly regulated [32, 118], it is not unexpected that PFO has evolved to maximize the recognition of a particular cholesterol accessibility [39].

PFO contacts the target membrane via D4 [26], the loops at the bottom of the beta sandwich being the only segments of this domain that remain membrane inserted after oligomerization [Fig. 1, 60]. Comparison of the sequences for 28

CDC family members shows that the conserved undecapeptide (458-468, PFO sequence), L1 (488-493) and L2 (398-406) contain five, four, and four invariable residues, respectively [39]. The less conserved L3 (434-439) has no invariable residues. Multiple mutagenesis studies have shown that residues located in the undecapeptide , especially the conserved Trp residues, are very important for pore-formation [reviewed in 119], and this undecapeptide was initially considered the cholesterol binding site of the CDCs. However, it has been shown that the L1-L3 loops are responsible for the interaction of PFO with cholesterol containing membranes [83]. More recently, it has been suggested that only two invariable residues located in L1 are essential for cholesterol recognition: Thr 490 and Leu 491 [85]. While it is clear that the side chain of T490 and L491 are critical for cholesterol binding, direct cholesterol interaction with these two residues has not been shown. It may be possible that these two mutations affected a membrane-dependent conformational transition required for cholesterol interaction, and not the interaction with cholesterol itself. Moreover, the analysis of other invariable residues located in L1 (Gly488 and Pro493), and in L2 (H398, G400, and A404) has not been done, and therefore the exact location of a cholesterol binding site (if any) deserves further characterization. We have shown here either the mutation of L491 (a putative cholesterol binding residue) or V403 (not previously related to cholesterol interaction) significantly altered the cholesterol threshold for PFO binding. Surprisingly, none of these residues affected PFO binding or pore-formation at high cholesterol concentration (Fig. 2.2). A similar effect was previously found for the C459A mutation in the undecapeptide [Fig. 2A, 20].

Moreover, elimination of the negative charge of Asp434 located in the poorly conserved L3 segment decreased the cholesterol threshold for PFO (Fig. 2.3B). It is therefore clear that the nature of amino acids located in D4 loops modulates the cholesterol accessibility required to trigger toxin binding, with residues located around the conserved Cys459 being the ones that affected the cholesterol threshold the most (Fig. 2.1B). In addition to single amino acid substitutions, changes that are likely to affect the conformation of the protein, like the pH of the medium, also alter the cholesterol threshold for toxin binding [18, 89]. Taken together, these data strongly suggest that the conformation of the PFO D4 dictates the cholesterol accessibility required to trigger toxin binding. The importance of sensing an optimal cholesterol chemical activity is reflected in the highly conserved amino acid sequences at the membrane interacting loops of the CDCs.

Another important characteristic of PFO binding to cholesterol containing membranes is the typical step-wise increase that in our experiments was detected by the intrinsic Trp fluorescence change that follows the exposure of the aromatic residues to the membrane surface [18, 21, 26, 95]. This membrane-dependent fluorescence change constitutes an efficient approach to determine PFO binding (Fig. 2.3A). The association of PFO with membranes can also be detected by the formation of SDS-resistant oligomers using SDS-PAGE [18, 21, 48, 65]. Both approaches have independently shown PFO transition from no binding to complete binding in a very narrow window of cholesterol concentrations. In agreement with these results, we have shown, using simultaneous determinations of PFO binding and pore-formation, that the cholesterol-dependent response is

regulated during the initial binding step of the toxin [20]. The molecular basis for this sharp cooperative cholesterol-dependent PFO binding remains unknown. It has been suggested that either a sharp change in the cholesterol chemical activity or oligomerization preceded by a reversible PFO-cholesterol equilibrium may be responsible for the sharp change in the binding profile [21]. Similar binding profiles have been observed on membranes containing different levels of cholesterol (e.g., plasma membrane or ER membranes), indicating that similar cholesterol accessibilities can be obtained on membranes with very different cholesterol concentrations [21]. Independent of the mechanism, the effect on the cholesterol threshold for PFO binding observed when the phospholipid composition is modified, indicates that the cholesterol accessibility plays a critical role on the initial PFO-membrane interaction [18-20]. This cholesterol-dependent transition has been used to image membranes containing high cholesterol [120-122]. Originally, it was suggested that PFO binds exclusively to cholesterol rich domains or membrane rafts [123, 124]. However it has become clear that PFO binding and membrane localization is not limited to the presence of a particular membrane domain [18-20, 62, 81]. Therefore, we reasoned that by combining the sharp on/off membrane association properties of PFO with the ability to alter the cholesterol binding threshold of the toxin would provide unique tools to study and clarify the cholesterol dependent binding mechanism of PFO to cellular membranes.

Using site-directed mutagenesis we modified D4 of $_{F}$PFO and obtained two derivatives, $_{F}PFO^{D434S}$ and $_{F}PFO^{L491S}$, each showing a distinctive cholesterol

dependent profile on model membranes. Binding of $_{F}$PFO^{D434S} required ~3 mol% less cholesterol than $_{F}$PFO, while binding of $_{F}$PFO^{L491S} required ~7 mol% more cholesterol than the parental $_{F}$PFO derivative (Fig. 2.3B). Based on the cholesterol dependent response obtained for $_{F}$PFO on RAW 264.7 cells (Fig. 2.4), we determined if the differential binding properties of the proteins were conserved when using cellular membranes. In contrast to model membranes, the distribution and availability of cholesterol on cellular membranes could be affected by many factors, including membrane traffic, synthesis and modifications of lipids, presence of membrane proteins, and/or the association of the membrane with the cytoskeleton [125, 126]. The availability of cholesterol on the plasma membrane of these cells was varied using incubations with mβCD alone or different mβCD:cholesterol mixtures [110]. The amount of mβCD was maintained constant at 2.5 mM in all assays to account for any non-specific effect that this compound may have on membranes (e.g., removal of other lipids). Interestingly, similar cholesterol dependent properties were observed for PFO derivatives on biological membranes. Only $_{F}$PFO and $_{F}$PFO^{D434S} interacted with RAW 264.7 cells (Fig. 2.6). No significant binding of $_{F}$PFO^{L491S} was detected on RAW 264.7 cells unless the cells were treated with the lowest mβCD:cholesterol ratios (i.e., the highest cholesterol levels achieved with this procedure). In contrast, $_{F}$PFO^{D434S} was bound to cells treated with mβCD alone (i.e., the lowest cholesterol level achieved). Based on the brighter spots observed along some faint outlines of the plasma membrane, we can speculate that there is heterogeneity in the distribution of cholesterol in the plasma membrane. As observed with model membranes, the

binding properties of the parental $_{F}$PFO derivative on the membranes of RAW 264.7 cells were intermediate when compared with the properties observed for $_{F}$PFO^{D434S} and $_{F}$PFO^{L491S} (Fig. 2.6).

In summary, we have shown here that modifications on PFO D4 altered the cholesterol binding properties of the toxin. Moreover, engineered PFO derivatives differentially bind to model and biological membranes containing different cholesterol levels. The plasticity of the PFO-cholesterol interaction combined with engineered PFO derivatives will allow us and others to create novel molecular probes to study cholesterol distribution and dynamics on cellular membranes.

2.4 Methods

2.4.1 Preparation of PFO Derivatives

The expression and purification of the PFO derivatives were done as described previously [19, 127, 128]. The PFO derivative containing the native sequence (amino acids 29−500) plus the polyhistidine tag that came from the pRSETB vector (Invitrogen) is named nPFO [19]. The PFO Cys-less derivative (nPFO^{C459A}, where Cys459 is replaced by Ala) is named rPFO [128]. The single-Cys lysis-impaired parental derivative used in this study (rPFO$^{E167C\ -F318A}$) was named $_{F}$PFO. The E167C mutation on domain 1 (D1) provides a site for specific probe attachment [56], and the F318A mutations on D3 eliminate the lytic activity of the toxin on liposomes [66]. Mutagenesis of PFO was done using the QuickChange (Stratagene) procedure as described previously [129].

2.4.2 Steady-State Fluorescence Spectroscopy

Steady-state fluorescence measurements were taken using a Fluorolog-3 photon-counting spectrofluorometer as described previously [105]. Samples were equilibrated at 25 ^{o}C before fluorescence determinations.

2.4.3 Assay for Binding

Binding to liposomes was done using the change in the Trp emission intensity produced by the binding of PFO to cholesterol containing membranes as described previously [105]. Briefly, emission for Trp fluorescence was recorded at 348 nm (4 nm bandpass) with the excitation wavelength fixed at 295 nm (2 nm bandpass). The signal of monomeric PFO derivatives were obtained with samples containing 200 nM protein in buffer A (HEPES 50mM, NaCl 100mM, DTT 1mM, EDTA 0.5mM, pH 7.5) using 4 mm x 4 mm quartz cuvettes [130]. The net emission intensity (F_0) for monomers was obtained after subtracting the signal of the sample before the protein was added. Liposomes were added (~200 μM total lipids) and the samples were incubated 20 min at 37^{o}C. Trp emission after membrane incubation was measured after re-equilibration of the sample at 25 ^{o}C, and the signal from an equivalent sample lacking the protein was subtracted (F). Fraction of protein bound was determined as $(F-F_0)/(F_f-F_0)$, where Ff is the emission intensity when all the protein is bound. Binding of PFO derivatives to cholesterol dispersions in aqueous solutions was done as described previously [127].

2.4.4 Urea unfolding equilibrium studies

Unfolding was done as described previously [105]. The conformational stability of the proteins ($\Delta G_{U\text{-}F}^{water}$), was calculated assuming a two-state unfolding model for the PFO monomers.

2.4.5 Fluorescent protein labeling

Fluorescent labeling was done as previously described [66],[131]. Maleimide derivatives of Alexa 488 or 633 were mixed with the PFO derivative of interest and incubated at room temperature for 2 h in buffer B (50 mM HEPES, 100 mM NaCl, pH 8). Labeled PFO was separated from free dye by using size exclusion chromatography using Sephadex G-25 [1.5 cm (I.D.) x 25 cm column].

2.4.6 Preparation of Lipids and Liposomes

Non-sterol lipids were obtained from Avanti Polar Lipids (Alabaster, AL), and cholesterol was from Steraloids (Newport, RI). Large unilamellar vesicles were generated as described previously [132]. Briefly, equimolar mixtures of 1-palmitoyl-2-oleoyl-sn-glycero-3-phosphocholine (POPC), 1-palmitoyl-2-oleoyl-sn-glycero-3-phosphoethanolamine (POPE), and sphingomyelin (SM, porcine brain), were combined with the indicated amount of cholesterol (5-cholesten-3β-ol) in chloroform. The thin film of lipids formed after chloroform evaporation was resuspended in buffer A and passed through an extruder equipped with 0.1 μm filter 21 times. Liposomes were stored on ice and discarded after three weeks.

2.4.7 Lipid determination

The percentage of cholesterol in liposomes used in Fig. 2.3A was determined using the Amplex® Red Cholesterol Assay Kit (Invitrogen). Total phosphate quantification assay as described in Chen et al. [133]. Briefly, the lipid

samples (30 µL) were added to a mixture of 0.45 mL of 8.9 M sulfuric acid and 0.15 mL of hydrogen peroxide (30 % v/v) and heated at 200-215 °C for 30 min. The sample is then allowed to cool down for 5 min at 20-23 °C and 3.9 mL of water, 0.5 mL of ammonium molybdate 20 mM, and 0.5 mL of ascorbic acid 0.57 M were added and mixed after each addition. Samples were then heated at 100 °C for 5 min and the absorbance at 800 nm was determined after equilibration at 25 °C. Readings were then compared to a standard curve obtained in parallel with samples of potassium phosphate of known concentrations to determine the concentration of individual samples. The mol% cholesterol in each sample was calculated as total cholesterol/(total phosphate + total cholesterol). For other experiments the concentration of lipids was calculated using the concentration of stock solutions (usually between ± 3% of measured concentrations).

2.4.8 Preparation of cyclodextrin complexed with cholesterol

Methyl-β-cyclodextrin (mβCD) and cholesterol were from Sigma-Aldrich Canada Ltd (Oakville, ON, Canada). mβCD: cholesterol complexes were prepared as described by Christian et al. [134]. Briefly, cholesterol dissolved in chloroform:methanol (1:1 by volume) was transferred to a glass tube and the solvent was evaporated under N2 gas passed through a 0.2 µm syringe filter. mβCD (2.5 mM in Dulbecco's modified Eagle's medium) was added to the cholesterol residue to the desired molar ratio of mβCD:cholesterol. Cholesterol was dissolved by sonication for 30 min in a bath sonicator, followed by mixing overnight at 37 ºC. Samples were sterilized by passage through 0.45 µm syringe filters and used immediately thereafter. All procedures were performed in glass.

2.4.9 Cell culture

All reagents for cell culture were from Life Technologies Inc (Burlington, ON Canada). RAW 264.7 murine macrophage-like cells were cultured in Dulbecco's modified Eagle's medium containing 10 % fetal bovine serum (heat inactivated), 2 mM L-glutamine, 50 units/mL penicillin and 50 µg/mL streptomycin. Cells were passaged when they reached 75% confluence by gentle scraping and plated at 1:5 in fresh media. Prior to each experiment, 3x105 cells were seeded into each well of 8-well Nunc LabTek Chambered Coverglass (Thermo Scientific) and cultured for 24 h.

2.4.10 Treatment of cells, labeling, and fluorescence microscopy

Cells were treated for 1-3 h at 37 °C with media containing either filipin (5 µg/mL; Sigma-Aldrich Canada Ltd, Oakville, ON, Canada), mβCD (at the concentrations indicated), 2.5 mM mβCD complexed to cholesterol at different mβCD:cholesterol ratios, or with no additions. Cells were then washed twice with PBS [KH_2PO_4 0.88 mM, Na_2HPO_4 6.4 mM, NaCl 136.8 mM, KCl 2.7 mM, pH 7.4 (PBS) supplemented with 1mM CaCl2], fixed for 30 min at 23-25 °C with 2.5% paraformaldehyde (freshly made in PBS), and washed twice with PBS. Cells were incubated with fluorescently labeled PFO derivatives (38 nM in PBS containing 1 mg/mL bovine serum albumin) as indicated, for 90 min at 37°C. In some experiments, cholera toxin subunit B (CTxB) labeled with Alexa 594 (5 µg/ml; Life Technologies Inc, Burlington ON Canada) was included in the incubation. Cells were then washed once with PBS at 23-25 oC and for some experiments cells were stained with DAPI (4',6-diamidino-2-phenylindole, 300 nM, 1 min in PBS at 20-23°C; Life Technologies Inc, Burlington ON Canada).

Cells were washed another three times with PBS at 23-25 °C and cPBS containing 0.5 mM ascorbic acid (Sigma Chemical Co, St Louis, MO) was added. Cells were immediately imaged by wide-field fluorescence microscopy using either a Zeiss Axiovert 200 M or a Leica DMI 6000B fluorescent microscope.

2.4.11 Hemolysis assay

Washed sheep RBC were suspended in buffer 10 mM sodium phosphate, 1.74 mM potassium phosphate, 137 mM NaCl, 2.7mM KCl, pH 7.4 to 0.5 %. PFO of varied concentration was then added to 685 μL of the RBC suspension in addition to BSA to maintain overall protein levels. This mixture was then incubated for 30 min at 37°C [129]. Unlysed RBC were removed from samples by centrifugation at 6000g for 5 min. The extent of hemoglobin release was quantified by measuring the absorbance of the supernatants at 540 nm. Controls were determined by osmotic shock of an identical amount of RBC with deionized water (100% lysis) or by incubation with no PFO (0% lysis).

CHAPTER 3

DESIGN OF A PROBE TO MEASURE MEMBRANE CHOLESTEROL ACCESSIBILITY BASED ON THE CHOLESTEROL RECOGNITION AND BINDING PROPERTIES OF PERFRINGOLYSIN O

3.1 Introduction

Due to its highly hydrophobic nature, cholesterol locates below the surface of the membrane, with only the small, polar hydroxyl group oriented towards the water-membrane interface. The interaction of cholesterol with other membrane lipids dictates the accessibility of cholesterol to interact with water-soluble molecules located outside of the membrane [27, 28, 32]. Interactions of the sterol with other molecules at the surface of the membrane will be dictated not only by total concentration, but also by the lipid composition of the membrane.

Cholesterol accessibility is an important biologically property of cellular membranes. Changes in cholesterol accessibility have been suggested to affect cholesterol homeostasis, modulate cell signaling, protein binding, and sterol transport (reviewed in [32, 21]). Current probes to study membrane cholesterol, such as filipin, can efficiently detect overall cholesterol concentration in membranes. Cholesterol accessibility does not directly correlate with sterol content, but is modulated by cholesterols interaction with the other membrane components. As a result subtle changes in cholesterol content can have profound

effect on cholesterol accessibility and cell signaling [21]. Novel molecular probes to determine cholesterol accessibility, and not total cholesterol concentration, are required for these studies.

Previous studies in our lab have shown that the binding of the bacterial toxin, Perfringolysin O (PFO), to cholesterol containing membranes has a strong response to small changes on the cholesterol content of the lipid bilayer. The transition from no binding to full binding occurs at a particular cholesterol level. The concentration of cholesterol at which the binding transition from off-on is referred to as the cholesterol threshold to trigger membrane binding. This threshold can be modulated by changes in the lipid composition of the membrane [19].

Our lab has also shown that the cholesterol threshold for PFO binding can be modulated by amino acids substitutions at the C-terminus of the toxin (Fig. 2.2A). We were able to both lower and raise the concentration of cholesterol that is required for binding (Fig. 2.3B), thus allowing for the detection of varied cholesterol accessibilities. These results greatly increased the usefulness of PFO as a probe for cholesterol accessibility, however, the FPFO probe used in my previous work proved ineffective for testing on live cells due to high levels of cell mortality. In this chapter, I aimed to create a completely nonlytic probe for membrane cholesterol and used it to assay cholesterol associability on live cells.

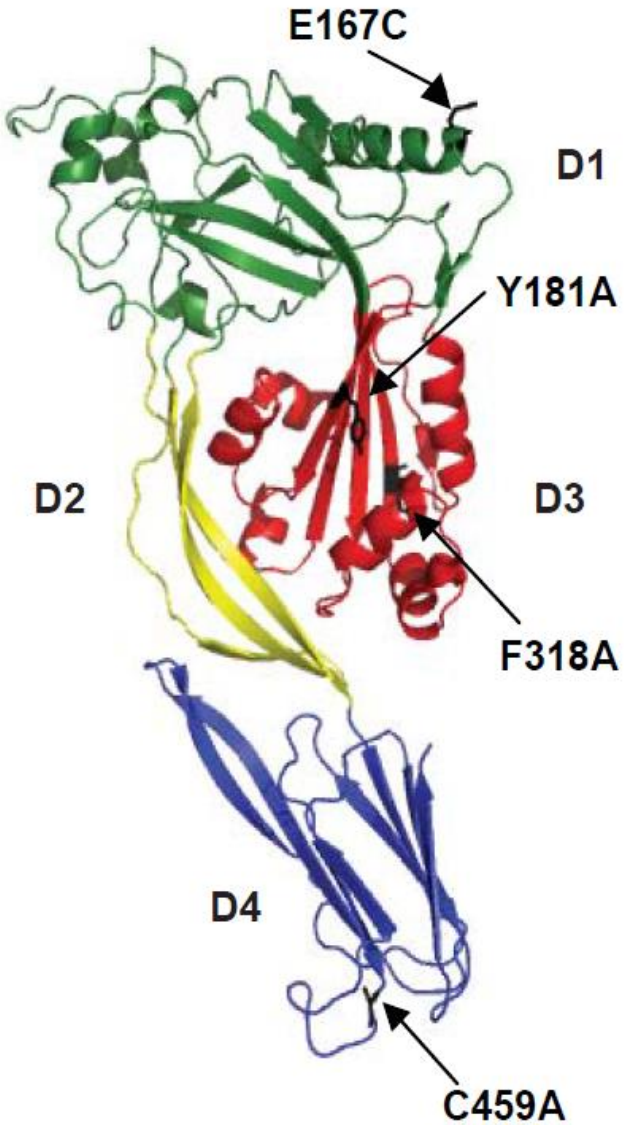

Figure 3.1: Molecular structure of monomeric water-soluble Perfringolysin O Crystal structure of PFO in a ribbon representation showing the mutations contained in the pPFO non-lytic parental derivative. The mutations E167C located in D1 (green) and C459A in D4 (blue) allows for specific labeling with a single fluorescent probe. The mutations in D3 (blue) Y181A and F318A produce a non-lytic PFO derivative. (PDB ID: 1PFO)

3.2 Results

3.2.1 Construction of a non-lytic PFO scaffold to be used in the development of probes to detect membrane cholesterol accessibility.

In my initial probe design, I used the $_{F}$PFO background which contained three modifications, two of which, C459A and E167C, were used to move the sole cysteine in the protein out of D4 to D1 where fluorescent labels would not affect binding (Fig. 3.1A). The third modification, F318A, had been reported to eliminate PFO pore forming activity when tested with model membranes [66]. However, when tested with live RAW 264.7 cells the $_{F}$PFO derivative caused considerable cell death and presumably maintained lytic activity (Fig. 3.2A). As detection of cholesterol accessibility required no (or minimal) alterations to the analyzed membrane (i.e., no lipid removal due to pore formation), a non-lytic PFO scaffold must be constructed for the analysis of live cells.

Amino acid substitutions in D3 have been previously been shown to reduce the lytic activity of PFO, for example the Y181A modification, which was shown to eliminate pore formation activity of PFO on model membranes [66]. The lytic activity of PFO derivatives containing modifications in D3 was tested using sheep erythrocytes, and quantified by hemoglobin release. The PFO derivative with Y181A modification, like those containing the F318A modification, proved to be considerably less lytic than the native PFO, but they were still lytic at high concentrations (Fig. 3.2B).

A.

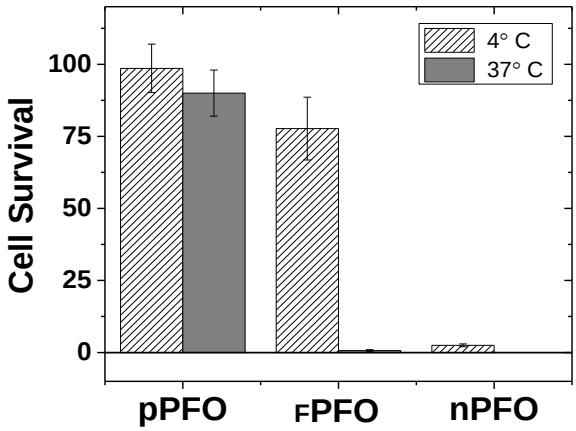

B.

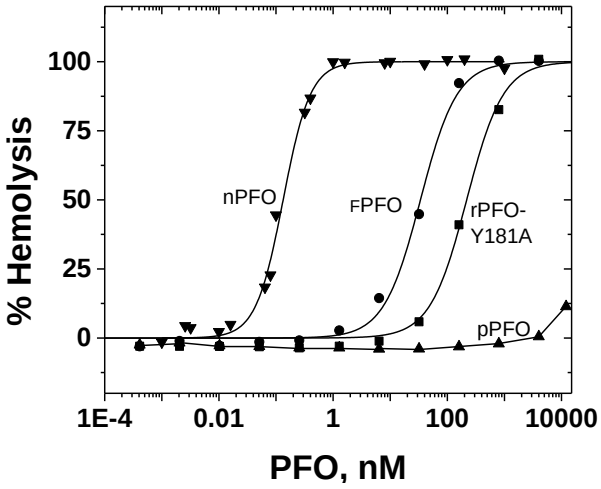

Figure 3.2: Two modifications in domain 3 are required to abolish PFO cytolysis. A. Quantification of cell death for RAW 267.4 cells incubated with the indicated PFO derivatives for 20 min at 37°C (shaded bars) or 4°C (crosshatched bars). The graph shows the percentage of live cells after incubation with the indicated PFO derivative (final concentration 1µM) when compared to cells that were not exposed to the PFO derivative. Cell survival was determined counting death cells with trypan blue stain before and after incubation with PFO derivatives. **B**. Hemolytic activity of PFO derivatives shown by the quantity required to lyse sheep erythrocytes. The indicated amount of the pPFO(▲), FPFO(●), rPFO^{-Y181A}(■), and nPFO(▼) was incubated with a 0.5 % solution of stacked erythrocytes for 20 min at 37°C in a 96 well plate (final volume 200µL). Percent hemolysis was determined by measuring hemoglobin release post-incubation using absorbance at 540 nm in a plate reader. Total hemoglobin released was determined by osmotic lysis of erythrocytes with water.

When both modifications were introduced simultaneously, the resulting PFO derivative was 100,000 fold less lytic than the native PFO, and showed minimal cell death at 37°C for concentrations up to 10µM. The Y181A modification was therefore added to our $_{F}$PFO background. The resulting construct, named probe PFO (pPFO), was used as the background for all further testing.

3.2.2 Modification of Y181A in D3 altered the cholesterol binding properties of the distal D4

While the introduction of the F318A modification into rPFO did not alter the cholesterol dependent properties of the toxin, I found that introduction of the Y181A modification into the $_{F}$PFO derivative to obtain pPFO shifted the threshold for the cholesterol concentration required for toxin binding to levels very similar to the one observed for nPFO (Fig 3.3). Allosteric coupling between D3 and D4 has been previously reported [135], however I showed here, that modifications in D3 not only effect the kinetics of protein binding, but also the mol% of cholesterol required to trigger binding (or threshold). It is worth noting that residues in D3 are more than 70Å away from the tip of D4, which is directly involve in cholesterol recognition. This indicated that mutations in D3, far from the binding domain (D4), can significantly affect the cholesterol binding threshold of the protein.

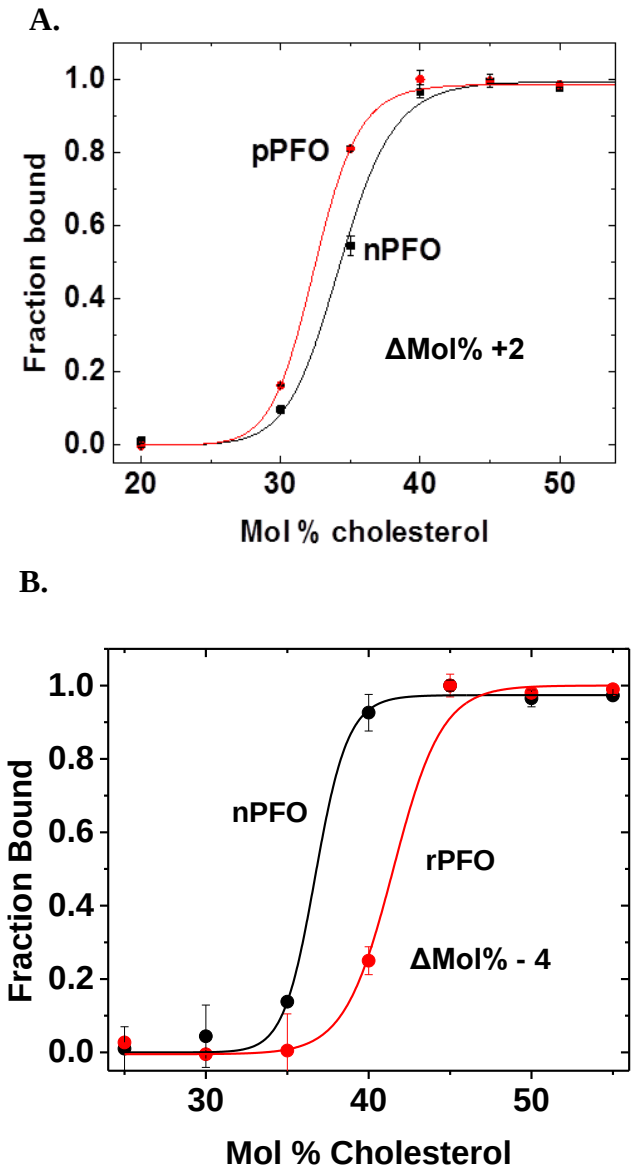

Figure 3.3: Shift in binding created by Y181A modification A. Cholesterol dependent binding of pPFO (red) and nPFO (black). Binding measurements were done as indicated in Fig. 2.2 **B**. Cholesterol dependent binding of rPFO (red) and nPFO (black). Binding measurements were done as indicated in Fig. 2.2. Data points are the average of at least two measurements and their range or standard deviation is indicated**.**

A.

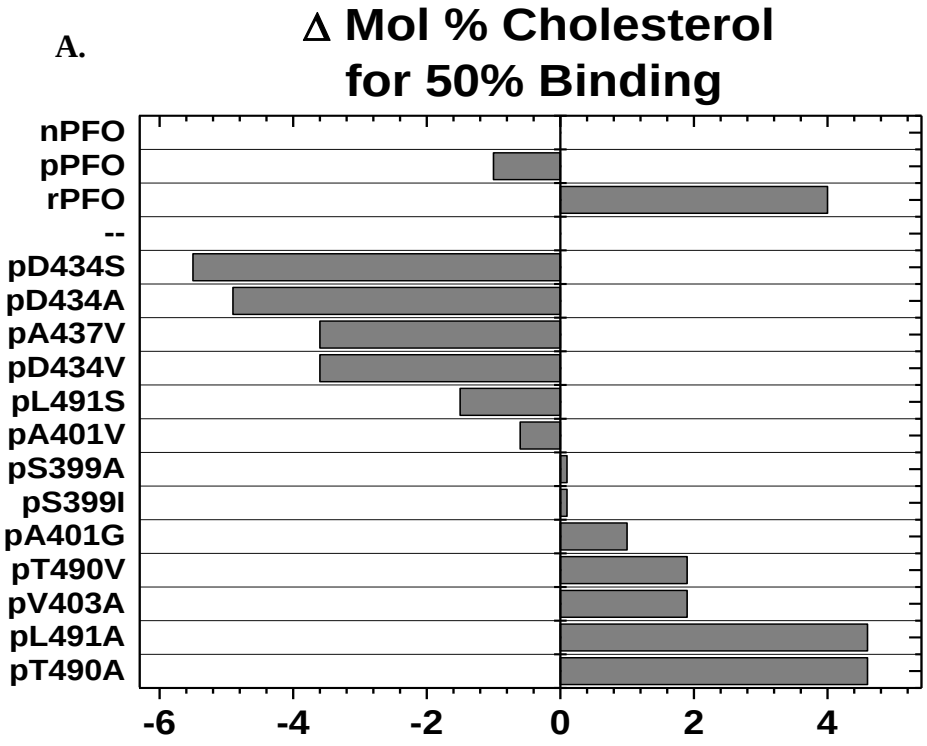
Δ Mol % Cholesterol
for 50% Binding
nPFO
pPFO
rPFO
--
pD434S
pD434A
pA437V
pD434V
pL491S
pA401V
pS399A
pS399I
pA401G
pT490V
pV403A
pL491A
pT490A
-6
-4
-2
0
2
4

B.

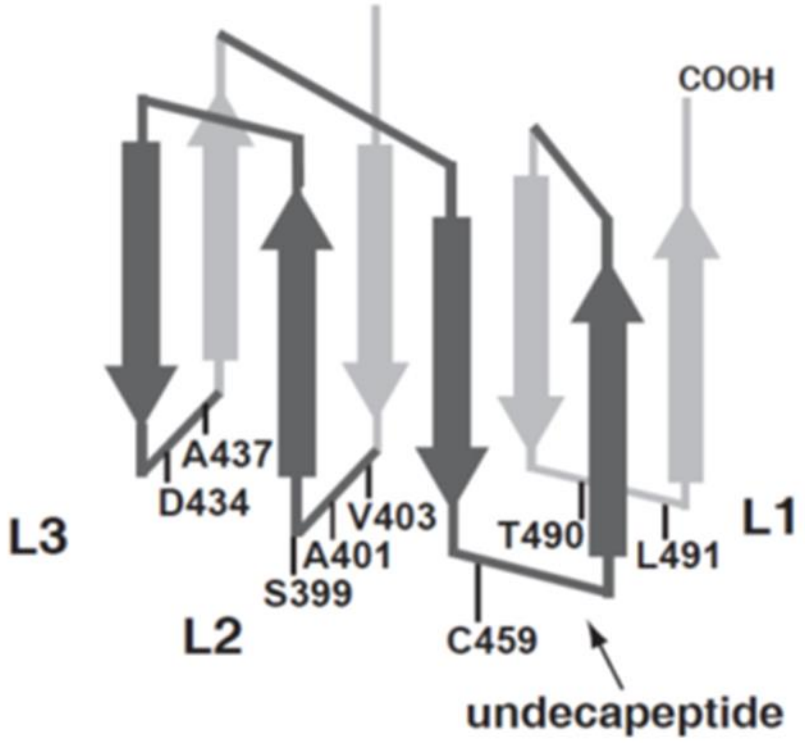
COOH
A437
D434
V403
A401
S399
T490
L491
L1
L3
L2
C459
undecapeptide

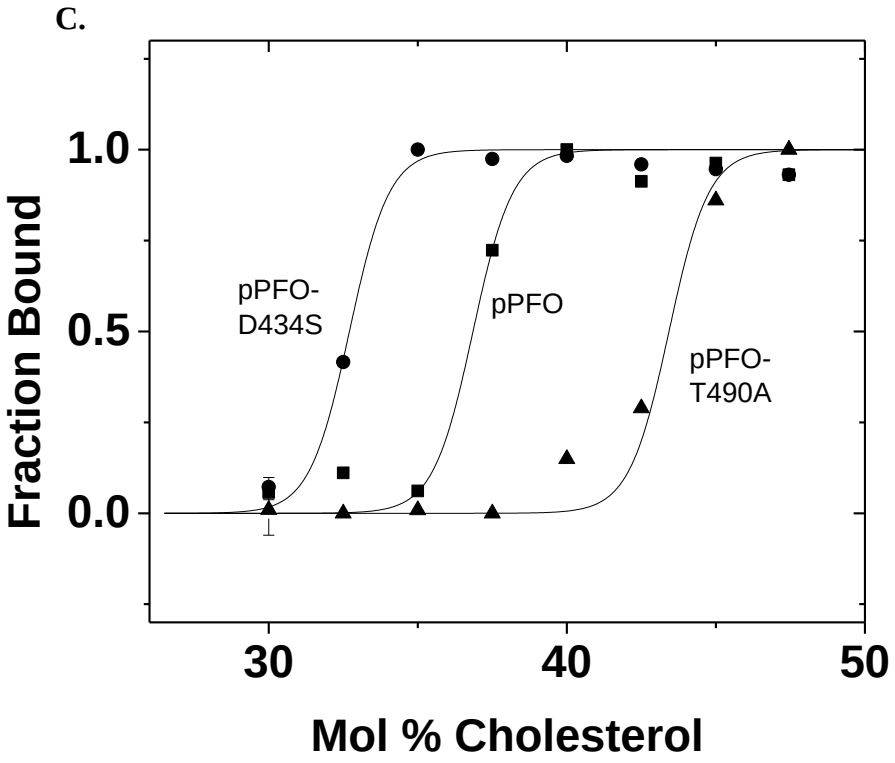

Figure 3.4: pPFO derivatives with different cholesterol binding thresholds. **A.** Relative change on the cholesterol threshold for different pPFO derivatives compared to nPFO. The fraction of bound PFO derivatives (final concentration of 0.2 μM) to liposomes of varying cholesterol content and POPC, POPE, and SM in a constant 1:1:1 molar ratio (final total lipid concentration of 0.2 mM) was determined using intrinsic Trp fluorescence as described in Experimental Procedures. The cholesterol threshold is the amount of cholesterol required in the membrane to bind 50% of a given PFO derivative. Each pPFO derivative binding threshold is represented by the Δmol % between its binding and that of nPFO with the same membrane preparation. A positive value indicating the need for more cholesterol and a negative value indicating the need for less cholesterol. **B.** A cartoon depiction of the beta-sheets that make up D4. The loops that interact with the membrane and the location of modified amino acids are indicated. **C.** Cholesterol dependent binding of $pPFO^{D434S}$(●), pPFO(■), and $pPFO^{T490A}$(▲). These derivatives were selected for further live cell testing. Binding measurements were done as indicated in Fig. 2.2.

3.2.3 Modifications in PFO D3 also affect how modifications in D4 change the threshold for the cholesterol concentration required to trigger binding

As shown in Fig. 2.3B, introduction of the D434S and L491S into FPFO both increased and decreased the binding threshold for cholesterol, respectively. Unexpectedly, when the L491S modification was re-introduced into the non-lytic pPFO derivative, I observed a slight increase in the binding threshold for cholesterol (Fig. 3.4A). This effect showed the complexity of the allosteric coupling between D3 and D4, that regulates the cholesterol dependent oligomerization of the toxin.

Structural analysis of the water-soluble PFO derivatives showed that the modification of Y181A induced a conformational change in D4, as revealed by the changes in the Trp fluorescence spectrum (Fig. 3.5A). Since 6 of the 7 Trp in PFO are located in D4, a change in the overall Trp fluorescence spectrum is a good indicator of conformational changes taking place in this domain. The pPFO spectrum shows a significant red shift compared to that of the rPFO of nPFO suggesting movement of one or more Trp to a more polar environment.

Changes in the overall secondary structure content were also observed when the CD spectrum of pPFO is compared with the one of nPFO. The CD spectra of pPFO shows less intensity at 215 nm compared to the nPFO and rPFO spectra, this indicating less beta structure in the protein (Fig. 3.5B). Therefore, the opposite effects observed when the same L491S modification was introduced in FPFO or pPFO can be explained by conformational changes induced by the Y181A modification in D3.

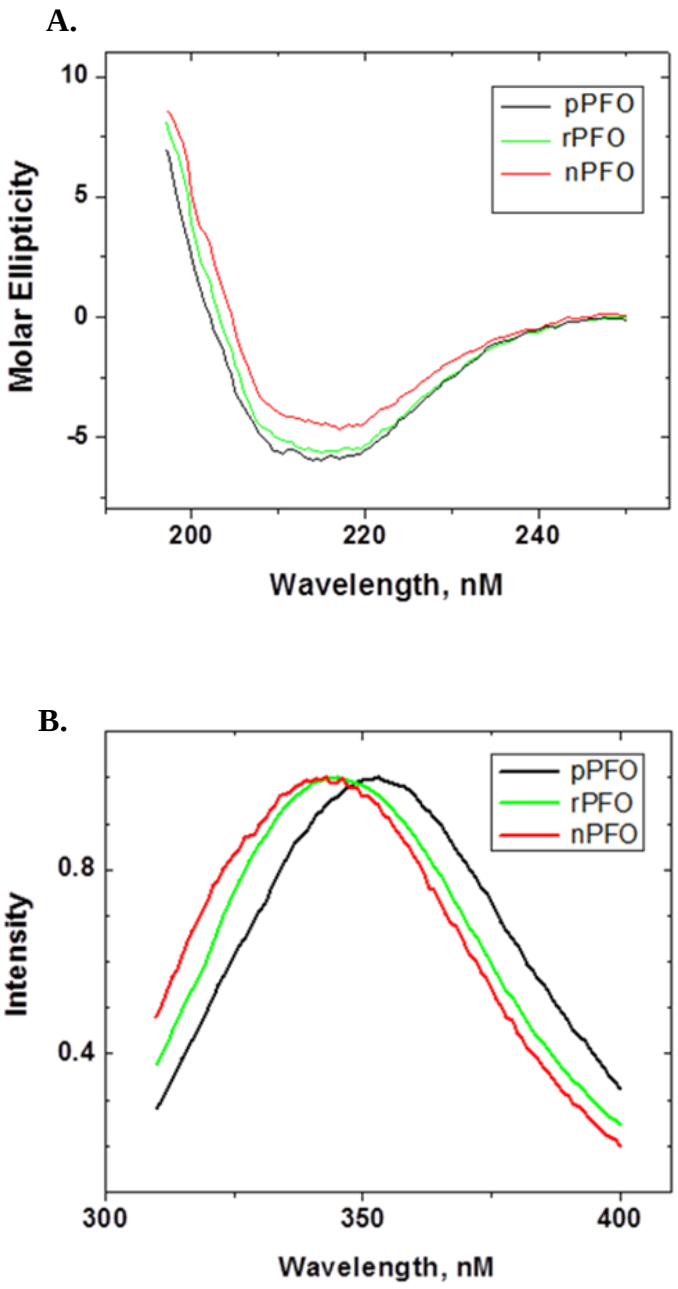

Figure 3.5: Characterization of pPFO background A. Far-UV CD spectra of nPFO and pPFO in 10 mM sodium phosphate buffer pH 7.5 at a total protein concentration of 2.0 μM. B. Normalized fluorescence emission spectra of nPFO and pPFO recorded in HBS buffer (hepes 50 mM, NaCl 100 mM EDTA 1 mM, DTT 1 mM). The spectra were taken between 310-400 nm with an excitation wavelength of 295 nm, and the total protein concentration was 500 nM.

3.2.4 Modification of domain 4 loops results in changes to the cholesterol binding threshold of pPFO derivatives

In addition to the D434S and L491S modifications mentioned above, other amino acids located in the D4 loops were modified in the new pPFO parental derivative to analyze the effect of changes to the side chains (modifications for Ala) or the effect of introducing a hydrophobic amino acid (modifications for Val or Ile) (Fig. 3.4 A and B). Major effects were observed when the native side chains were replaced with Ala at positions D434 in loop 3, and for T490 and L491 in loop 1. These last two amino acids were proposed to be the cholesterol binding motif in PFO [98]. However, modification of the hydrophobic L491 by Ser, or the hydrogen bond former Thr490 for Val, showed only minor effects on the cholesterol binding properties of pPFO, suggesting that the role of these two residues in loop 1 may differ from a specific sterol binding motif.

Modifications at loop 2 (S399 to A or I, A401to G or V, and V403 to A) showed only minor effect on the cholesterol binding threshold. Interestingly, modification of A437 in loop 3 for the bulky and hydrophobic Val residue decreased the cholesterol binding threshold, suggesting that hydrophobic residues in these loops may increase the interaction of the toxin with membranes. However, modification of the negatively charged D434 by Val showed a smaller effect on the cholesterol binding threshold than that for the modification of D434 for the polar Ser.

Based on the results discussed above, two modifications were selected for the studies of cholesterol accessibility on live cells: D434S and L491A. These modifications showed significantly lower and higher cholesterol binding

thresholds, respectively when compared with the pPFO background (Fig. 3.4C). These two modifications, plus the pPFO background itself, constitute a set of derivatives that cover a broad range in cholesterol accessibilities. These three PFO derivatives were used to explore how cholesterol manipulations in cells with cyclodextrins alter cholesterol accessibility at the membrane surface.

3.2.5 Manipulation of cell membrane cholesterol with cholesterol:methyl-β-cyclodextrin complexes results in only moderate changes in cholesterol accessibility

Having created completely non-lytic PFO derivatives that could recognize various cholesterol levels on model membranes, I moved into testing live cell membranes. As a proof of concept, I took RAW 264.7 cells and manipulated their plasma membranes with cyclodextrin/cholesterol complexes. Using these complexes in different ratios, I was able to both add and remove cholesterol from the plasma membrane. Any changes in cholesterol accessibility on the RAW cell membranes were detected using fluorescently labeled PFO derivatives and flow cytometry.

The binding isotherms for the PFO derivatives were obtained using live RAW 264.7 cells pre-treated with different cholesterol:MβCD ratios (Fig 3.6 . Interestingly, the range of cholesterol:MβCD ratios that did not induced considerable cell death, did not modified cholesterol accessibility enough to allow the binding of the $pPFO^{T490A}$ derivative. Attempts to add more cholesterol to the plasma membrane of the RAW 264.7 cell resulted in cell death. Moreover, the pPFO and $pPFO^{D434S}$ binding to live RAW cells containing various cholesterol levels did not show the sigmoidal response observed with model membranes

(compare Fig. 3.4C and Fig. 3.6).Therefore, I conclude that cholesterol levels in RAW cell membranes are tightly regulated, and cannot reach levels as high as the ones obtained when using model membranes. This also indicates live cells ability to readily adjust the cholesterol levels in their cell membranes.

3.2.6 Membranes with identical cholesterol content bind different amounts of pPFO derivatives

When tested on RAW cells, the binding of $pPFO^{D434S}$ was always higher than that observed for pPFO (Fig 3.6), independently of the overall cholesterol content of the cell membrane. This unexpected observation may result from the higher concentration of PFO derivatives used in the assay, which were required PFO detection in flow cytometry. These results suggested that at saturation binding levels, a particular membrane could accommodate more $pPFO^{D434S}$ molecules than pPFO molecules. In order to investigate this possibility, I tested the binding saturation of pPFO and $pPFO^{D434S}$ on both model membranes and live cells.

Using model membranes, 38% cholesterol was chosen as it is a concentration slightly over that required for 50% pPFO binding (Fig. 3.4C). At a 1:1000 protein lipid ratio, only part of the added pPFO was bound, but $pPFO^{D434S}$ showed maximal binding. The binding of the pPFO and $pPFO^{D434S}$ derivatives were measured on these membranes using intrinsic Trp fluorescence as described previously. Samples containing increasing amount of protein were incubated with the same amount of total lipids. The binding of the pPFO derivative was lower

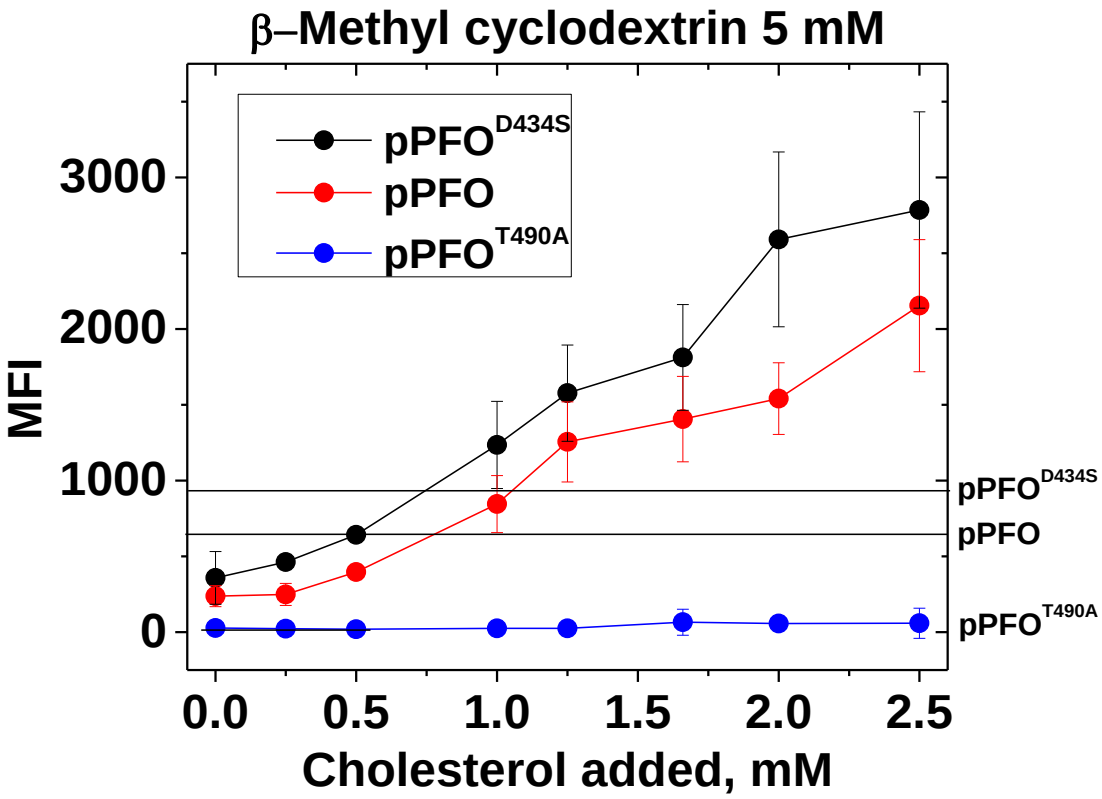

Figure 3.6: Differential binding of pPFO derivatives to RAW cells with altered cholesterol content. Quantification of binding of Alexa 488 labeled pPFO^{D434S} (Black), pPFO(Red), and pPFO^{T490A}(Blue) to RAW cells pretreated with varied levels of cholesterol complexed with mβCD (5 mM, 1 hr incubation at 37°C). Cells were washed twice after incubations with mβCD/cholesterol and after incubation with pPFO derivatives (0.5 µM protein, for 20 min at 4 ^{o}C) and binding was quantified using flow cytometry as described in experimental procedures. Horizontal lines indicate binding of each derivative to untreated cells. The pPFO^{T490A} derivative showed no binding to the cholesterol activity that could be achieved through treatment with mβCD:cholesterol complexes. Both the pPFO and pPFO^{D434S} showed differential binding in response to cholesterol treatment.

than the one observed for pPFO^{D434S} independently of how much protein was used in the assay (Fig. 3.7A). A similar effect was observed when binding to live RAW 267.4 cells was measured as a function of protein concentration using flow cytometry (Fig. 3.7B). However, a stable saturation level was difficult to obtain with live cells because at high protein concentrations, endocytosis starts to contribute to the overall fluorescent signal due to the internalization of protein despite using low temperatures. It is clear from these data that the D434S modification increased the number of protein molecules that can bind to a membrane at a particular cholesterol concentration. These observations suggested that PFO binds cholesterol and remains bound to it after oligomerization.

3.2.7 PFO binding decreased the cholesterol accessibility of the membrane

The differential binding observed for pPFO and pPFO^{D434S} in model and natural membranes could be explained by two alternative hypothesis. The first hypothesis postulates that some pPFO derivatives require more cholesterol molecules than others, and therefore, for a certain cholesterol level, the derivative that required less cholesterol molecules will have a higher saturation point. The second hypothesis postulates that protein binding sequester cholesterol molecules up to the point that the accessibility drops below the binding threshold of the PFO derivative and not more binding is observed.

In order to determine which of these hypotheses is correct, I used a sequential binding assay (Fig.3.8A). In this assay the membrane is first saturated with one PFO derivate, and the binding of a second PFO derivative is subsequently evaluated on the already saturated membrane. If the PFO

A.

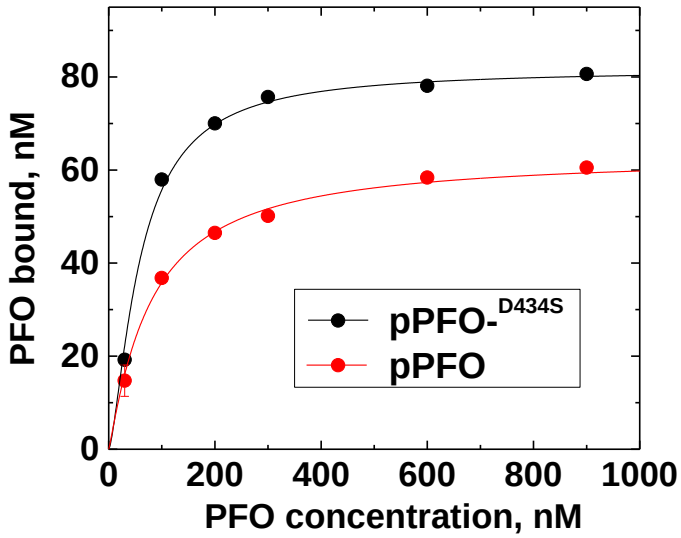

B.

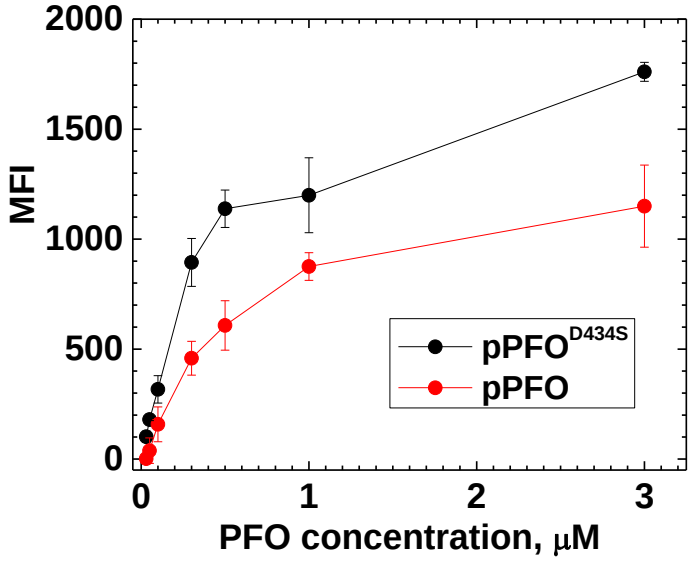

Figure 3.7 Binding saturation Curves A. Binding saturation of pPFO (red) and pPFO^{D434S} (black) to liposomes containing 38% cholesterol content and POPC, POPE, and SM in a constant 1:1:1 molar ratio. Samples containing increasing concentrations of pPFO or pPFO^{D434S} were incubated with liposomes for 20 min at 37°C. Binding was determined as indicated in Fig. 2.2. **B.** Binding saturation of pPFO (red) and pPFO^{D434S} (black) to live RAW 264.7 cells. Concentration dependent binding of Alexa 488 labeled pPFO and pPFO^{D434S} (20 min incubation at 4°C) to RAW cells determined using flow cytometry as described in Fig. 3.6.

derivatives bind different number of cholesterol molecules, no binding will be observed for the second derivative because all accessible cholesterol molecules will be bound to the first added derivative. In contrast, if binding of a PFO derivative decreases the overall cholesterol accessibility, at the saturation point for one derivative the cholesterol accessibility at the membrane surface will be just below the binding threshold for this derivative. Upon this point, only derivatives that require less cholesterol accessibility will bind to the membrane.

The sequential binding assay was done using pPFO and pPFO^{D434S}, two derivatives that showed a ~5 mol% difference in their cholesterol threshold required to trigger binding on model membranes (Fig. 3.4C). To maximize visualization of any difference in pPFO binding I used liposomes containing ~37 mol% cholesterol, approximately the cholesterol threshold of pPFO. Based on the isotherm showed in Fig. 3.4 C, only 30-40% of the added pPFO derivative will bind to these membranes, while saturation levels are expected for the pPFO^{D434S} derivative.

Binding was independently determined a) using the change in Trp emission intensity that follow membrane interaction as described in Section 3.4.9 (Fig. 3.8B), and b) using a membrane floatation assay based on ultra-centrifugation through different sucrose cushions (Fig. 3.8C). In both cases, I observed that saturation of the membrane with pPFO did not eliminate the binding of the pPFO^{D434S} derivative. In contrast, when the addition of the derivatives was done in the reverse order, saturation with the pPFO^{D434S} blocked the binding of pPFO.

These data clearly support the hypothesis that postulate that the binding of a derivative reduced the cholesterol accessibility at the membrane surface. Binding of pPFO reduced accessibility to the point where no more binding of this derivative can occur. However, since the $pPFO^{D434S}$ has a lower threshold for cholesterol, it could bind to membranes saturated with pPFO. Moreover, the total amount of toxin bound was similar independently of the order of addition. The amount of pPFO bound during the first step of the assay was equivalent to the reduction in biding observed for $pPFO^{D434S}$ in the second step when compared to its biding to membranes not pre-incubated with pPFO.

3.3 Discussion

These studies have demonstrated the non-lytic nature of the pPFO background as well as the determination of the effects many mutations to D4 have on the cholesterol binding threshold of the protein. These determinations established a library of mutations for the purposes of cholesterol accessibility determination. From this library, we selected three PFO derivatives for live cell testing. pPFO and $pPFO^{D434S}$ both showed binding that mirrored the modulation of the cells cholesterol concentration, but not the sigmoidal binding that was shown on model membranes. Saturation binding curves demonstrated that different concentrations of PFO derivatives could bind to identical membranes. This led us to testing the sequential binding of two pPFO derivatives that showed that PFO derivative sequester cholesterol when they bind and there for lower the cholesterol accessibility of the membrane. The culmination of these studies is not only a versatile probe for membrane cholesterol accessibility but also a better understanding of how PFO recognizes accessible cholesterol.

My recent studies revealed the need for a less lytic PFO derivative to serve as the scaffold for the cholesterol accessibility probe. Though both the Y181A and the F318A mutations were shown to completely eliminate the ability of PFO to form pores on model membranes and "exhibit less than 1% of the hemolytic activity of PFO^{C459A} on human erythrocytes" [136, 66] ,I still encountered significant cell death when using this background for live cell testing. As the data shows, when the concentration of toxins used is increased, the lytic activity of the derivatives is regained. This discrepancy is indicative of the manner in which PFO derivatives are generally tested. The usage of percent hemolysis compared to the native toxin is problematic because it is highly influenced by the toxin/RBC or model membrane ratio. I have also shown that the effects of mutations are very dependent to how much cholesterol is available on the surface of the membrane. This has led me to define my mutants based on their cholesterol threshold relative to wild type or Δmol % cholesterol (section 2.2.2). This system better represents the differences between mutants without the effects presented by concentration and other membrane constituents.

I showed in Fig. 3.2A that a significantly high level of toxin is required to lyse sheep RBC compared to the same mutant in Fig 2.4. While I maintain the same concentration and ratio from previous testing, the discrepancy is due to the fact that previous samples contained 10% glycerol. I have seen that glycerol

A.

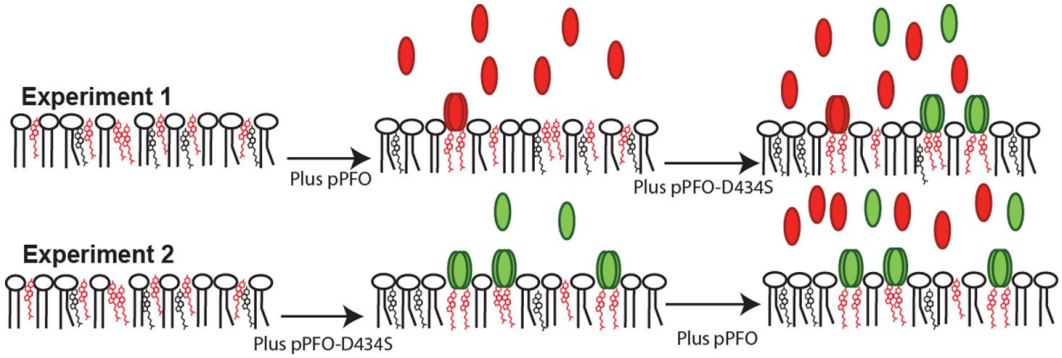
Experiment 1
Plus pPFO
Plus pPFO-D434S
Experiment 2
Plus pPFO-D434S
Plus pPFO

B.

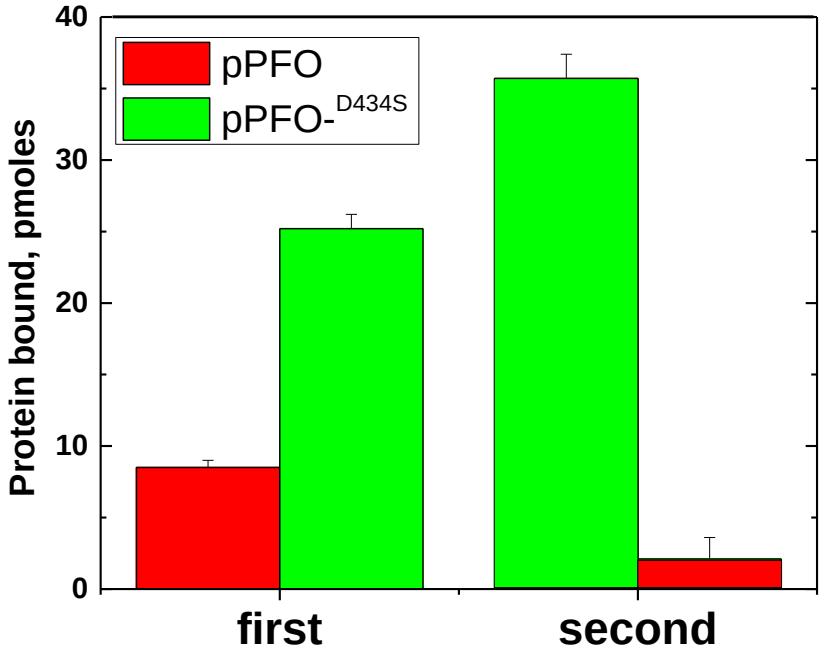
40
30
20
10
0
Protein bound, pmoles
pPFO
pPFO-D434S
first
second

C.

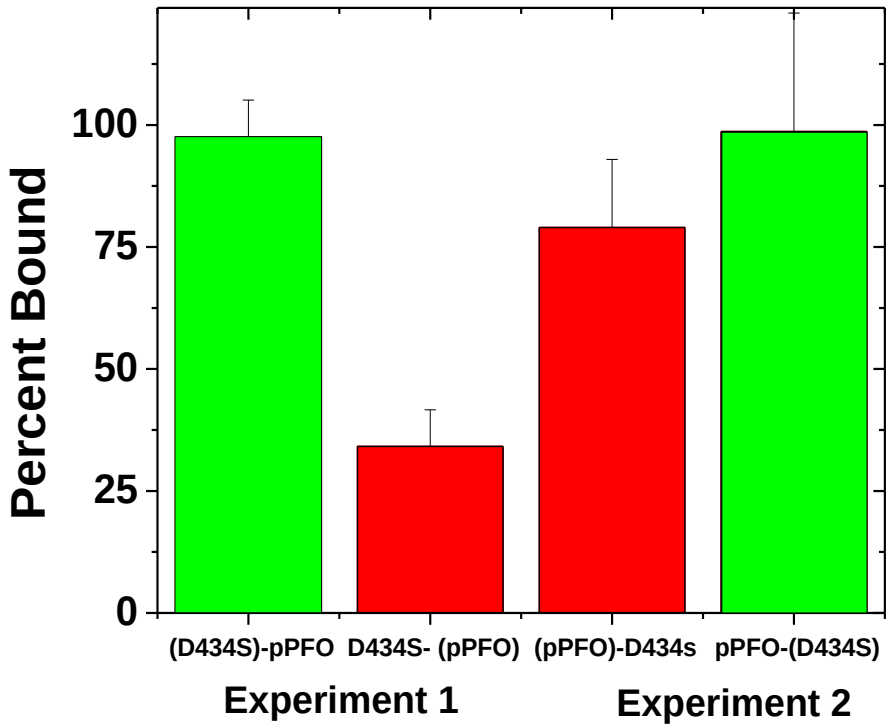

Figure 3.8: Sequential binding of pPFO derivatives showed that PFO binding reduced cholesterol accessibility. A. Carton representation of experimental method from Part B. In brief two binding reaction take place to the same set of liposomes in succession with total binding being determined for each reaction. Each reaction contain a PFO derivative with either a high (red ovals) or low (green ovals) cholesterol binding threshold. **B.First exsperiment** Liposomes with cholesterol content just above the threshold for pPFO binding were saturated with pPFO (100 nM protein, 100 µM total lipids) and incubated for 20 min at 37^{o}C. After equilibration, bound protein was quantified using intrinsic Trp fluorescence as indicated in Fig. 2.2A Subsequently an equimolar amount of pPFO^{D434S} was added to the sample, incubated for additional 20 min at 37^{o}C, and bound protein determined as indicated in section 3.4.9 **Second experiment**. Same experiment described in A was performed but liposomes were first incubated with pPFO^{D434S}, and subsequently incubated with the derivative with a lower cholesterol threshold pPFO. **C**. pPFO (red) and pPFO^{D434S} (green) were bound in two separate sequential binding assays to the same liposomes as in A. The proteins were added in two sequential incubation in the order indicate one the graphs with the protein in parentheses tracked via an Alexa 488 tag. The percent of bound protein was determined after both incubations using separation with ultra-centrifugation and, tracking of the fluorescence of the Alexa dyes.

significantly destabilized the membranes of cells and increased the lytic activity of the toxin. These current data represent a more accurate representation of the lytic activity of the protein, with slight variations from the age and health of the RBC notwithstanding.

The addition of the Y181A mutation to my probe, while resulting in the almost completely non-lytic pPFO derivative, did have some unforeseen results. Residue Y181 is located in D3, far away from the cholesterol binding interface of the protein, but has seemed to causes a distortion in D4 (Fig. 3.1). The Y181 residue is thought to be involved in oligomerization by way of a π-stacking interaction that aids in aligning the beta sheets of the protein for insertion see section 1.5.2.2 [47]. As a result, this mutation has affected both the cholesterol binding threshold of pPFO, as well as the combined effect of other mutations upon the construct. The effect of the Y181A mutation would seem to indicate a previously proposed interplay between D3 and D4 [127]. It is also possible that oligomerization affects the cholesterol threshold of the mutant. PFO binding is very cooperative in nature, as shown by its sharp sigmoidal shaped binding isotherm. A significant part of the oligomerization process is the disruption of the interface between D2 and D3 which is thought to be caused by a shift in D4. The Y181 residue is located near the interface of D2 and D3 and may weaken the interaction between the two domains, thus, making the shift in D4 more energetically favorable.

In order to find pPFO derivatives with varied cholesterol thresholds similar to our previous work, I mutated key amino acids in D4. As a whole, I observed that mutations on the well conserved loops L1 and L2 have neutral or negative effects, whereas mutations to L3 had neutral or positive affects in terms of cholesterol threshold. The two mutations with the most positive effect on cholesterol threshold, D434S and A437V, are both located in L3. The mutation with the largest negative effect was T490A, which has been put forth as half of a cholesterol binding motif that also contains L491. While the mutation of T490 significantly affects the binding of the protein, it still binds to membranes containing high cholesterol. The same is true for the L491 residue. A binding motif contains only two amino acids is unlikely to be able to afford losing either amino acid. While these two amino acids are clearly very important for binding, further study is needed to determine if additional amino acids are involved.

My live cell testing shows a gradual increase in the binding levels of my probe when cholesterol in the cell membranes was increased or decreased (Fig. 3.6). This is not what I observed on model membranes where sharp sigmoidal isotherms were shown. I attribute these results to the fact that live cells were used. Cholesterol accessibility is involved in many important cellular functions including cholesterol homeostasis. The addition of cholesterol to the plasma membrane would have resulted in the trafficking of cholesterol to the ER for esterification and storage. Over time this would have reduced the cholesterol accessibility of the plasma membrane back to equilibrium.

By showing that PFO sequesters cholesterol upon binding I can also infer that the interaction of PFO with cholesterol is not transient and that it persists after oligomerization. The sequestration of cholesterol by PFO also suggests that PFO is lowering the cholesterol accessibility of the membrane by its binding. This indicates that any PFO derivative will lower the accessibility of cholesterol on the cell membrane to that of its binding threshold if its binding is saturated. PFO derivatives could hypothetically be used to reduce the level of accessible cholesterol on a cell membrane for the purpose of initiating trafficking of cholesterol to that membrane. This could open up an entirely novel use of PFO as a scientific tool.

3.2 Methods

3.4.1 Cell culture

RAW264.7 macrophages were cultured in RPMI 1640: 10% FCS with 50 units/mL penicillin and 50 µg/mL streptomycin at 37°C with 5% CO_2. Cell were passaged at 70-80% confluence by removal of nonadherent cells and adherent removed by gently pipetting cell were replated with fresh media in a one to ten dilution.

3.4.2 Hemolysis of sheep red blood cells

pPFO derivatives were dialyzed twice in 4 liters of PBS (10 mM sodium phosphate, 1.74 mM potassium phosphate, 137 mM NaCl, 2.7 mM KCl, pH 7.4) for 4 hrs to exchange buffers and remove cryoprotectant glycerol. Washed RBC were suspended in PBS to 1%. pPFO was serially diluted in a 96 well plate and then combined with an equal volume of the RBC dilution to a final concentration

of 250 µL per well. This mixture was then incubated for 30 min at 37°C. Non-lysed RBC were pelleted from the samples by centrifugation at 3500g for 10 min and 200 µL of supernatant was transferred to a new plate. The extent of hemoglobin release was quantified by measuring the absorbance at 540 nm of cell free supernatants. Controls were determined by osmotic shock of an identical amount of RBC with deionized water (100% lysis) or by incubation of RBC in the absence of PFO (0% lysis).

3.4.3 Flow cytometry

Aliquots of 1 million cultured RAW 264.7cells were washed in PBS: 1%FCS (Fetal calf serum) and then incubated at 37 °C for 30 min in 0.5 ml of PBS: 1% FCS with 5 mM MβCD complexed with varied concentration of cholesterol. The cells were then wash and incubated at 4 °C for 20 min with 0.5 µM of the indicated PFO derivative in 100 µL of PBS: 1% FCS. The cells were analyzed in a LSRII flow cytometer (BD Biosciences) to determine mean fluorescent intensity.

3.4.4 Lysis of RAW 264.7 cells

Cultured RAW cell were counted using a hemocytometer, and re-suspended in PBS: 1% FCS. Aliquots of 1 million cells were washed in PBS: 1%FCS and then incubate at 4 °C and 37°C for 20 min with 1 µM of the indicated PFO derivative in 100 µL of PBS: 1% FCS. Cells were then washed and recounted and compared to a sample containing no protein.

3.4.5 Preparation of lipids and liposomes

Large unilamellar vesicles were generated as described previously in section 2.4.6. Briefly, equimolar mixtures of 1-palmitoyl-2-oleoyl-*sn*-glycero-3-

phosphocholine (POPC), 1-palmitoyl-2-oleoyl-*sn*-glycero-3-phosphoethanolamine (POPE), and sphingomyelin (brain, porcine), were combined with the indicated amount of cholesterol (5-cholesten-3β-ol).

3.4.6 Florescent protein labeling

Florescent labeling with Malemide derivatives of Alexa 488 or 633 was done as previously described in Section 2.4.5

3.4.7 Assay for PFO binding to liposomes

Binding assay was done using the change in the Trp emission intensity produced by the binding of PFO to cholesterol containing membranes as described previously Section 2.4.3

3.4.8 Preparation of PFO derivatives

The expression and purification of the PFO derivatives were done as described previously in Section 2.4.1 Aditional the Y181A mutation on D3 in conjunction with the F318A mutation eliminate the lytic activity of the toxin [66], [105].

3.4.9 Sequential binding of PFO derivatives determined using intrinsic tryptophan fluorescence

The consecutive binding of two different PFO derivatives with different cholesterol binding thresholds was tested on model membranes containing 36 mol % cholesterol. The first PFO derivative was added to a cuvette and Trp fluorescence was determined as described in (2.4.3). Liposomes were then added and the sample was incubated for 20 min at 37 ºC. Bound PFO was determined by the net increase in Trp fluorescence (after blank subtraction and dilution corrections) that follows the interaction with the membrane (section 2.4.3). A

second PFO derivative was then added to the same cuvette and incubated for another 20 min at 37 ºC and the final fluorescence was determined. The Trp emission intensity of the sample was recorded, and the fluorescence increase calculated from as the difference between the emission before and after incubation with the second PFO derivative. The Trp fluorescence corresponding to the unbound second derivative was determined in a separate cuvette in the absence of membranes. The binding of the second PFO derivative was then determined using the increase in the Trp fluorescence as described above.

3.4.10 Sequential binding of PFO derivatives determined by ultracentrifugation

Sequential binding of two pPFO derivatives was tested using ultracentrifugation to separate the bound and unbound protein. Binding of pPFO or pPFO^{-D434S} was determined by using one protein labeled with Alexa 488. Four reactions were set up, in which the proteins were bound sequentially. Two of the reactions were when the pPFO was bound first and the remaining two more were when the pPFO was bound second. In each reaction, only one protein was fluorescently labeled. Reaction involved one protein (200nM) being added to liposomes 200 µM in HBS (50 mM HEPES, 100 mM NaCl, pH 7.5) and incubated for 20 min at 37 ºC, follow by the addition of the second protein and a second identical incubation. Controls of labeled protein without liposomes and unlabeled protein with liposomes were also done. Each reaction mixture was then centrifuged for 1 hr at 95000G using a Beckman optima MAX TL with a TLA 120.2 rotor. Each reaction was then split into three equal fractions: bottom, middle, and top. The amount of bound protein was determined by the

fluorescence of the top fraction. This was assayed using a Fluorolog fluorometer, EX 493 nm and EM 520 nm with slit of 2 nm and 4 nm.

3.4.11 Preparation of cyclodextrin complexed with cholesterol

Sterol/ MβCD complex solutions of cholesterol in methanol-chloroform (2:1 v/v) were added dropwise to a stirred solution of MβCD in PBS on a water bath (80 °C) [137]. Once the sterol was added to the MβCD solution, a cloudy precipitate formed. Complete dissolution of the sterol was achieved after allowing the mixture to stir for about 30-45 minutes.

3.4.12 Steady-State Fluorescence Spectroscopy

Steady-state fluorescence measurements were taken using a Fluorolog-3 photon-counting spectrofluorometer as described previously [105]. Samples were equilibrated at 25 ^{o}C before fluorescence determinations.

3.4.13 Circular Dichroism (CD) Spectroscopy

Measurements were taken as previously described [131]. Briefly protein sample were made 2 μM in 10 mM sodium phosphate buffer pH 7.5. Five spectra were recorded and averaged for each sample.

CHAPTER 4

CONCLUSIONS

4.1 Future Research

4.1.1 *In vivo* cell testing of cholesterol accessibility

My work on the development of a probe for cholesterol accessibility has opened up a wide range of areas to explore. The testing done up to this point has been mostly focused on proof of concept. Now that I have demonstrated the viability of the probe, there are several outstanding questions that can be investigated. The two areas that are the most interesting, as well as promising, are the effect of cholesterol reducing drugs on cholesterol accessibility and that of cholesterol transport and homeostasis are regulated.

Statin drugs are very widely used in cases of heart disease to reduce the risk of arterial plaques. They have also been shown to reduce cholesterol serum levels in humans. In several cultured cell types, Lovastatin, a statin drug, has been shown to significantly lower membrane cholesterol concentrations by approximately a 50% reduction [24-26]. While much is known about statins reduction of cholesterol concentration, the effect of the drug class on cholesterol accessibility is still unclear and many questions remain to be addressed. The first question would be if cells are able to modulate their membrane to maintain cholesterol accessibility in the face of reduced cholesterol levels. It is likely that cells will try to compensate for the reduction in cholesterol concentration by modulating their membranes to maintain cholesterol accessibility. An example of this would be reducing concentrations of sphingomyelin and other lipids that

interact strongly with cholesterol [23, 27] as this will increase the accessibility of their reduced cholesterol concentration.

Initial testing would take place in cultured cells, which would be exposed to increasing levels of Lovastatin. The effect of the drug on the cell overall cholesterol accessibility would be assayed using our probes in conjunction with flow cytometry. The sensitivity of the PFO probes would allow for detection of fine change in cholesterol accessibility that could not previously be determined. I would test the cells at many time points, on the order of hours to days after treatment with the statin to see how the cell adapts over time to the reduction in cholesterol and how long this process takes. The cholesterol accessibility of the cells treated with statin would be compared to untreated cell to determine if they recover was partial or complete. If indeed an adaptation is seen, then the next step would be to determine what that adaptation involved. This would be started by looking at concentration of various membrane constituents, specifically those that interact strongly with cholesterol like sphingomyelin.

Cholesterol trafficking, as discussed in section 1.2.6, remains poorly understood. Cholesterol accessibility has been proposed to play a significant role in the homeostasis of this system. One part of this system that is yet to be elucidated is how the cholesterol gradient between the ER and the plasma membrane is maintained. As discussed in Section 1.3, while the cholesterol concentration of the ER and plasma membrane are very different, their cholesterol accessibility is thought to be very similar. It is clear that cholesterol accessibility is involved in the regulation of this system. Through the use of our probes, I aim

to determine what this regulation entails. There are two ways in which I would go about this investigation; the first would be to see if cholesterol accessibility affects binding of cholesterol transport proteins *in vitro*. The second would be to use kinetics experiment to see which proteins, or methods of vesicular transport, effect cholesterol transport and accessibility.

The possible cholesterol transport proteins, e.g. SCP-2, would first be tested in an *in vitro* system. This would be done in a split well plate with membranes of different composition in each well. These plates have pores that would allow for diffusion of proteins, but not the larger membranes between the wells. A cholesterol transport protein, such as SCP-2, would then be added to the system. After the system was allowed to come to equilibrium, I would then determine if the transport protein had caused the two membranes to equalize to the cholesterol concentration or the cholesterol accessibility. This would be done by determination of both the cholesterol concentration through the colorimetric assay described in section 2.4.7 and cholesterol accessibility through the using our probes.

This test would be run on membranes containing increasing concentrations of sphingolipids in one of the well. If the transport protein in question uses cholesterol accessibility as a means of recognizing cholesterol for transport than, as sphingolipids are increased the cholesterol concentration would increases in that well but the cholesterol accessibility of both wells will remain constant. If the opposite happens and cholesterol concentration remains equal and cholesterol accessibility becomes skewed then the transportof cholesterol by the protein is

driven by cholesterol concentration. A number of transport proteins would be tested in this way and what drives there transport of cholesterol determined.

The regulation of cholesterol transport and homeostasis is a very complicated and redundant system. This has hindered progress in determining the mechanisms by which it is regulated or even in the exact proteins involved. In previous studies, knocking down anyone one part of the system has shown mostly limited effects. Due to this, I will have to look at how removing one part of the system affects the speed of cholesterol transport. In the initial live cell testing, it became apparent that cell whose membrane were loaded with cholesterol would equilibrate quickly, if given the opportunity By testing the kinetics of the equilibration of cholesterol accessibility, after either add or removing cholesterol to the cell membrane, I should be able to determine the importance of individual protein or vesicle transport systems.

The key to the live cell testing would be the ability to complete it in a rapidly and precisely timed manner. My probe is well suited to this task its binding it very fast on the order of seconds to a minute and the cell can be tested as soon as the excess probe can be washed away. The transport of cholesterol out of the plasma membrane take place on the order of several minutes but this could be slowed if necessary by a reduction in temperature. In this manner, both vesicle and non-vesicle transport could be assessed through the use of inhibitors and knockdown off specific transporters using RNAi as well as other inhibitors.

I would use any incites gained from the *in vitro* testing of transport proteins to prioritize transport proteins to test. I would, first, determine how long untreated cells require for the equilibration of cholesterol accessibility after a standard amount of cholesterol is added. This measurement would then be compared to the same process in the presence of an inhibited transport protein. Then, based on the additional time it takes for the system to equilibrate, one can rank transport methods in order of importance. By doing the experiments in this manner, the pitfalls of redundant systems that have plagued previous attempts should be avoided. The ability of my probes for quick and easy determination of cholesterol accessibility levels, makes this finer determination of the effect of removing any one pathway from the system possible.

4.1.2 Creation of a reversible probe using a D4- GFP fusion protein

My current probe, like all CDC's, oligomerizes into large ring shaped pre-pore complexes on the surface of the membrane. Formation of large oligomers, in addition to perturbing the membrane and artificially grouping the probe, is also thought to be responsible for the irreversibility of PFO binding. D4, the binding domain of PFO, is an isolated domain made up of an eight stranded beta-sandwich. If one could isolate just D4, and fuse it to a fluorophore like GFP, one would have a monomerically, and reversible, binding probe. This probe would be extremely useful for the assay of dynamic changes in cells inner and outer membranes, as well as the ER and other organelles. This probe could also provide insight into the link between oligomerization and the sharp nature of the sigmoidal binding curve of the protein.

Some work has already been completed towards this goal and is discussed in appendix 2. Our lab currently possesses a PFO-GFP fusion protein that contains the entire PFO protein connected to GFP by a peptide linker. Several constructs of the truncated protein have been created and purified with limited success as all of the constructs had serious stability issues. In addition to this, the one construct that was finally purified failed to show any binding to high cholesterol membranes. Due to this, it has become clear that a simple truncation will not be successful.

There are several avenues by which this problem can be approached in the future. The first would be to try to mutate the extremely hydrophobic top of D4 that is now exposed in the fusion protein. The amino acids in this highly hydrophobic interface between D3 and D4 are responsible for holding to protein together. When D3 is removed, these amino acids become solvent exposed, and therefore, problematic. I would mutate these amino acids to either a more neutral amino acid, such as alanine, or something more hydrophilic, such as threonine or lysine. This should aid with the folding and increase the stability of the protein fusion construct.

The second possible solution would be to try other more stable and faster folding GFP constructs. Our current fusion probe has a standard EmGFP. I would swap out this GFP for one that will aid in the stability of the overall fusion construct. Several GFP proteins have been developed that fold and maturated faster, as well as, those that have additional outer charges for increased solubility. A super folding GFP would allow for low temperature growth of the protein that

may help in the proper folding of D4. A GFP with increased solubility will increase the solubility of the overall complex, but will not help if D4 is miss-folded and nonfunctional. Careful testing of the cholesterol depended binding of the probe will be necessary after these constructs are made.

The third solution would be to try a different CDC-D4 that is reported to be more stable. One of our colleagues at a conference indicated that domain four from other CDCs is more stable than that of PFO, specificity alveolysin. While this would likely solve the problem, an issue would lie with having to retest all of the D4 mutation we have already done. While alveolysin has a 75/87 identity/ similarity (Fig. 1.4) to PFO, the fact that it is more stable indicated that the effect of mutation on the cholesterol threshold may not be the same in this protein. Due to the amount of work this would entail, this option if somewhat less desirable.

4.2 Summary

As I have illustrated in this work, a new detection method is needed for the determination of cholesterol accessibility. As the scope and importance of cholesterol accessibility has become more elucidated, it has become clear that cholesterol accessibility plays a vital role in many physiologically systems; the most important, and well documented, of which is the regulation of cholesterol homeostasis. Currently, there are no probes available to detect cholesterol accessibility. Testing for cholesterol oxidation has only proved moderately useful. While cholesterol oxidase does only bind to accessible cholesterol, the oxidation process drastically changes the physical property of cholesterol and

greatly perturbs the membrane being tested. The lack of adequate detection methods for cholesterol accessibility allows it to remain as a poorly defined membrane property. A better, more quantitative probe would allow for a clearer determination of what cholesterol accessibility represents and the role that is plays in many physiological systems. This is the void that my work, and future work on this topic, aims to fill as the creation of better detection methods is paramount to expanding our understanding of cholesterol accessibility.

Throughout my work I have strived to optimize PFO for the detection of membrane cholesterol accessibility. I have created an almost completely non-lytic PFO derivative to serve as the scaffold of the probe. This scaffold is over a hundred thousand times less lytic than the parental strain and can be easily labeled with a fluorophore for detection via a single cysteine added on the top of the protein. Our lab discovered that mutations to the binding domain could alter the cholesterol threshold PFO requires for binding. By carefully testing dozens of mutations on model membranes, I was able to build up a library of mutated PFO derivatives with varied effects on the cholesterol binding threshold of the protein. I have categorized PFO derivatives which both raise and lower the cholesterol threshold the protein requires for binding; with derivatives being able to recognize a wide range of over 10 mol% cholesterol in our model system.

In collaboration with Bernardo L. Trigatti at McMaster University, the initial testing of the probe was performed on both live and fixed cells using both epifluorescent microscopy and flow cytometry. I demonstrated that the probes responded accordingly when the cholesterol concentration in the cells was

artificially raised and lowered using cyclodextrin. The fixed cells exhibited a pattern similar to what had been observed on model membranes. The live cells, though, showed a more moderate response to the cholesterol loading. The data showed a more gradual rise in cholesterol accessibility, with levels never reaching the binding threshold of the pPFO-T490A derivative. From this, I concluded that the live cells were able to modulate my attempts to artificially raise the cholesterol accessibility through cholesterol loading. Cholesterol accessibility is a tightly regulated parameter of the plasma membrane. Our future testing will need to be done on a shorter time scale to see the true effects of cholesterol loading on the cholesterol accessibility cell membrane.

I was also able to show that PFO binding sequesters cholesterol and lowers the cholesterol accessibility of the membrane. This fact could be exploited to modulate cholesterol accessibility in a cell membrane. Rather than remove cholesterol from a membrane, one could simply use PFO probes to reduce cholesterol accessibility and trigger a cellular response similar to cholesterol removal. This would be more precise and result in less disruption of the membrane than removing cholesterol. Refinements to the probe will continue, but the probe stands ready to be utilized for the intended purpose of assaying cholesterol accessibility.

The probes that I have created can now be used to detect cholesterol accessibility quickly and easily in a large number of systems. Cholesterol accessibility is still an ill-defined term because, up to this point, it was hard to quantify its effects in most systems. Giving the scientific community a means by

which to easily assay for cholesterol accessibility will allow for a better understanding of the role it plays in many cellular functions.

There are numerous areas where this tool could be useful, one of which is in cholesterol trafficking and homeostasis. This system has long been shown to be controlled by cholesterol concentration but more recently it has been suggested that it is cholesterol accessibility that controls this system. How the stark gradient in cholesterol concentration between the ER and the plasma membrane is maintained has long been an outstanding question in the field. With the demonstration that both membranes have the same level of cholesterol accessibility, a possible, and very plausible, explanation has emerged. This theory is that cholesterol accessibility determines transport between the plasma membrane and the ER and not cholesterol concentration. Through the use of our probes, we will be able to quickly assay and detect how perturbation of the systems affects cholesterol accessibility. This should allow for the determination of what role cholesterol accessibility plays in the maintenance of cholesterol homeostasis. I believe that this endeavor is the future of this project and will discuss it in more depth in the Future Directions (section 4.1.1).

There are several other cellular functions that cholesterol has been shown to play an important role in; protein activation is another examples. Many membrane proteins such, as ion channels, are activated by the binding of cholesterol molecules. This process is thought to be controlled by cholesterol concentration but it is very possible that when cholesterol is sequestered in the membrane it is not accessible to activate some of these channels. Our probe could

be used to determine whether changes in cholesterol accessibility and activation of the channels are linked.

There are many outstanding questions when it comes to cholesterol accessibility and I hope that the probes we have created will help to provide answer to some of them. As this research continues I am excited to see what can be determined about cholesterol accessibility as the project moves forward.

APPENDIX 1

SIZE DETERMINATION OF PORE COMPLEXES FORMED BY DIFFERENT PPFO DERIVATIVES

Rational: All CDC's oligomerize into large ring shaped complexes on the surface of the membrane. This oligomerization is thought to aid binding to the membrane, and be at least partially responsible for the steep rise in the binding curve of the CDCs. I showed that mutations in D3 meant to effect oligomerization and pore formation have affected the cholesterol binding threshold of the protein (section 3.2.3). This asks the question, have our mutation to D4 changed the cholesterol recognition threshold of the protein or simply effected oligomerization, and therefore, the cooperative binding of the protein. It became prudent to determine if the D4 mutations I made were having any effect on the oligomerization of the protein in terms of size of the pore, shape of the pore, or completion of the rings. I determined that the best method to determine the size of the complex was electron microscopy imaging (EM) due to the large size of the PFO complex.

Methods:

Liposomes were created as described in section 2.4.6 and their binding was tested as described in section 2.4.3. For the EM experiment, 500 nM of the given PFO derivative was incubated for 20 min at 23-25°C with 500 μM total lipids. A drop

of these samples was then placed on a carbon grid (CARBON TYPE A 300M CU) and allowed to adhere for 1 min. The excess liquid was them removed with tissue paper and the samples were stained for 30 sec with 2% uranyl acetate. After 30 seconds, the excess acid was removed with tissue paper and the grids were left to dry for 2 hrs. The imaging was then done on the JEOL JEM-2000FX microscope. 15 to 25 images were taken for each sample with an attempt being made to pick images that contained complete rings. The determination of size was done using ImageJ.

Results/Discussion:

Liposomes with cholesterol levels close to the binding threshold of the PFO derivatives pPFO and $pPFO^{D434S}$ were created. These liposomes were then tested using intrinsic tryptophan fluorescence to determine which batch gave closest to 50 percent pPFO binding. Based on these data, the 31 mol % and 37 mol % liposomes were selected as the transition for $pPFO^{D434S}$ and pPFO respectively. The 47 mol% derivative was used for full binding of both.

The PFO derivatives were bound to liposomes placed on a carbon grid and stained with uranyl acetate. Sample images for each of the samples are shown in fig. A1. The drying of the samples to the carbon grid seemed to have caused a large amount of ring breakage, only 15-20% of the rings were complete in each sample. Due to this, and the fact that I had selected for complete rings, I did not feel confident determine the percentage of complete to incomplete rings, but the samples appeared to be qualitatively similar. Forty complexes were measured and averaged for each sample (Table A1). There was a slight difference in size

between the rings created by pPFO and those created by the D434S mutation. Due to the fact that PFO oligomers contain a varied number of monomers in each ring the error bars are too large to make the difference between the two statistically relevant

Table A1	Average Size nm	Standard deviation		Average Size nm	Standard deviation
pPFO 47 mol %	36.1	2.0	$pPFO^{D434S}$ 47 mol %	38.1	2.4
pPFO 37 mol%	36.6	1.6	$pPFO^{D434S}$ 31 mol%	37.7	2.0

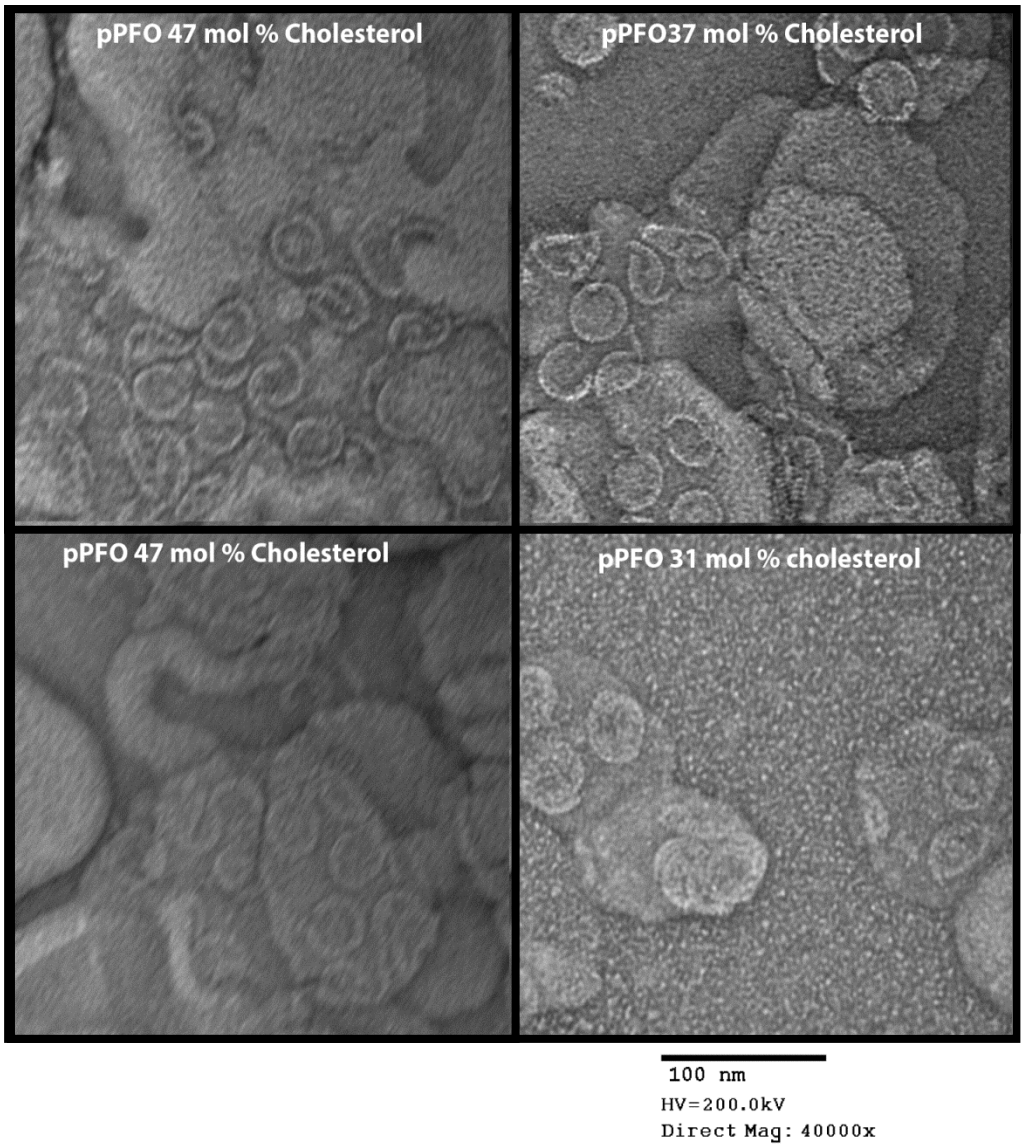

Figure A.1 Sample images for EM determination of pore size of PFO Derivatives. The oligomeric structure of the indicated PFO derivative were formed on liposomes containing the indicated mol% cholesterol and subsequently transferred to carbon grids. The grids were negatively stained with uranyl acetate Scale Bar 100 nm.

APPENDIX 2

GFP-D4 FUSIONS

Rational:

All CDCs, including PFO, oligomerize into large ring shaped pre-pore complexes on the surface of the membrane.[138] It is thought that this is responsible for the irreversible binding and cooperative binding of PFO indicated by its sharp sigmoidal binding curve. As detailed in section 1.5, D4, the binding domain, and the rest of the protein, including D3, the domain responsible for oligomerization [139], are only connected by one poly-peptide chain. As a result, it should be easy to separate the part of the protein that recognizes and binds to cholesterol and the part that oligomerizes and forms a pore. Such a construct would contain all of the properties wanted such as monomeric binding, reversible binding, and being completely non-lytic. Similar constructs has been previously created[121],[140] , but had some solubility issues. However, the fusion probe was able to be purified, and its binding was demonstrated.

Creation of GFP-PFO fusion protein:

Creation and testing of the initial full length GFP-PFO fusion was completed by other members of the Heuck lab. The creation of the construct was completed by Dr. Fabian Romano-Cherñac and the purification and testing was done by Ms. Lindsey Gouvin. In brief, the DNA codifying for pPFO was cut into an EmGFP construct vector (Invitrogen) using PCR, followed by the addition of

two point mutations to create the EmGFP-pPFO^{D434S}, and EmGFP-pPFO^{T490A} derivatives. These three constructs were then purified using standard lab procedures as described section 2.4.1. The constructs purified easily and showed no instability issues. The binding of the probe was then tested on model membranes using intrinsic tryptophan fluorescence, as described in section 2.4.3. The binding data was similar to that observed with non GFP pPFO derivatives, but was slightly shifted, ~5 mol% cholesterol lower. (Figure B.1) This shift may be because of the addition of the GFP or simply due to the cholesterol composition of the liposomes created being slightly skewed. This result would have to be confirmed before further uses of these probes could continue.

Creation of EmGFP-D4:

I used the full length EmGFP-PFO construct as a base for the EmGFP-D4 construct. The undesired parts (D1-3) of the PFO molecule were simple cut out. GFP-D4 fusions had proven to have stability problems in the past; I decided that creating several constructs that contained small amount of D3 left in the protein may stabilize the protein. The three constructs are shown in Figure B.2. The deletion of the first three domains was completed by using a single step PCR mediated deletion method. [141] Primers were created containing 16 to 20 bases from either side of the section to be deleted. The PCR reaction then extended the primer to copy all but the undesired section of the plasmid.

Purification of EmGFP-D4:

Initial attempts at purification of the EmGFP-D4 were met with some complications, mostly due to insolubility and protein precipitation. Attempts were made to purify all three of the constructs as described in section 2.4.1 with relatively limited success. My initial work was focused on the constructs with linker segments, because of reported instability of the straight GFP-D4 constructs. Though, this assumption did not prove helpful as the linkers were found to increase the likelihood of the protein to precipitate.

In the initial purification of both the long and short linkers, the protein was found entirely in the insoluble pellet after breaking the cells. A number of different growth conditions were tried in an attempted to increase the solubility of these fusion proteins. These included low temperature, high salt, addition of proline, and overgrowth. The overgrowth involved inducing the protein at an OD of 1.2 as opposed to the standard 0.6. In this case, the protein would be produced more slowly due to lack of nutrients. This had the opposite of the desired effect, increasing precipitation of the protein. Proline was added at the time of induction to act as a quasi-chaperon, but produced no noticeable effect. Purifying under high salt conditions was moderately successful. The buffers for the IMAC column were spiked with 300 mM NaCl. This resulted in a small amount of soluble protein, but most of the protein had already precipitated prior to purification and was still in the insoluble aggregate. A low temperature induction (18°C) helped the solubility, but lead to the GFP chromophore not maturating. I found that raising the temperature of the induction to 37°C for the last 20-30 minutes would

result in full maturation of the GFP. A very small amount of the short linker protein was able to be purified, but aggregated upon concentration. At this point, I set aside the constructs containing linkers, and focused my attempts at purifying the no linker construct.

The construct with no linker was marginally soluble and only precipitated in the dialysis between the IMAC and ion exchange columns due to the low salt. To solve the problem, I added 100 mM of NaCl to the dialysis buffer after the IMAC column and did three one hour dialysis followed immediately by the ion exchange column the same day. This reduced the degradation and precipitation significantly. This led to a moderate amount of pure, and surprisingly, stable protein. This protein was then tested for binding. The results were not promising, as the protein did not show any binding to liposomes, even one containing high cholesterol levels. (Figure B.3)

As I mentioned in the rational for this appendix, another group has created a GFP-D4 fusion which did show binding, although they too had solubility issues. This raises the question why did mine fail. There are only two real differences between the two. The first is the GFP they used a standard GFP while ours is an EmGFP. It seems unlikely that this would have any effect on the stability of the construct. The difference is only a couple of point mutations around the chromophore of the GFP. The other difference is I cut PFO off in the same place the other group added a cleavage site between D4 and the GFP. This may have aided in folding in some fashion. For further discussion of future work and possible solution to these problems see Section 4.2.2

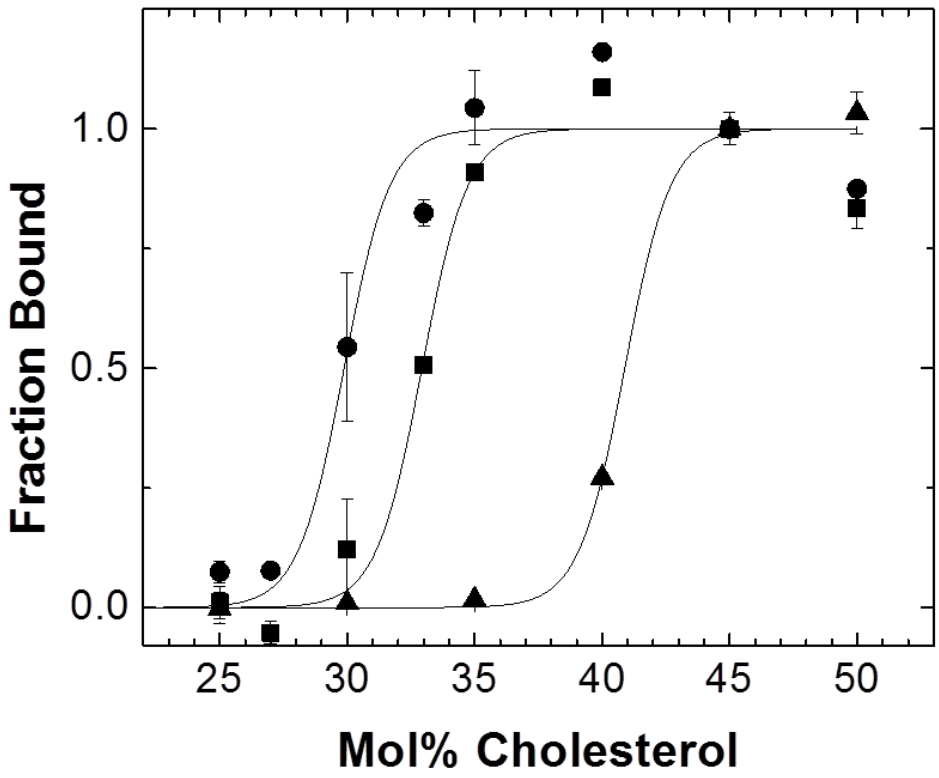

Figure B.1 Binding of Full length GFP-pPFO derivatives Cholesterol dependent binding of GFP-pPFO (squares), GFP-pPFO-^{D434S} (circles) and GFP-pPFO-^{T490A} (triangles) Binding measurements were done as indicated in Fig. 2.2 Data points are the average of at least two measurements.

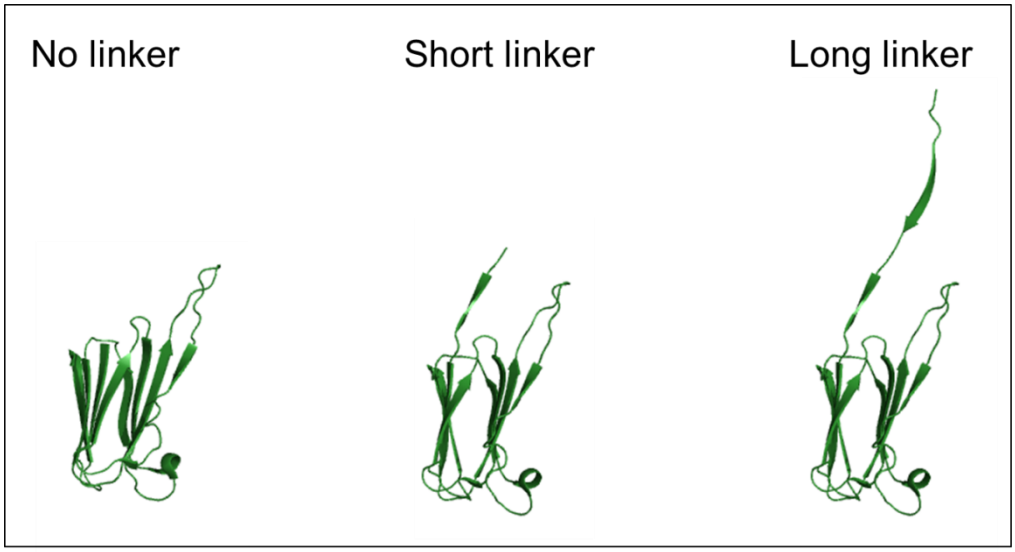

Figure B.2 Structural representation of D4 truncations. Crystal structure of PFO in a ribbon representation showing D4 and the linker region of D3 that was added to each construct.

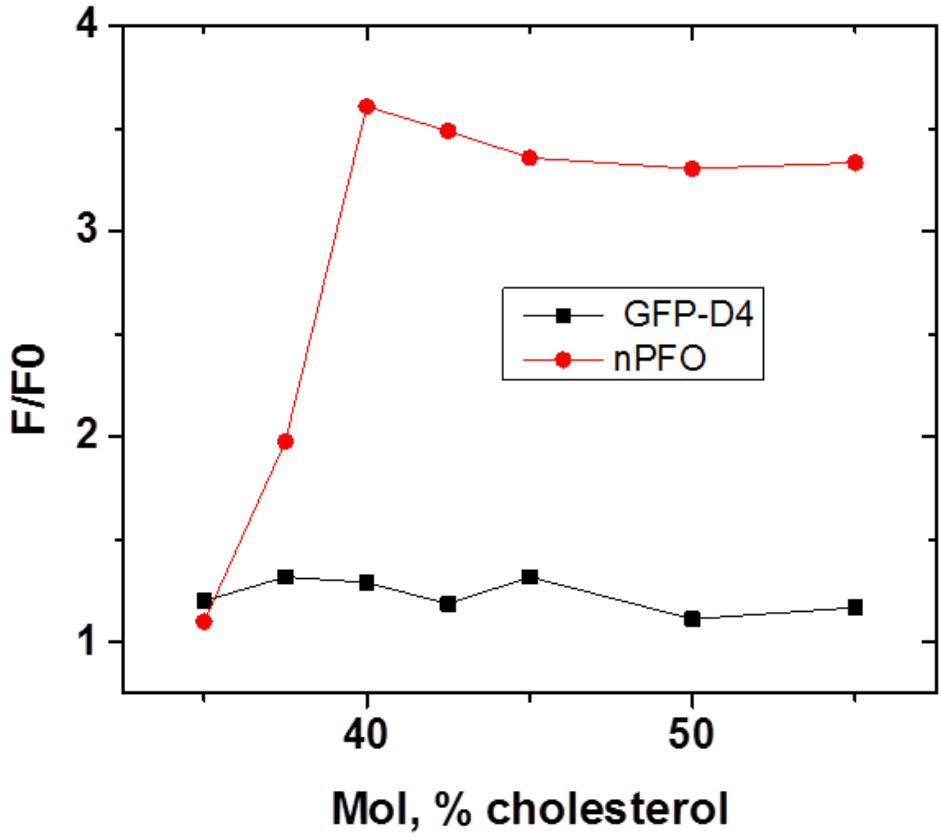

Figure B.3 Binding of GFP-D4 no-linker derivative. The graph depicts the cholesterol dependent binding of GFP-D4 no-linker (squares), and nPFO (circles). Binding measurements were done as indicated in Fig. 2.2.

BIBLIOGRAPHY

1. Ikonen, E., *Mechanisms for Cellular Cholesterol Transport: Defects and Human Disease.* Physiological Reviews, 2006. **86**(4): p. 1237-1261.

2. Maxfield, F.R., Tabas, Ira, *Role of cholesterol and lipid organization in disease.* Nature, 2005. **438**(7068): p. 612-21.

3. Puglielli, L., Tanzi, Rudolph E.,Kovacs, Dora M., *Alzheimer's disease: the cholesterol connection.* Nat Neurosci, 2004. **6**(4): p. 345-51.

4. Goedeke, L. and C. Fernández-Hernando, *Regulation of cholesterol homeostasis.* Cellular and Molecular Life Sciences, 2012. **69**(6): p. 915-930.

5. van der Wulp, M.Y.M., H.J. Verkade, and A.K. Groen, *Regulation of cholesterol homeostasis.* Molecular and Cellular Endocrinology, 2013. **368**(1–2): p. 1-16.

6. Janine K Kruit, A.K.G., Theo J van Berkel and Folkert Kuipers, *Emerging roles of the intestine in control of cholesterol metabolism.* World J Gastroenterol, 2006. **12**(40): p. 6429-39.

7. Gong, Y., et al., *Sterol-regulated ubiquitination and degradation of Insig-1 creates a convergent mechanism for feedback control of cholesterol synthesis and uptake.* Cell Metabolism, 2006. **3**(1): p. 15-24.

8. Goldstein, J.L., R.A. DeBose-Boyd, and M.S. Brown, *Protein Sensors for Membrane Sterols.* Cell, 2006. **124**(1): p. 35-46.

9. Brown, M. and J. Goldstein, *A receptor-mediated pathway for cholesterol homeostasis.* Science, 1986. **232**(4746): p. 34-47.

10. Yokoyama, S., *Release of cellular cholesterol: molecular mechanism for cholesterol homeostasis in cells and in the body.* Biochimica et Biophysica Acta (BBA) - Molecular and Cell Biology of Lipids, 2000. **1529**(1–3): p. 231-244.

11. Prinz, W.A., *Non-vesicular sterol transport in cells.* Progress in Lipid Research, 2007. **46**(6): p. 297-314.

12. Field, F.J., et al., *Transport of cholesterol from the endoplasmic reticulum to the plasma membrane is constitutive in CaCo-2 cells and differs from the transport of plasma membrane cholesterol to the endoplasmic reticulum.* Journal of Lipid Research, 1998. **39**(2): p. 333-343.

13. Seedorf, U., P. Ellinghaus, and J. Roch Nofer, *Sterol carrier protein-2.* Biochimica et Biophysica Acta (BBA) - Molecular and Cell Biology of Lipids, 2000. **1486**(1): p. 45-54.

14. Kriska, T., et al., *Sterol carrier protein-2 (SCP-2) involvement in cholesterol hydroperoxide cytotoxicity as revealed by SCP-2 inhibitor effects.* Journal of Lipid Research, 2010. **51**(11): p. 3174-3184.

15. Martin, S. and R.G. Parton, *Caveolin, cholesterol, and lipid bodies.* Seminars in Cell & Developmental Biology, 2005. **16**(2): p. 163-174.

16. Radhakrishnan, A. and H.M. McConnell, *Chemical activity of cholesterol in membranes.* Biochemistry, 2000. **39**(28): p. 8119-24.

17. Lange, Y., J. Ye, and T.L. Steck, *Activation of Membrane Cholesterol by Displacement from Phospholipids.* J. Biol. Chem., 2005. **280**(43): p. 36126-36131.

18. Nelson, L.D., A.E. Johnson, and E. London, *How interaction of perfringolysin O with membranes is controlled by sterol structure, lipid structure, and physiological low pH: insights into the origin of perfringolysin O-lipid raft interaction* J. Biol. Chem., 2008. **283**(8): p. 4632-4642.

19. Flanagan, J.J., et al., *Cholesterol Exposure at the Membrane Surface Is Necessary and Sufficient to Trigger Perfringolysin O Binding.* Biochemistry, 2009. **48**(18): p. 3977-3987.

20. Moe, P.C. and A.P. Heuck, *Phospholipid hydrolysis caused by Clostridium perfringens a-toxin facilitates the targeting of perfringolysin O to membrane bilayers.* Biochemistry, 2010. **49**(44): p. 9498-9507.

21. Sokolov, A. and A. Radhakrishnan, *Accessibility of cholesterol in endoplasmic reticulum membranes and activation of SREBP-2 switch abruptly at a common cholesterol threshold.* Journal of Biological Chemistry, 2010. **285**(38): p. 29480-29490.

22. Ohvo-Rekilä, H., et al., *Cholesterol interactions with phospholipids in membranes.* Prog. Lipid Res., 2002. **41**(1): p. 66-97.

23. Mason, P.R., T.N. Tulenko, and R.F. Jacob, *Direct evidence for cholesterol crystalline domains in biological membranes: role in human pathobiology.* Biochim. Biophys. Acta, 2003. **1610**(2): p. 198-207.

24. Bach, D. and E. Wachtel, *Phospholipid/cholesterol model membranes: formation of cholesterol crystallites.* Biochim Biophys Acta, 2003. **1610**(2): p. 187-97.

25. Ziblat, R., L. Leiserowitz, and L. Addadi, *Crystalline Domain Structure and Cholesterol Crystal Nucleation in Single Hydrated DPPC:Cholesterol:POPC Bilayers.* Journal of the American Chemical Society, 2010. **132**(28): p. 9920-9927.

26. Heuck, A.P., et al., *Mechanism of membrane insertion of a multimeric b-barrel protein: perfringolysin O creates a pore using ordered and coupled conformational changes.* Mol. Cell, 2000. **6**(5): p. 1233-1242.

27. Huang, J. and G.W. Feigenson, *A Microscopic Interaction Model of Maximum Solubility of Cholesterol in Lipid Bilayers.* Biophysical Journal, 1999. **76**(4): p. 2142-2157.

28. McConnell, H.M. and A. Radhakrishnan, *Condensed complexes of cholesterol and phospholipids.* Biochimica et Biophysica Acta (BBA) - Biomembranes, 2003. **1610**(2): p. 159-173.

29. Lange, Y. and T.L. Steck, *Cholesterol homeostasis and the escape tendency (activity) of plasma membrane cholesterol.* Progress in Lipid Research, 2008. **47**(5): p. 319-332.

30. Mesmin, B. and F.R. Maxfield, *Intracellular sterol dynamics.* Biochimica et Biophysica Acta (BBA) - Molecular and Cell Biology of Lipids, 2009. **1791**(7): p. 636-645.

31. Olsen, Brett N., et al., *The Structural Basis of Cholesterol Accessibility in Membranes.* Biophysical Journal, 2013. **105**(8): p. 1838-1847.

32. Steck, T.L. and Y. Lange, *Cell cholesterol homeostasis: Mediation by active cholesterol.* Trends in Cell Biology, 2010. **20**(11): p. 680-687.

33. Radhakrishnan, A., et al., *Switch-like Control of SREBP-2 Transport Triggered by Small Changes in ER Cholesterol: A Delicate Balance.* Cell Metabolism, 2008. **8**(6): p. 512-521.

34. Soccio, R.E. and J.L. Breslow, *Intracellular Cholesterol Transport.* Arteriosclerosis, Thrombosis, and Vascular Biology, 2004. **24**(7): p. 1150-1160.

35. Chailley, B. and E. Boisvieux-Ulrich, *Detection of plasma membrane cholesterol by filipin during microvillogenesis and ciliogenesis in quail oviduct.* Journal of Histochemistry & Cytochemistry, 1985. **33**(1): p. 1-10.

36. Gimpl, G. and K. Gehrig-Burger, *Probes for studying cholesterol binding and cell biology.* Steroids, 2011. **76**(3): p. 216-231.

37. Grechishnikova, I.V., et al., *New fluorescent cholesterol analogs as membrane probes.* Biochimica et Biophysica Acta (BBA) - Biomembranes, 1999. **1420**(1–2): p. 189-202.

38. Tweten, R.K., *Cholesterol-dependent cytolysins, a family of versatile pore-forming toxins.* Infect. Immun., 2005. **73**(10): p. 6199-6209.

39. Heuck, A.P., P.C. Moe, and B.B. Johnson, *The cholesterol-dependent cytolysins family of Gram-positive bacterial toxins,* in *Cholesterol binding proteins and cholesterol transport*, J.R. Harris, Editor. 2010, Springer. p. 551-577.

40. Gilbert, R.J., *Cholesterol-dependent cytolysins.* Adv Exp Med Biol, 2010. **677**: p. 56-66.

41. Rampersaud, R., et al., *Inerolysin, a Cholesterol-Dependent Cytolysin Produced by Lactobacillus iners.* Journal of Bacteriology, 2011. **193**(5): p. 1034-1041.

42. Jost, B.H., et al., *Arcanolysin is a cholesterol-dependent cytolysin of the human pathogen Arcanobacterium haemolyticum.* BMC Microbiology, 2011. **11**(1): p. 239.

43. Hotze, E.M., et al., *Identification and Characterization of the First Cholesterol-Dependent Cytolysins from Gram-Negative Bacteria.* Infection and Immunity, 2013. **81**(1): p. 216-225.

44. Kara S Giddings, J.Z., Peter J Sims & Rodney K Tweten, *Human CD59 is a receptor for the cholesterol-dependent cytolysin intermedilysin.* Nature Structural & Molecular Biology, 2004. **11**: p. 1173-78.

45. Giddings, K.S., A.E. Johnson, and R.K. Tweten, *Redefining cholesterol's role in the mechanism of the cholesterol-dependent cytolysins.* Proceedings of the National Academy of Sciences, 2003. **100**(20): p. 11315-11320.

46. Palmer, M., et al., *Kinetics of Streptolysin O Self-Assembly.* European Journal of Biochemistry, 1995. **231**(2): p. 388-395.

47. Hotze, E.M., et al., *Monomer-Monomer Interactions Propagate Structural Transitions Necessary for Pore Formation by the Cholesterol-dependent Cytolysins.* Journal of Biological Chemistry, 2012. **287**(29): p. 24534-24543.

48. Shepard, L.A., et al., *The mechanism of pore assembly for a cholesterol-dependent cytolysin: formation of a large prepore complex precedes the insertion of the transmembrane beta-hairpins.* Biochemistry, 2000. **39**(33): p. 10284-10293.

49. Dang, T.X., et al., *Prepore to pore transition of a cholesterol-dependent cytolysin visualized by electron microscopy.* Journal of Structural Biology, 2005. **150**(1): p. 100-108.

50. Shatursky, O., et al., *The Mechanism of Membrane Insertion for a Cholesterol-Dependent Cytolysin: A Novel Paradigm for Pore-Forming Toxins.* Cell, 1999. **99**(3): p. 293-299.

51. Shepard, L.A., et al., *Identification of a membrane-spanning domain of the thiol-activated pore-forming toxin Clostridium perfringens perfringolysin O: an a-helical to b-sheet transition identified by fluorescence spectroscopy.* Biochemistry, 1998. **37**(41): p. 14563-14574.

52. Rossjohn, J., et al., *Structure of a cholesterol-binding, thiol-activated cytolysin and a model of its membrane form.* Cell, 1997. **89**(5): p. 685-692.

53. Polekhina, G., et al., *Comparative three-dimensional structure of cholesterol-dependent cytolysins*, in *The Comprehensive Sourcebook of Bacterial Protein Toxins*, J.E. Alouf and M.R. Popoff, Editors. 2006, Academic Press: Oxford, England. p. 659-670.

54. Bourdeau, R.W., et al., *Cellular Functions and X-ray Structure of Anthrolysin O, a Cholesterol-dependent Cytolysin Secreted by Bacillus anthracis.* Journal of Biological Chemistry, 2009. **284**(21): p. 14645-14656.

55. Xu, L., et al., *Crystal structure of cytotoxin protein suilysin from Streptococcus suis.* Protein & Cell, 2010. **1**(1): p. 96-105.

56. Ramachandran, R., R.K. Tweten, and A.E. Johnson, *The domains of a cholesterol-dependent cytolysin undergo a major FRET-detected rearrangement during pore formation.* Proceedings of the National academy of Sciences of the United States of America, 2005. **102**(20): p. 7139-7144.

57. Czajkowsky, D.M., et al., *Vertical collapse of a cytolysin prepore moves its transmembrane beta-hairpins to the membrane.* EMBO Journal, 2004. **23**(16): p. 3206-3215.

58. Tilley, S.J., et al., *Structural basis of pore formation by the bacterial toxin pneumolysin.* Cell, 2005. **121**(2): p. 247-256.

59. Ramachandran, R., R.K. Tweten, and A.E. Johnson, *Membrane-dependent conformational changes initiate cholesterol-dependent cytolysin oligomerization and intersubunit beta-strand alignment.* Nat. Struct. Mol. Biol., 2004. **11**(8): p. 697-705.

60. Ramachandran, R., et al., *Structural insights into the membrane-anchoring mechanism of a cholesterol-dependent cytolysin.* Nat. Struct. Mol. Biol., 2002. **9**(11): p. 823-827.

61. Olofsson, A., H. Hebert, and M. Thelestam, *The projection structure of Perfringolysin O (Clostridium perfringens q-toxin).* FEBS Letters, 1993. **319**(1-2): p. 125-127.

62. Heuck, A.P., et al., *Conformational changes that effect oligomerization and initiate pore formation are triggered throughout perfringolysin O upon binding to cholesterol.* J. Biol. Chem., 2007. **282**(31): p. 22629-22637.

63. Gilbert, R.J.C., et al., *Self-interaction of pneumolysin, the pore-forming protein toxin of Streptococcus pneumoniae.* Journal of Molecular Biology, 1998. **284**(4): p. 1223-1237.

64. Solovyova, A.S., et al., *The solution structure and oligomerization behavior of two bacterial toxins: pneumolysin and perfringolysin O.* Biophysical Journal, 2004. **87**(1): p. 540-552.

65. Hotze, E.M., et al., *Arresting pore formation of a cholesterol-dependent cytolysin by disulfide trapping synchronizes the insertion of the transmembrane beta-sheet from a prepore intermediate.* Journal of Biological Chemistry, 2001. **276**(11): p. 8261-8.

66. Rajesh Ramachandran, R.K.T., Arthur E Johnson, *Membrane-dependent conformational changes initiate cholesterol-dependent cytolysin oligomerization and intersubunit bold beta-strand alignment.* Nature Structural & Molecular Biology, 2004. **11**: p. 697-705.

67. Rossjohn, J., et al., *Structures of Perfringolysin O Suggest a Pathway for Activation of Cholesterol-dependent Cytolysins.* J. Mol. Biol., 2007. **367**(5): p. 1227-1236.

68. Heuck, A.P., R.K. Tweten, and A.E. Johnson, *beta-Barrel Pore-Forming Toxins: Intriguing Dimorphic Proteins.* Biochemistry, 2001. **40**(31): p. 9065-9073.

69. Hadders, M.A., D.X. Beringer, and P. Gros, *Structure of C8 a-MACPF Reveals Mechanism of Membrane Attack in Complement Immune Defense.* Science, 2007. **317**(5844): p. 1552-1554.

70. Rosado, C.J., et al., *A Common Fold Mediates Vertebrate Defense and Bacterial Attack.* Science, 2007. **317**(5844): p. 1548-1551.

71. Dunstone, M.A. and R.K. Tweten, *Packing a punch: the mechanism of pore formation by cholesterol dependent cytolysins and membrane attack complex/perforin-like proteins.* Current Opinion in Structural Biology, 2012. **22**(3): p. 342-349.

72. Sato, T.K., R.K. Tweten, and A.E. Johnson, *Disulfide-bond scanning reveals assembly state and beta-strand tilt angle of the PFO beta-barrel.* Nature Chemical Biology, 2013. **9**(6): p. 383-389.

73. Heuck, A.P. and A.E. Johnson, *Membrane Recognition and Pore Formation by Bacterial Pore-forming Toxins*, in *Protein-Lipid Interactions. From Membrane Domains to Cellular Networks*, L.K. Tamm, Editor. 2005, Wiley-VCH: Weinheim. p. 163-186.

74. Heuck, A.P., R.K. Tweten, and A.E. Johnson, *Assembly and topography of the prepore complex in cholesterol-dependent cytolysins.* J. Biol. Chem., 2003. **278**(33): p. 31218-31225.

75. Palmer, M., et al., *Assembly mechanism of the oligomeric streptolysin O pore: the early membrane lesion is lined by a free edge of the lipid membrane and is extended gradually during oligomerization.* EMBO Journal, 1998. **17**(6): p. 1598-1605.

76. Gilbert, R.J., *Inactivation and activity of cholesterol-dependent cytolysins: what structural studies tell us.* Structure (Camb), 2005. **13**(8): p. 1097-1106.

77. Praper, T., et al., *Human Perforin Employs Different Avenues to Damage Membranes.* Journal of Biological Chemistry, 2010. **286**(4): p. 2946-2955.

78. Alving, C.R., et al., *Cholesterol-dependent tetanolysin damage to liposomes.* Biochimica et Biophysica Acta, 1979. **551**: p. 224-228.

79. Rosenqvist, E., T.E. Michaelsen, and A.I. Vistnes, *Effect of streptolysin O and digitonin on egg lecithin/cholesterol vesicles.* Biochim. Biophys. Acta, 1980. **600**: p. 91-102.

80. Ohno-Iwashita, Y., et al., *Effect of lipidic factors on membrane cholesterol topology - mode of binding of q-toxin to cholesterol in liposomes.* Biochimica et Biophysica Acta, 1992. **1109**(1): p. 81-90.

81. Nelson, L.D., S. Chiantia, and E. London, *Perfringolysin O Association with Ordered Lipid Domains: Implications for Transmembrane Protein Raft Affinity.* Biophysical journal, 2010. **99**(10): p. 3255-3263.

82. Lin, Q. and E. London, *Altering Hydrophobic Sequence Lengths Shows That Hydrophobic Mismatch Controls Affinity for Ordered Lipid Domains (Rafts) in the Multitransmembrane Strand Protein Perfringolysin O.* Journal of Biological Chemistry, 2013. **288**(2): p. 1340-1352.

83. Soltani, C.E., et al., *Structural elements of the cholesterol-dependent cytolysins that are responsible for their cholesterol-sensitive membrane interactions.* Proceedings of the National academy of Sciences of the United States of America, 2007. **104**(51): p. 20226-20231.

84. Soltani, C.E., et al., *Specific Protein-Membrane Contacts Are Required for Prepore and Pore Assembly by a Cholesterol-dependent Cytolysin.* J. Biol. Chem., 2007. **282**(21): p. 15709-15716.

85. Farrand, A.J., et al., *Only two amino acids are essential for cytolytic toxin recognition of cholesterol at the membrane surface.* Proceedings of the National Academy of Sciences of the United States of America, 2010. **107**(9): p. 4341-6.

86. Johnson, B.B., et al., *Modifications in Perfringolysin O Domain 4 Alter the Cholesterol Concentration Threshold Required for Binding.* Biochemistry, 2012. **51**(16): p. 3373-3382.

87. Dowd, K.J. and R.K. Tweten, *The Cholesterol-Dependent Cytolysin Signature Motif: A Critical Element in the Allosteric Pathway that Couples Membrane Binding to Pore Assembly*. PLoS Pathogens, 2012. **8**(7): p. e1002787.

88. Cho, W. and R.V. Stahelin, *Membrane-protein interactions in cell signaling and membrane trafficking.* Annual Review of Biophysics and Biomolecular Structure, 2005. **34**: p. 119-151.

89. Bavdek, A., et al., *Sterol and pH interdependence in the binding, oligomerization, and pore formation of listeriolysin O.* Biochemistry, 2007. **46**(14): p. 4425-4437.

90. Flanagan, J.J., A.P. Heuck, and A.E. Johnson, *Cholesterol-Phospholipid Interactions Play an Important Role in Perfringolysin O Binding to Membrane.* FASEB J. , 2002. **16**(Part II): p. A929.

91. Polekhina, G., et al., *Insights into the action of the superfamily of cholesterol-dependent cytolysins from studies of intermedilysin.* Proceedings of the National academy of Sciences of the United States of America, 2005. **102**(3): p. 600-605.

92. Saunders, F.K., et al., *Pneumolysin, the thiol-activated toxin of Streptococcus pneumoniae, does not require a thiol group for in vitro activity.* Infection and Immunity, 1989. **57**(8): p. 2547-2552.

93. Pinkney, M., E. Beachey, and M. Kehoe, *The thiol-activated toxin streptolysin O does not require a thiol group for cytolytic activity.* Infection and Immunity, 1989. **57**(8): p. 2553-2558.

94. Michel, E., et al., *Attenuated mutants of the intracellular bacterium Listeria monocytogenes obtained by single amino acid substitutions in listeriolysin O.* Molecular Microbiology, 1990. **4**(12): p. 2167-2178.

95. Sekino-Suzuki, N., et al., *Contribution of individual tryptophan residues to the structure and activity of q-toxin (perfringolysin O), a cholesterol-binding cytolysin.* Eur. J. Biochem., 1996. **241**: p. 941-947.

96. Korchev, Y.E., et al., *A conserved tryptophan in pneumolysin is a determinant of the characteristics of channels formed pneumolysin in cells and planar lipid bilayers.* Biochem. J., 1998. **329**: p. 571-577.

97. Billington, S.J., J.G. Songer, and B.H. Jost, *The variant undecapeptide sequence of the Arcanobacterium pyogenes haemolysin, pyolysin, is required for full cytolytic activity.* Microbiology, 2002. **148**(12): p. 3947-3954.

98. Farrand, A.J., et al., *Only two amino acids are essential for cytolytic toxin recognition of cholesterol at the membrane surface.* Proceedings of the National Academy of Sciences, 2010. **107**(9): p. 4341-4346.

99. Giepmans, B.N.G., et al., *The Fluorescent Toolbox for Assessing Protein Location and Function.* Science, 2006. **312**(5771): p. 217-224.

100. Wüstner, D., *Fluorescent sterols as tools in membrane biophysics and cell biology.* Chemistry and Physics of Lipids, 2007. **146**(1): p. 1-25.

101. Coxey, R.A., et al., *Differential accumulation of cholesterol in Golgi compartments of normal and Niemann-Pick type C fibroblasts incubated with LDL: a cytochemical freeze-fracture study.* Journal of Lipid Research, 1993. **34**(7): p. 1165-76.

102. Miller, R.G., *The use and abuse of filipin to localize cholesterol in membranes.* Cell Biol. Int. Rep, 1984. **8**: p. 519-35.

103. Ikonen, E. and M. Hölttä-Vuori, *Cellular pathology of Niemann–Pick type C disease.* Seminars in Cell & Developmental Biology, 2004. **15**(4): p. 445-454.

104. Waheed, A.A., et al., *Selective binding of perfringolysin O derivative to cholesterol-rich membrane microdomains (rafts).* Proceedings of the National Academy of Sciences, 2001. **98**(9): p. 4926-4931.

105. Moe, P.C. and A.P. Heuck, *Phospholipid Hydrolysis Caused by Clostridium perfringens α-Toxin Facilitates the Targeting of Perfringolysin O to Membrane Bilayers.* Biochemistry, 2010. **49**(44): p. 9498-9507.

106. Gimpl, G., K. Burger, and F. Fahrenholz, *Cholesterol as modulator of receptor function.* Biochemistry, 1997. **36**(36): p. 10959-74.

107. Pang, L., M. Graziano, and S. Wang, *Membrane cholesterol modulates galanin-GalR2 interaction.* Biochemistry, 1999. **38**(37): p. 12003-11.

108. Wolf, A.A., Y. Fujinaga, and W.I. Lencer, *Uncoupling of the cholera toxin-GM1 ganglioside receptor complex from endocytosis, retrograde Golgi trafficking, and downstream signal transduction by depletion of membrane cholesterol.* Journal of Biological Chemistry, 2002. **277**(18): p. 16249-16256.

109. Zidovetzki, R. and I. Levitan, *Use of cyclodextrins to manipulate plasma membrane cholesterol content: Evidence, misconceptions and control strategies.* Biochimica et Biophysica Acta, 2007. **1768**(6): p. 1311-1324.

110. Christian, A.E., et al., *Use of cyclodextrins for manipulating cellular cholesterol content.* J. Lipid Res., 1997. **38**(11): p. 2264-2272.

111. Patzer, E.J. and R.R. Wagner, *Cholesterol oxidase as a probe for studying membrane organisation.* Nature, 1978. **274**(5669): p. 394-5.

112. Lange, Y., H.B. Cutler, and T.L. Steck, *The effect of cholesterol and other intercalated amphipaths on the contour and stability of the isolated red cell membrane.* Journal of Biological Chemistry, 1980. **255**(19): p. 9331-9337.

113. Leventis, R. and J.R. Silvius, *Use of cyclodextrins to monitor transbilayer movement and differential lipid affinities of cholesterol.* Biophysical Journal, 2001. **81**(4): p. 2257-2267.

114. Huang, J. and G.W. Feigenson, *A microscopic interaction model of maximum solubility of cholesterol in lipid bilayers.* Biophys. J., 1999. **76**(4): p. 2142-2157.

115. McConnell, H.M. and A. Radhakrishnan, *Condensed complexes of cholesterol and phospholipids.* Biochim. Biophys. Acta, 2003. **1610**(2): p. 159-73.

116. Lange, Y., J. Ye, and T.L. Steck, *How cholesterol homeostasis is regulated by plasma membrane cholesterol in excess of phospholipids.* Proceedings of the National Academy of Sciences of the United States of America, 2004. **101**(32): p. 11664-7.

117. Mesmin, B. and F.R. Maxfield, *Intracellular sterol dynamics.* Biochimica et Biophysica Acta 2009. **1791**(7): p. 636-645.

118. Maxfield, F.R. and G. van Meer, *Cholesterol, the central lipid of mammalian cells.* Current Opinion in Cell Biology, 2010. **22**(4): p. 422-429.

119. Alouf, J.E., S.J. Billington, and B.H. Jost, *Repertoire and general features of the family of cholesterol-dependent cytolysins*, in *The Comprehensive Sourcebook of Bacterial Protein Toxins*, J.E. Alouf and M.R. Popoff, Editors. 2006, Academic Press: Oxford, England. p. 643-658.

120. Reid, P.C., et al., *A novel cholesterol stain reveals early neuronal cholesterol accumulation in the Niemann-Pick type C1 mouse brain.* J. Lipid Res., 2004. **45**(3): p. 582-591.

121. Hayashi, M., et al., *Detection of cholesterol-rich microdomains in the inner leaflet of the plasma membrane.* Biochemical and Biophysical Research Communications, 2006. **351**(3): p. 713-718.

122. Koseki, M., et al., *Increased lipid rafts and accelerated lipopolysaccharide-induced tumor necrosis factor-a secretion in Abca1-deficient macrophages.* J. Lipid Res., 2007. **48**(2): p. 299-306.

123. Waheed, A., et al., *Selective binding of perfringolysin O derivative to cholesterol-rich membrane microdomains (rafts).* Proceedings of the National Academy of Sciences of the United States of America, 2001. **98**: p. 4926-4931.

124. Ohno-Iwashita, Y., et al., *Perfringolysin O, a cholesterol-binding cytolysin, as a probe for lipid rafts.* Anaerobe, 2004. **10**: p. 125-134.

125. Silvius, J., *Lipid microdomains in model and biological membranes: how strong are the connections?* Quarterly Reviews of Biophysics, 2005. **38**(4): p. 373-83.

126. Gaus, K., et al., *Domain-specific lipid distribution in macrophage plasma membranes.* Journal of Lipid Research, 2005. **46**(7): p. 1526-38.

127. Heuck, A.P., et al., *Conformational Changes That Effect Oligomerization and Initiate Pore Formation Are Triggered throughout Perfringolysin O upon Binding to Cholesterol.* Journal of Biological Chemistry, 2007. **282**(31): p. 22629-22637.

128. Rajesh Ramachandran, A.P.H., Rodney K. Tweten & Arthur E. Johnson, *Structural insights into the membrane-anchoring mechanism of a cholesterol-dependent cytolysin.* Nature Structural & Molecular Biology, 2002. **9**: p. 823-7.

129. Shepard, L.A., et al., *Identification of a Membrane-Spanning Domain of the Thiol-Activated Pore-Forming Toxin Clostridium perfringens Perfringolysin O: An α-Helical to β-Sheet Transition Identified by Fluorescence Spectroscopy.* Biochemistry, 1998. **37**(41): p. 14563-14574.

130. Solovyova, A.S., et al., *The Solution Structure and Oligomerization Behavior of Two Bacterial Toxins: Pneumolysin and Perfringolysin O.* Biophysical journal, 2004. **87**(1): p. 540-552.

131. Romano, F.B., et al., *Efficient Isolation of Pseudomonas aeruginosa Type III Secretion Translocators and Assembly of Heteromeric Transmembrane Pores in Model Membranes.* Biochemistry, 2011. **50**(33): p. 7117-7131.

132. Heuck, A.P., R.K. Tweten, and A.E. Johnson, *Assembly and Topography of the Prepore Complex in Cholesterol-dependent Cytolysins.* Journal of Biological Chemistry, 2003. **278**(33): p. 31218-31225.

133. Chen, P.S., T.Y. Toribara, and H. Warner, *Microdetermination of Phosphorus.* Analytical Chemistry, 1956. **28**(11): p. 1756-1758.

134. Christian, A.E., et al., *Use of cyclodextrins for manipulating cellular cholesterol content.* Journal of Lipid Research, 1997. **38**(11): p. 2264-72.

135. Heuck, A.P., et al., *Mechanism of Membrane Insertion of a Multimeric βeta-Barrel Protein: Perfringolysin O Creates a Pore Using Ordered and Coupled Conformational Changes.* Molecular cell, 2000. **6**(5): p. 1233-1242.

136. Hotze, E.M., et al., *Monomer-Monomer Interactions Drive the Prepore to Pore Conversion of a β-Barrel-forming Cholesterol-dependent Cytolysin.* Journal of Biological Chemistry, 2002. **277**(13): p. 11597-11605.

137. Klein U, G.G., Fahrenholz F., *Alteration of the myometrial plasma membrane cholesterol content with beta-cyclodextrin modulates the binding affinity of the oxytocin receptor.* biochemistry, 1995. **34**(42).

138. Hotze, E.M., et al., *Monomer-Monomer Interactions Drive the Prepore to Pore Conversion of a βeta-Barrel-forming Cholesterol-dependent Cytolysin.* Journal of Biological Chemistry, 2002. **277**(13): p. 11597-11605.

139. Ramachandran, R., et al., *Structural insights into the membrane-anchoring mechanism of a cholesterol-dependent cytolysin.* Nat Struct Mol Biol, 2002. **9**(11): p. 823-827.

140. Ohno-Iwashita, Y., et al., *Perfringolysin O, a cholesterol-binding cytolysin, as a probe for lipid rafts.* Anaerobe, 2004. **10**(2): p. 125-134.

141. Hansson, M.D., et al., *PCR-mediated deletion of plasmid DNA.* Analytical Biochemistry, 2008. **375**(2): p. 373-375.